

**MATHEMATICAL MODELLING APPROACH TO INVESTIGATE  
TRANSMISSION DYNAMICS OF COVID-19 WITH SOME CONTROL  
PARAMETERS**

**James Nicodemus Paul**

**A Dissertation Submitted in Partial Fulfilment of the Requirements for the Degree of  
Master's in Mathematical and Computer Sciences and Engineering of the Nelson Mandela  
African Institution of Science and Technology**

**Arusha, Tanzania**

**June, 2022**

## ABSTRACT

COVID-19 is a world pandemic that has affected and continues to affect human lives, socially and economically. Worldwide governments enforced preventive measures aimed at reducing the disease transmission due to its social and economic impact. Examples of such measures are physical separation, quarantine, hand-washing, travel bans and border restrictions, lockdown, and the use of hand sanitizers. Some of the control measures like quarantine was the most stressful strategy for people to manage. To examine the impact of stress on the transmission of COVID-19, this dissertation developed a mathematical model with six compartments; Susceptible-Exposed-Quarantine-Infectious-Hospitalized-Recovered (*SEQIHR*). The model was then analyzed both theoretically and numerically. In theoretical analysis, terms like positivity, bounded region, existence, uniqueness of the solution, model existence of free and endemic equilibrium points, local and global stability are all utilized. The basic reproduction number ( $R_0$ ) was calculated using the next-generation matrix approach. When  $R_0 < 1$ , the disease-free equilibrium is globally asymptotically stable, whereas when  $R_0 > 1$ , the endemic equilibrium is globally asymptotically stable. The Partial Rank Correlation Coefficient (PRCC) was used to evaluate the relationship between model parameters and  $R_0$ . The model was numerically solved using the fourth-order Runge-Kutta method, and parameter identifiability was achieved using least square and Markov Chain Monte Carlo (MCMC) methods. The formulated deterministic model explored the impact of stress in quarantine to the human population and revealed that when an individual's mental health is good, the body immunity becomes strong. Conclusively, the control parameters have a considerable impact on COVID-19 transmission minimization.

## DECLARATION

I, **James Nicodemus Paul**, do hereby declare to the Senate of Nelson Mandela African Institution of Science and Technology that this dissertation titled: *Mathematical modelling Approach to Investigate Transmission Dynamics of COVID-19 with some Control Parameters*, is my own original work and that it has neither been submitted nor presented for similar awards in any other institution.



---

James Nicodemus Paul  
(Candidate)

20/07/2022

Date

The above declaration is confirmed:



---

Dr. Silas Steven Mirau  
(Supervisor 1)

20/07/2022

Date



---

Dr. Isambi Sailon Mbalawata  
(Supervisor 2)

20/07/2022

Date

## **COPYRIGHT**

This dissertation is copyright material protected under the Berne Convention, the Copyright Act of 1999 and other international and national enactments, in that behalf, on intellectual property. It must not be reproduced by any means, in full or in part, except for short extracts in fair dealing; for researcher private study, critical scholarly review or discourse with an acknowledgement, without the written permission of the office of Deputy Vice Chancellor for Academic, Research and Innovation on behalf of both the author and the Nelson Mandela African Institution of Science and Technology.

## CERTIFICATION

The undersigned certify that they have read and hereby recommend for acceptance by the Nelson Mandela African Institution of Science and Technology the dissertation entitled: *Mathematical modelling Approach to Investigate Transmission Dynamics of COVID-19 with some Control Parameters*, in fulfilment of the requirements for the Master's degree in Mathematical and Computer Science and Engineering of the Nelson Mandela African Institution of Science and Technology.



---

Dr. Silas Steven Mirau

(Supervisor 1)

Date: ..... 20/07/2022 .....



---

Dr. Isambi Sailon Mbalawata

(Supervisor 2)

Date: ..... 20/07/2022 .....

## **ACKNOWLEDGEMENTS**

I am indebted to Almighty GOD eternally and the Holy Spirit who never and will never leave me as I trust in Him no matter what happens.

Very special thanks to my supervisors: Dr. Silas Steven Mirau and Dr. Isambi Sailon Mbalawata, for their encouragement and guidance throughout my studies. I sincerely appreciate not just their supervision but also their mentorship in assisting me on achieving my goals.

Special thanks to the NM-AIST management and personnel for their assistance during my studies.

Very special thanks to my really wonderful mate Lemjini Masandawa who supported me and encouraged me during the preparation of this dissertation.

All of my lecturers, Professor Dr-Ing. Verdiana Grace Masanja, Professor Dmitry, and other lecturers (both classical and contemporary) at NM-AIST, deserve my deepest gratitude.

Not only, but also my deepest appreciation goes to Dr. Nkuba Nyerere, Dr. Jean Claude, Dr. Joshua Mwasunda, Dr. Aristide Lambura, Dr. Miracle Amandi, Dr. Jean Muhirwa and Dr. Taiwo Adewumi for their contribution towards this study.

Special thanks to my beloved wife, Mrs Alice James for taking all family responsibilities during my absence and thanks to my lovely children Gracious, Gracian and Gladness for their encouragement and prayers.

## **DEDICATION**

This dissertation is dedicated to my loving and caring wife Alice P. Shemkai, my lovely children Gracious James, Gracian James and Gladness James. They have been the source of motivation and encouragement throughout my studies. Furthermore I dedicate this study to my parents, my brother Felix Nicodemus Paul, and sisters, whose supported me unconditionally to accomplish my studies.

## TABLE OF CONTENTS

<b>ABSTRACT</b> . . . . .	<b>i</b>
<b>DECLARATION</b> . . . . .	<b>ii</b>
<b>COPYRIGHT</b> . . . . .	<b>iii</b>
<b>CERTIFICATION</b> . . . . .	<b>iv</b>
<b>ACKNOWLEDGEMENTS</b> . . . . .	<b>v</b>
<b>DEDICATION</b> . . . . .	<b>vi</b>
<b>TABLE OF CONTENTS</b> . . . . .	<b>vii</b>
<b>LIST OF TABLES</b> . . . . .	<b>x</b>
<b>LIST OF FIGURES</b> . . . . .	<b>xi</b>
<b>LIST OF ABBREVIATIONS</b> . . . . .	<b>xii</b>
<b>CHAPTER ONE</b> . . . . .	<b>1</b>
<b>INTRODUCTION</b> . . . . .	<b>1</b>
1.1 Background of the Problem . . . . .	1
1.2 Problem Statement . . . . .	5
1.3 Research Rationale . . . . .	7
1.4 Research Objectives . . . . .	7
1.4.1 Main Objective . . . . .	7
1.4.2 Specific Objectives . . . . .	7
1.5 Research Questions . . . . .	8
1.6 Significance of the Study . . . . .	8
1.7 Delineation of the Study . . . . .	8
<b>CHAPTER TWO</b> . . . . .	<b>9</b>
<b>LITERATURE REVIEW</b> . . . . .	<b>9</b>
2.1 History of Mathematical Models in Medical Applications . . . . .	9
2.2 COVID-19 Mathematical Models . . . . .	11
2.3 Related Mathematical Models with stress component . . . . .	13



2.4	Related Survey Studies . . . . .	13
2.5	Conclusion . . . . .	17
<b>CHAPTER THREE . . . . .</b>		<b>18</b>
<b>MATERIALS AND METHODS . . . . .</b>		<b>18</b>
3.1	Introduction . . . . .	18
3.2	Model Formulation . . . . .	18
3.2.1	Model Assumptions . . . . .	20
3.2.2	Model Compartments and Dynamics . . . . .	21
3.2.3	The <i>SEQIHR</i> Model Equations . . . . .	23
3.3	Model Analysis . . . . .	23
3.3.1	Properties of the Model . . . . .	23
3.3.2	Model Positivity . . . . .	23
3.3.3	Invariant (Boundedness) Region . . . . .	25
3.3.4	The Existence and Uniqueness of the Solution . . . . .	27
3.3.5	The Existence of Disease-Free Equilibrium Point ( $E_0$ ) . . . . .	32
3.3.6	The Basic Reproduction Number ( $R_0$ ) . . . . .	33
3.4	Stability Analysis . . . . .	38
3.4.1	Local Stability of the Disease-Free Equilibrium ( $E_0$ ) . . . . .	38
3.4.2	Existence of Endemic Equilibrium Point . . . . .	41
3.4.3	The Global Stability of Disease-Free Equilibrium Point ( $E_0$ ) . . . . .	42
3.4.4	The Global Stability of Endemic Equilibrium Point, $E_*$ . . . . .	43
3.5	Conclusion . . . . .	45
<b>CHAPTER FOUR . . . . .</b>		<b>46</b>
<b>RESULTS AND DISCUSSION . . . . .</b>		<b>46</b>
4.1	Introduction . . . . .	46
4.2	Numerical Simulation . . . . .	46
4.3	Sensitivity Analysis and Uncertainty . . . . .	46
4.4	Dynamic Population simulation on a <i>SEQIHR</i> Model . . . . .	48
4.5	Relationship between Parameters and $R_0$ . . . . .	49
4.6	Simulation of Stability Analysis for Endemic Equilibrium Point of <i>SEQIHR</i> Model . . . . .	52
4.7	Control Parameters . . . . .	53

4.8	Parameter identifiability and model fitting by least square method . . . . .	55
4.9	Parameter identifiability by Markov Chain Monte Carlo (MCMC) . . . . .	58
4.10	Discussion . . . . .	61
<b>CHAPTER FIVE . . . . .</b>		<b>63</b>
<b>CONCLUSION AND RECOMMENDATIONS . . . . .</b>		<b>63</b>
5.1	Conclusion . . . . .	63
5.2	Recommendations . . . . .	63
5.2.1	Future Work . . . . .	64
5.2.2	Study Limitations . . . . .	64
<b>REFERENCES . . . . .</b>		<b>65</b>
<b>APPENDICES . . . . .</b>		<b>77</b>
<b>MATLAB CODES . . . . .</b>		<b>77</b>
<b>RESEARCH OUTPUTS . . . . .</b>		<b>84</b>

## LIST OF TABLES

Table 1:	Description of state model variables . . . . .	21
Table 2:	Model parameters description . . . . .	22
Table 3:	Sensitivity indices for $R_0$ parameters . . . . .	47
Table 4:	Parameter identifiability . . . . .	56
Table 5:	Estimated parameters using least square and MCMC methods . . . . .	59

## LIST OF FIGURES

Figure 1:	Strong immune system (Smith, 2020) . . . . .	6
Figure 2:	Weak immune system (Kateman, 2020) . . . . .	6
Figure 3:	Schematic flow diagram showing dynamics of COVID-19 . . . . .	21
Figure 4:	Boundedness Region . . . . .	27
Figure 5:	Sensitivity analysis and PRCC results for $R_0$ . . . . .	48
Figure 6:	$SEQIHR$ Model dynamic simulation . . . . .	49
Figure 7:	Effect of stress $\eta_1$ and contact rate $\beta$ on $R_0$ . . . . .	50
Figure 8:	Effect of quarantined rate $\theta$ and hospitalized rate $\omega$ on $R_0$ . . . . .	50
Figure 9:	Effect of infected rate $\eta_2$ and recovered rate $\nu$ on $R_0$ . . . . .	51
Figure 10:	Effect of recruitment rate $\mu$ and uninfected rate $\alpha$ on $R_0$ . . . . .	51
Figure 11:	Effect of natural death $b$ and death due to disease $\delta$ on $R_0$ . . . . .	51
Figure 12:	Effect of $q$ on $R_0$ from exposed class to hospitalized and infected class . .	52
Figure 13:	Endemic equilibrium for susceptible and exposed human population . . .	52
Figure 14:	Endemic equilibrium for quarantined and infected human population . . .	53
Figure 15:	Endemic equilibrium for hospitalized and recovered human population . .	53
Figure 16:	Variation of contact rate $\beta$ in susceptible and infected population . . . . .	54
Figure 17:	Variation of $\eta_1$ in susceptible and infected population . . . . .	54
Figure 18:	Variation of $\eta_2$ in infected and hospitalized population . . . . .	55
Figure 19:	Variation of $\nu$ in infected and recovered population . . . . .	55
Figure 20:	Parameter estimations . . . . .	57
Figure 21:	Model Fitting . . . . .	57
Figure 22:	Trace plots . . . . .	60
Figure 23:	Scatter plots . . . . .	60
Figure 24:	Histograms . . . . .	61
Figure 25:	Distribution density . . . . .	61

## LIST OF ABBREVIATIONS

PRCC	Partial Rank Correlation Coefficient
MCMC	Markov Chain Monte Carlo
DFEP	Disease-Free Equilibrium Point
$SI$	System International
$R_0$	Basic Reproduction Number
NM-AIST	Nelson Mandela African Institution of Science and Technology
AIMS	African Institute of Mathematical Science
WHO	World Health Organization
TB	Tuberculosis
EE	Endemic Equilibrium
MCerr	Markov Chain errors
LSQE	Least Square Estimates

## CHAPTER ONE

### INTRODUCTION

#### 1.1 Background of the Problem

Coronavirus disease-2019 (COVID-19) is an infectious disease caused by the severe acute respiratory syndrome coronavirus-2 (SARS-CoV-2). SARS-CoV-2, like the other two COVID-19, SARS-CoV-1 and MERS-CoV, is thought to have originated in bats, which have long served as reservoirs for many deadly COVID-19. Although the exact mechanism by which SARS-CoV-2 is transmitted from bats to humans is uncertain, rapid human-to-human transmission has been widely confirmed (Khan *et al.*, 2021).

Coronavirus are categorized into four classes: alpha, beta, gamma, and delta coronavirus. Human coronavirus such as HCoV-NL63 and HCoV-229E are examples of alpha coronavirus. Human coronavirus such as HCoV-HKU1, Severe Acute Respiratory Syndrome Human Coronavirus (SARS-HCoV), and Middle Eastern Respiratory Syndrome Coronavirus, on the other hand, are seen in beta coronavirus (MERS-CoV). Viruses from birds and pigs make up the delta coronavirus, whereas viruses from birds and whales make up the gamma coronavirus (Harapan *et al.*, 2020; Velavan, 2020).

Coronavirus were found as human diseases for the first time in the mid-1960s whereby SARS-CoV-1, MERS-CoV, SARSCOV-2, HCoV-229E, HCoV-HKU1, HCoV-OC43, and HCoV-NL63 are the seven types of coronavirus (Steardo *et al.*, 2020). In comparison to other coronavirus, SARS-CoV-1, MERS-CoV, and SARS-CoV-2 are well-known. SARS-CoV-1 first appeared in Guangdong, China's southern province, in November 2002, and quickly spread to Vietnam, Canada, Singapore, and other countries (Koh *et al.*, 2005). In March 2003, one study found that a new coronavirus was the causal agent of SARS-CoV-1, with palm civet cats and dromedary camels serving as intermediate animal sources (Peiris *et al.*, 2003). Bats may be a natural reservoir for SARS-CoV-1, according to research. Human-to-human transmission occurs via respiratory droplet fomite-based contact and direct touch. In the year 2004, SARS-CoV-1 spread to 29 countries, producing 8096 confirmed cases, 774 deaths, and disappeared (Tsang *et al.*, 2003; Garba *et al.*, 2020).

MERS-CoV was first discovered in Saudi Arabia in September 2012, and it has since spread to

27 countries, resulting in 2494 confirmed cases and 858 deaths (Garba *et al.*, 2020). Nonetheless, the virus was spread naturally by dromedary camels and civet cats. The novel beta coronavirus was detected in a male patient who died of acute pneumonia after many of his body organs failed, according to one study (Hui *et al.*, 2021). MERS-CoV is spread by intimate contact with droplets or by coming into contact with fomite (Zaki *et al.*, 2012).

Infectious diseases have impacted negatively on cultures all across the world throughout history. According to the World Health Organization (WHO), more than 20 infectious agents have caused disease outbreaks and epidemics around the world over the past decade. Several of these epidemics were caused by novel infectious diseases like H1N1 and MERS. Over the past two decades, the rise of COVID-19-associated diseases (SARS and MERS) has posed a global threat to public health systems. SARS-CoV-2 (the disease-causing coronavirus) is the most recent addition to the growing list of novel agents that aren't welcome (Balkhair, 2020).

The first incidence of this pandemic was recorded in Wuhan, China, in December 2019, and it spread to other parts of the world in early 2020 (Ali *et al.*, 2020; Ivorra *et al.*, 2020). The WHO declared COVID-19 disease a global pandemic on March 12, 2020, after reporting 125,260 confirmed cases and 4613 deaths in less than 24 hours (Organization *et al.*, 2020; Maier & Brockmann, 2020).

This disease alarmed world leaders because of how quickly it spread from person to person and the social and economic impact it had on their countries. The WHO and country leaders focused on developing ways to reduce disease transmission by implementing new technologies such as Lockdown, quarantine, border closures, travel bans, and isolation centers are some of the tactics that have been used by the researchers (Prem *et al.*, 2020; Daks *et al.*, 2020; Morato *et al.*, 2020; Savi *et al.*, 2020). COVID-19 is transmitted from person to person by inhaling respiratory droplets given out by an infected person's mucous membranes (eye, mouth, and nose) when sneezing, coughing, talking, or exhaling. Because these respiratory droplets are too heavy to float in the air, they are influenced by gravity and move not more than one meter before crashing to the floor or surface, hence a social distance of two meters or more is recommended by the WHO. Furthermore, the disease can be transmitted through fomites. In most cases, infection is spread by breathing respiratory droplets from a close touch with an infected individual (Peter *et al.*, 2021; Mbogo, 2021).

When compared to young adults, the condition is substantially more severe in the 65+ age range. Long-term diseases that reduce the body's immune, such as cancer, chronic respiratory disease, diabetes, hypertension, and cardiovascular disease, are more likely to cause serious sickness in humans (Peter *et al.*, 2021). Tiredness, sleep disturbances, throat infection, nausea, vomiting, diarrhea, severe headache, muscle discomfort, runny nose, dry cough, red eyes, exhaustion, sneezing, loss of smell, and test results are all common symptoms of this condition (Gostic *et al.*, 2020; Ahmad *et al.*, 2021). Breathing issues, persistent chest pain, high blood pressure, kidney failure, and a lack of voluntary movement are all highly serious clinical symptoms (Baba *et al.*, 2021).

Mathematical models are essential tools for evaluating various infectious disease transmission and control intervention approaches. From the beginning of this human-disrupting disease, a lot of mathematical models on COVID-19 pandemic have been constructed.

According to Pancani *et al.* (2021), the length of the isolation time, which was recorded in days after lockdown began, resulted in loneliness and mental health difficulties. During the pandemic in China, the impact of COVID-19 quarantine on mental health was discussed. The impacts of loneliness on psychological well-being, rather than addressing whether by confining the general population for an extended period of time, which can lead to a decline in mental health. The research conducted by Jurblum *et al.* (2020) on the Psychological effects of social isolation and quarantine during the COVID-19 epidemic, finding that quarantine is linked to an increase in suicide, acute stress disorder, anger, posttraumatic stress disorder, and depression. These symptoms continue for a long time even after the quarantine period ends, whereby the patients need further psychological support.

Dagnino *et al.* (2020) conducted a survey in Chile on the Psychology effects of social isolation caused by quarantine and discovered that quarantine causes high levels of stress and bad psychological impact in people's life. Younger participants are more affected by the situation, according to the survey carried in Latin American, because of concerns about employment, finances, stigma, and mental health in general.

In their study, López Steinmetz *et al.* (2020) analyzes the negative mental health effects of quarantine and suggests that quarantine time is an important factor to consider when quantifying such effects. Long periods of quarantine have a significant impact on patients due to a lack of family support while in quarantine, causing the patient to experience excessive stress and become



psychologically affected.

Khan *et al.* (2020) conducted a research on the use of lockdown and quarantine in Bangladesh that has had consequences on daily living, mental and physical. They discussed the relationship between COVID-19 and mental health in their study. During the COVID-19 epidemic, many people were subjected to lockdown and quarantine, which created mental health problems and distress. Many people became more affected during this period because they were isolated from their loved ones and the community in general. Ullah (2020) explored several ways such as social-distancing, self-isolation, quarantine, and hospitalization and then concluded that these are the best ways to curb COVID-19. But these ways are certainly very tough for society because they are very stressful.

Dos Santos (2020) in his review studied the effects of social distancing and social isolation measures as good ways to fight against the disease, although they lead to social stress which influence the spread of the disease. In early 2020, some mathematical models for COVID-19 were developed and published. In this study, it shows that most of the isolated individuals became mentally affected. Also, Dhanwant & Ramanathan (2020) explored how the social distancing in India during the pandemic helped to reduce COVID-19 disease transmission by social contact. Social distancing was found to be effective in India to fight against COVID-19 disease. In their study, discussed the impact of social-contact on the transmission of the disease from one person to another, so the government introduces the preventive measures to fight against the disease so as to avoid much spread throughout the country.

Khan (2020) discussed the interaction of bats and unknown hosts, and then the interaction of people in the seafood market where there is enough source of infection. They presented their results graphically to show how they can minimize the infections. According to Pfefferbaum (2020), in their research on mental health and the COVID-19 pandemic, explained that most people are affected emotionally by the pandemic (such as distress or psychiatric conditions) which is ubiquitous in affected populations.

Islam *et al.* (2020), discussed factors which lead to mental stress such as financial difficulties, losing of job (career), family isolation and sleep shortness which affect many families to lose their loved ones. During this time many individuals isolated from their families and loved ones which lead to the mental stress of the affected person.

The impact of quarantine on the transmission of COVID-19 disease was discussed by Ashcroft *et al.* (2021) showing that many countries impose quarantine to ensure the exposed people and those from abroad are isolated for a specific period of time to prevent the spread of the disease. However, these measures took a larger economical toll and affected the health of the isolated individuals. Moreover, Prati (2021) from Italy, discussed the national impacts of quarantine psychologically. In their online survey of 1569 people living in Italy, they found that there are psychosocial factors that influence the disease, such as media exposure to COVID-19 outbreak, financial loss, higher worry, and negative attitude towards quarantine leading to psychological impacts.

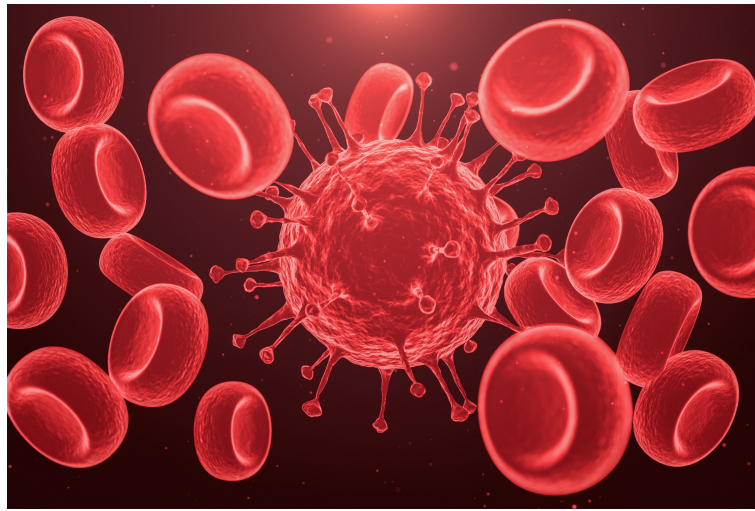
The mental health of public and healthcare professionals are affected by the pandemic, especially during quarantine time where hypervigilance arises because of fear and anxiety (Usher *et al.*, 2020; Khan *et al.*, 2020).

## **1.2 Problem Statement**

The efforts of WHO and the country leaders in fighting the COVID-19 disease have been made. During the pandemic, many scientists conducted several studies to overcome the transmission of the disease as considering the studies of Ali *et al.* (2020), Morato *et al.* (2020), Daks *et al.* (2020), Giordano *et al.* (2020) and Lin *et al.* (2020). The results from these studies showed the existence of COVID-19 disease and recommended different preventive measures to be taken to fight the disease, which are isolation, quarantine, self-distancing, wearing masks and washing hands every time. However, it was very important to introduce the parameter for the effects of stress and developed a mathematical model which is very essential to this study. The effect of stress in the human body affects the immune system especially for those with weak immunity who are affected much compared to those with a good immune system. Hence there is a need to introduce a new parameter of stress in modeling, which affects quarantined groups and infected groups. During quarantine time most people are stressed because they are isolated from their family members or community in which they develop fear and later develop stress through which the immune system is affected, hence causing the disease to fight the immune system easily. Stress affects many quarantined people whereby their immune system is disturbed by the COVID-19 and this is most likely because during quarantine, people are isolated from their families and community members, so they develop fear, and later the body becomes stressed which affects their immune system. When the immune system is disturbed, it fails to fight against the intruders, which leads to the fast spread of COVID-19 throughout the body. Therefore, this research aims to formulate

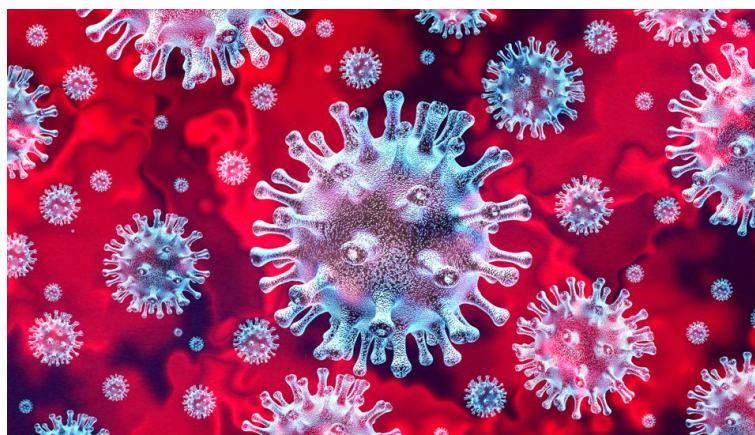
a mathematical model to explore the impact of stress in quarantine to the human population. The model has six compartmental classes (susceptible, exposed, quarantine, infectious, hospitalized, and recovered). The model is extended from the model given in Mandal *et al.* (2020) by incorporating the hospitalized class and introducing a stress parameter in a quarantined and infected class.

Figure 1, shows a strong immune system fighting the COVID-19 which leads to the failure of multiplying itself within the human body.



**Figure 1: Strong immune system (Smith, 2020)**

During quarantine and hospitalization time, most people become stressed because they think about dying with the disease and the immune system becomes weak. When the immune system is weak, COVID-19 multiplies within the body and destroys the immune system as in Fig. 2



**Figure 2: Weak immune system (Kateman, 2020)**

When the human body encounters COVID-19 disease for the first time, the immune system disturbed by the new intruder whereby the spread of the disease can occur. When an individual becomes stressed the immune system fails to fight back the virus so the virus attacks the white blood cells and starts to spread all over the respiratory system (Chowdhury *et al.*, 2020).

### **1.3 Research Rationale**

COVID-19 disease costs the African region and the world millions of dollars to fight for the spread of the disease from one person to another and from one country to another by introducing various measures to fight against the disease. To slow the spread of the disease, several vaccines were developed and distributed throughout the world. The whole world is suffering economic backlash due to the COVID-19 disease. This is because most of the businesses were closed to obey the control measures introduced by country leaders to avoid direct contact of people from one area/ or one country to another. Some of the ways introduced by the WHO and country leaders are social-distancing, social isolation, and quarantine. But some of these ways of fighting against the COVID-19 disease are stressful because people are isolated from their families and community members. Although many studies have been done on the COVID-19 disease and few done on mental health and stress, this study focused on a mathematical modeling approach to investigate transmission dynamics of COVID-19 with some control parameters.

### **1.4 Research Objectives**

This research is carried out with the help of the main objective and specific objectives.

#### **1.4.1 Main Objective**

To formulate and analyze a mathematical model for COVID-19 transmission dynamics that includes stress and other control parameters.

#### **1.4.2 Specific Objectives**

The study has the following specific objectives:

- (i) To formulate a mathematical model for COVID-19 transmission dynamics that includes stress and other control parameters.
- (ii) To perform and study a sensitivity analysis of a developed model by using Partial Rank Correlation Coefficient (PRCC) Analysis.
- (iii) To determine the conditions for equilibrium point existence and stability.

- (iv) To perform parameter estimation (identifiability) by Least Square and Markov Chain Monte Carlo (MCMC) methods.

## **1.5 Research Questions**

The study objectives can be met by examining and responding to the following questions:

- (i) How can mathematical models for the transmission dynamics of COVID-19 and control parameters including stress be formulated?
- (ii) What is the sensitivity analysis of the developed model to be analyzed by using PRCC?
- (iii) What are the conditions for equilibrium points to exist and be stable?
- (iv) How parameters converge?

## **1.6 Significance of the Study**

The study is significant among others, on the following reasons:

- (i) Reducing the transmission of COVID-19 in society.
- (ii) To know if quarantine helps to reduce the transmission of COVID-19 disease.
- (iii) This study helps to know how stress-free helps to reduce the transmission of COVID-19 disease.
- (iv) The research was utilized to fulfill a requirement for the NM-AIST master's degree in MCSE.

## **1.7 Delineation of the Study**

The transmission dynamics of COVID-19 in humans were investigated using a mathematical model with some control parameters in this study. This research builds on previous work done by Mandal *et al.* (2020) by incorporating the hospitalized class and introducing a stress parameter in a quarantined and infected class. This study shows that if stress is managed in the community especially during the quarantine period, the infection will be minimized from the community.

## CHAPTER TWO

### LITERATURE REVIEW

#### 2.1 History of Mathematical Models in Medical Applications

A mathematical model is a written representation of a system in terms of mathematics. A mathematical model is an essential tool for tracking the spread of infectious diseases and controlling them. Mathematical models are used to study and forecast how transmissible diseases spread in order to highlight the potential effects of an outbreak and provide public medical advice.

To define the parameters for various infectious diseases and to assess the effectiveness of various interventions such as mass vaccination and public awareness campaigns. Such models use a number of assumptions and mathematics which can also help with decisions about when and how to undertake interventions. Modeling of communicable diseases has been used to investigate disease transmission, forecast epidemics, and assess pandemic control techniques.

In 1766, a talented physician named Daniel Bernoulli conducted the first mathematical modeling study on disease transmission, creating a mathematical model to evaluate smallpox fatality in England. The model was used to illustrate that immunizing newborns against the disease could lengthen their lives by three years and two months (Bernoulli & Blower, 2004).

Lambert and Laplace built on Bernoulli's work by incorporating age-dependent elements into the model. Nonetheless, it wasn't until 1911 that their research emphasis was methodically refined, when Ross published a landmark study that founded contemporary mathematical epidemiology (Siettos & Russo, 2013).

The use of mathematical models to understand how to successfully manage diseases has a lengthy history, as well as some remarkable success. The river blindness disease (Onchocerciasis) control program in west Africa around the turn of the millennium shown that models may make significant pragmatic contributions to intervention programs if they are integrated into the broader program and participants understand what models can achieve and what cannot achieve as discussed by Macdonald (1950).

Mathematical models have become valuable tools in the study of infectious disease transmission and control. Despite the fact that chronic diseases such as cancer and heart disease receive greater

attention in wealthy countries, infectious diseases are the leading cause of misery and mortality in impoverished (developing) countries. Understanding the characteristics of infectious disease transmission in communities, regions, and countries can help to develop more effective disease-prevention methods. Mathematical models can be used to develop and test ideas, as well as to compare, plan, implement, and evaluate various detection, preventive, therapy, and control programs.

Generally, several models developed with compartmental structures depending on the disease type. Some of the compartmental models have classes such as; susceptible-infection-recovered (SIR), Susceptible-Infected-Susceptible (SIS), Susceptible - Exposed - Infected - Recovered (SEIR), Susceptible - Exposed - Infected (SEI), Susceptible - Infection (SI), and Susceptible - Exposed - Infected - Recovered - Susceptible (SEIRS) (Hethcote, 1994).

Since these early days, epidemiology has come a long way, and advances in immunology, cellular and molecular biology have provided many methods to aid in the measurement of infection patterns in human populations. Despite this progress, there is indeed a reluctance often in medical education and research today to use the disciplines of natural populations, mathematics, and statistics to help in the explanation of observed phenomena of infection within communities and the design of infection and disease control programs as presented by Anderson and May (1992).

Furthermore, it is impossible to deny that epidemic diseases have a negative impact on business and productivity. They may also lead to immigration as a result of the dread of death. Scientists have always been looking for the best techniques to combat pandemic diseases. Although medicines, vaccinations, and other techniques have had some success, many diseases have not been totally eradicated. Prior to the onset of epidemics, such diseases are primarily combated. To reduce/minimize the negative social and economic repercussions, it is critical to take proper safeguards and anticipate the impact of diseases. As a result, mathematical models are used, with the SIR (Susceptible-Infected-Recovered) model being the most extensively used to simulate infectious diseases including influenza, SARS, measles, and mumps, in which one-shot epidemic waves can occur with high mortality or recovery implying immune system as studied by Cilli *et al.* (2019).

## 2.2 COVID-19 Mathematical Models

Many studies on the COVID-19 pandemic have been done to examine the disease's dynamical transmission and control. In this section, some studies from other researchers are evaluated to show what has been done and what has been left out in order to establish the foundation for this research. The other researchers work aids in identifying the study gap of this work.

Mandal *et al.* (2020) provided a mathematical model with five compartments which are; susceptible ( $S$ ), quarantined ( $Q$ ), exposed ( $E$ ), recovered ( $R$ ), and infected ( $I$ ). They used reproduction number sensitivity analysis to show that when the contact rate is reduced, the exposed and susceptible population becomes a critical factor in disease prevention. The model's dynamical behavior was thoroughly explored in terms of the basic reproduction number. Furthermore, a sensitivity analysis of the basic reproduction number demonstrated that the most important component in disease prevention is reducing interaction between exposed and susceptible individuals.

Carvalho *et al.* (2020) introduced eight classes of the SINDROME model in which it consists, susceptible ( $S$ ), quarantine ( $Q$ ), exposed ( $E$ ), asymptomatic infection ( $A$ ), symptomatic infection ( $I$ ), diagnosed ( $D$ ), recovered ( $R$ ) and mortality ( $M$ ). Despite the transmission rate of environmental mediation as a parameter they did not discuss the effects of social isolation which creates stress of an individual and causes immune disturbance. Patients with COVID-19, whether confirmed or suspected, may be worried about the effects of contracting a potentially deadly new virus, while those in quarantine may be bored, lonely, and angry. Furthermore, signs of infection, such as fever, hypoxia, and cough, as well as treatment side effects, such as corticosteroid-induced sleeplessness, can exacerbate anxiety and produce mental discomfort. People's perceptions may mediate the psychological effects of stressful events associated with an infectious disease outbreak. In addition, to alleviate their sense of uncertainty and dread, health staff and patients should receive clear communication with regular and accurate information regarding the COVID-19 outbreak.

Okuonghae (2020) formulated a mathematical model to investigate the impacts of COVID-19 in a population and control measures on how it spread. The model used by the government in non-pharmaceutical control techniques to examine the transmission of COVID-19 disease in the city of Lagos, Nigeria. Their model divided the total population  $N(t)$  into susceptible ( $S$ ), exposed ( $E$ ), asymptomatic infectious ( $A$ ), symptomatic infectious ( $I$ ), infectious detected humans ( $I_D$ ) and recovered humans ( $R$ ). Their work did not consider the effects of stress in the population



for which this study is going to use it as a parameter. According to their findings, at least 55% of the population adheres to social distancing measures, with another 55% effectively using face masks in public, and the disease gradually fades out in the community over time. According to their study, the disease will be eradicated if the case detection rate for infected people is boosted to roughly 0.8 per day and about 55% of the population efficiently uses masks when in public.

Mpeshe (2021) formulated a mathematical model that combined COVID-19 and fear epidemics. Their research looked at the effects of fear on COVID-19 disease transmission and discovered that fear rates and transmission rates had an effect on  $R_0$ , the disease's initial transmission. Their research revealed that an education campaign regarding the nature of the disease and how it is transmitted, which helps to reduce fear among the community, is the mechanism for reducing fear and transmission in order to minimize  $R_0$ .

In their study, He *et al.* (2020) explored at the SEIR model for COVID-19 and its transmission dynamics. A particle swarm optimization approach was used to estimate parameters in this investigation. Furthermore, medication and quarantine were recognized as effective control techniques in the dynamics of COVID-19. When seasonality and stochastic infections of parameters were put into the model, they observed chaos in the system. Furthermore, their findings indicated that modifying the parameters would cause the model's dynamics to shift and then, revealed that treatment and quarantine were better suited to the SEIR model's dynamics.

Girona (2020) suggested a stochastic model to estimate the period required for confinement, which could prevent a second SARS-COV-2 outbreak in the United States and Spain. The most crowded cities, such as New York (US), San Francisco (US), and Madrid (Spain), are the cities targeted for the aforementioned goal (Spain). They looked at a population that isn't detected but is still a circulating infection in the community in their research. The findings revealed that proper management of suppression techniques was efficient in lowering confinement time. The duration required for house confinement and social isolation before the second wave, according to their model, is 110 days in New York, 80 days in San Francisco, and 70 days in Madrid.

A mathematical model was developed by Kouidere *et al.* (2021) to simulate the negative effects of quarantine on diabetic patients. Diabetics are the people who are most afflicted by COVID-19 disease and die the most as a result of the virus, therefore quarantine has a negative impact on them.

In their study, Meacci (2021) discusses the pandemic fatigue induced by the COVID-19 disease when stress levels grow above a certain level, leading to a person feeling demotivated to protect themselves and others. Because of pandemic fatigue caused on by fear of the disease implications in Italy, psychological effects had a direct impact on the COVID-19 disease transmission.

### **2.3 Related Mathematical Models with stress component**

Nemawejje *et al.* (2011) constructed a mathematical model to study how stress can make tuberculosis treatment more difficult. Many immunological diseases, such as diabetes, cancer, coronary heart disease, chronic TB, and other diseases requiring a strong immune system, are exacerbated by stress. The fight-or-flight response is triggered by stress. Both the sympathetic nervous and endocrine systems are affected. The sympathetic nervous system, which releases catecholamines like adrenaline and nor-adrenaline, stimulates the adrenal medulla. If stress is extended at this period, these chemicals overwhelm the body's immune system, making it more susceptible to infectious diseases.

The mathematical model on the impact of stress and stigma on tuberculosis transmission and how to control the disease to reduce the spread was developed by Lengiteng'i *et al.* (2016). They discussed about how people who go through low and fast progression are stressed. Also they have discussed health education to reduce stress among individuals affected with Tuberculosis. When stigma is high, disease prevalence and incidence are high, but they gradually reduce when both therapy and a health campaign are used together. Recommended that a health education campaign aimed at reducing stress and stigma among infected individuals be complemented with treatment of active TB patients to improve TB disease reduction.

### **2.4 Related Survey Studies**

Poudel (2020) in their research discussed impacts of COVID-19 pandemic in socioeconomic and mental health in Nepal, due to social distancing which reduces interaction among the people so as to reduce new infections. This has affected many areas in daily life activities; physically, mentally, socially and spiritual health of people. Some house owners have been claimed to have evicted nurses, doctors, and other healthcare providers from their rental homes, fearing the spread of the new COVID-19 in their neighborhood. Patients who have been treated are socially rejected and discriminated against when they return home, resulting in a drop in morale. Stigmatization may have a negative influence on individuals seeking medical treatment at a time when they are

most susceptible. People may hide their symptoms and avoid seeking medical attention as a result of stigma and social discrimination, making it more difficult for health care providers and the government to keep the disease under control. This stigmatization can discourage people from seeking healthy behaviors and drastically worsen their suffering, resulting in exhaustion, stress, and other mental health issues.

Furthermore, in Nepal from Singh and Subedi (2020) discussed that, frontline healthcare workers, who are critical in the fight against the crisis because they face stigma and discrimination at work and in their communities. Due to a variety of factors including as social isolation, stigma, and discrimination, frontline healthcare workers are put under a lot of stress during the outbreak by putting them at risk for psychological issues. Their focus and decision-making abilities may be affected as a result of their psychological issues, which could affect not only their mental health but also how they handle the ongoing crisis.

In the study of Di Fronso *et al.* (2020) discussed the relationship among people is very important because it built harmony and social well-being in the society, but during this pandemic in Italy as the most affected country at the beginning of this pandemic disease, isolation was the only way to reduce disease transmission. Most people die because of stress as they are isolated from their beloved ones. In Italy the pandemic shocked not only the society but also the government and led to the stress of the whole country because of anxiety, distressed, worried due to fear of contacting the virus, isolation and quarantine.

The purpose of their study, according to Fitzpatrick *et al.* (2020), was to investigate at the association between COVID-19 fear and social vulnerabilities as well as mental health implications among individuals in the United States. Fear and mental health consequences were found to have strong bivariate relationships with anxiety and depressive symptoms among socially susceptible respondents (female, Asians, Hispanics, foreign-born, families with children).

Emotions like dread and wrath must be considered and studied in order to comprehend the psychological and mental implications of a pandemic. Fear is a natural protective mechanism used by animals to ensure their survival. Preparing the body for a response to potentially dangerous events involves a number of biological mechanisms. It becomes harmful when it becomes chronic or extreme, and it can contribute to the development of psychological problems. In the case of a pandemic, fear raises anxiety and stress in healthy people while increasing symptoms in people

with mental problems (Ornell *et al.*, 2020).

According to Cullen *et al.* (2020), population psychological reactions are essential in determining both disease transmission and the emotional agony occurrence and social disorder during and after an infectious disease outbreak. Despite this, effective treatments for preventing or reducing the negative consequences of pandemics on mental health and well-being are rarely available. While this is appropriate in the early stages of an outbreak, when health services are focused on testing, transmission reduction, and crucial patient care, psychological and behavioral needs should never be overlooked when pandemic control is being implemented.

The international community is concerned about COVID-19 and its long-term consequences. It affects many aspects of life, including the economy, industries, global markets, agriculture, human health, and health care, to name a few. States and international agencies, like as the WHO, are focusing their efforts on controlling and minimizing the pandemic's impact by identifying, testing, and treating infected individuals, as well as developing medications, treatment regimens, and vaccines. Despite these efforts, the pandemic is still spreading. New measures such as self-isolation and quarantine are expected to have an impact on people's regular activities, routines, and livelihoods, potentially leading to a rise in stress, loneliness, anxiety, harmful alcohol, insomnia, and suicidal behavior (Zhou *et al.*, 2020).

According to Henssler *et al.* (2021), developed a random-effects model which was used to express the effect sizes of the studies that were included in their study. Quarantine and isolation both have many consequences but the main consequences are such as; depression, stress-related disorders, and anxiety. All reported secondary outcomes are psychological variables, such as rage. Individuals who were isolated or quarantined had a higher risk of negative mental health outcomes compared to controls, especially after a week or more of confinement. Elevated levels of rage were the most often reported secondary effect. Isolation and quarantine have been shown to have negative mental health effects, including sadness, stress-related disorders, anxiety, and aggression. The most frequent containment strategies used to protect the public by preventing the spread of contagious diseases are quarantine and isolation. Both strategies are primarily concerned with reducing movement and human connection. Quarantine is used for persons who may have been exposed to the disease, whereas isolation is used for people who are contagious and must be removed from those who are not affected.

People who have been exposed to COVID-19 are quarantined and isolated from moving in order to see if they become infected and spread the disease to others. Although the two names are sometimes used interchangeably, especially in public communication, isolation refers to the separation of persons who have been diagnosed with COVID-19 disease from those who have not. As part of the Brooks *et al.* (2020) project, the psychological impact of quarantine is being investigated to discover what consequences it may have on mental health and psychological well-being, as well as what factors may contribute to or alleviate these effects.

In a study conducted in Palestine, Mahamid *et al.* (2021) looked into the relationship between fear of COVID-19 disease and mental health issues. Individuals' psychological distress is worsened by their fear of COVID-19 disease. COVID-19 disease has negative repercussions such as depression, anxiety, and stress, as well as stigmatization and social exclusion of confirmed patients from their families, which increases the risk of developing health problems.

In their study, Serafini *et al.* (2020) discussed that during the COVID-19 epidemic, several psychological effects and major mental health repercussions, such as anxiety, stress, frustration, depression, and uncertainty, gradually arose. The researchers wanted to do a complete review of the studies on the impact of COVID-19 infection on mental health in the general population. The psychological impact of COVID-19 infection quarantine has also been documented, as well as the most relevant psychological reactions in the community in relation to the COVID-19 outbreak.

Saltzman and Hansel (2020) in their study discussed that, social support is a key role in psychological well-being of an individual. Social support is an important consideration for understanding the impacts of psychological problems during COVID-19 pandemic, in which helps in psychological recovery. Many people died because of being isolated from their families, and also loneliness affects many individuals psychologically. Huy *et al.* (2021) conducted a survey in 63 countries with 1871 responses to discuss the stress of quarantine and isolation during the COVID-19 outbreak. Suspected patients were required to be quarantined, which made them feel uncomfortable and increased the psychiatric problems. Both healthcare and non-healthcare professionals were included in the study. They observed that many factors, including female sex, higher education status, being single, and being a non-healthcare professional, can predict stress in COVID-19 pandemic and other different pandemics.

The majority of respondents in Torales *et al.* (2020)'s survey expressed a moderate level of self-

perceived stress as a result of the COVID-19 epidemic. To minimize the psychological impact of the epidemic, they suggested that mental health specialists provide phone-based or web-based assistance to the general public. This strategy may aid Paraguayans in obtaining mental health care, particularly during periods of social isolation.

## **2.5 Conclusion**

Generally, some researchers investigated on stress induced by COVID-19 disease through their studies and discovered that stress impacts much the immune system of the human body. Despite the fact that there are several survey research on stress, there is no COVID-19 mathematical model. The goal of this study was to develop a mathematical model and investigate the effects of stress on the spread of COVID-19 disease. In addition, to look at the transmission dynamics of COVID-19 disease using some control parameters.

## CHAPTER THREE

### MATERIALS AND METHODS

#### 3.1 Introduction

COVID-19 is a pandemic which affected human lives all over the world and still affects socially and economically. A deterministic model with six compartments is presented in this chapter: susceptible population  $S(t)$ , which represents those humans at risk of contacting the disease, exposed population  $E(t)$ , which represents those individuals who are infected but not infectious, quarantined population  $Q(t)$ , which represents those individuals who have been in contact with COVID-19 infected individuals but have not developed any symptoms, and infectious population  $I(t)$ , which represents those individuals with COVID-19 symptoms and capable to spread the disease, hospitalized population  $H(t)$  is made up of infectious people who have been admitted to a healthcare institution (active cases), while the recovered population  $R(t)$  is made up of those who have recovered from COVID-19. The next-generation matrix approach, as defined by Diekmann *et al.* (1990), was used to calculate the basic reproduction number  $R_0$ , which was utilized to determine whether or not the disease was present in the population. The disease will vanish if  $R_0 < 1$ , but if  $R_0 > 1$ , the disease will persist in the population. The Routh–Hurwitz criterion was used to demonstrate local stability in (Patil, 2021). The model stability points of disease-free and endemic equilibrium was examined using the Metzler matrix theory, showing that the disease-free equilibrium is globally asymptotically stable when  $R_0 < 1$  while the endemic equilibrium is globally asymptotically stable when  $R_0 > 1$ . The Lyapunov method and LaSalle (1976) invariance principle are used to investigate the global stability of endemic equilibrium.

#### 3.2 Model Formulation

A mathematical model for COVID-19 was formulated based on realistic assumptions. The human population was divided into six classes which are susceptible  $S(t)$ , exposed  $E(t)$ , quarantined  $Q(t)$ , infectious  $I(t)$ , hospitalized  $H(t)$ , and recovered  $R(t)$ . Currently, the way to detect whether the person is infected by COVID-19 virus or not is by using RT-PCR examination. From the exposed class, the population tested and the three groups obtained (rate of population to be hospitalized, Infectious and quarantined), after testing there are two results which are positive and negative. The population with negative results was taken to quarantine class (rate of quarantined population,  $\theta$ ) for 7 to 14 days to see if they were not developing symptoms. The population

with positive results was divided into two groups which are, proportion of exposed population with contradicting symptoms  $\omega$  who are taken to hospital for further treatment and proportion of exposed population with symptoms  $1 - \omega$  who are taken directly to the infected class for more treatment. Also  $q$  represents progression rate of disease from exposed class to hospitalized and infectious classes. In a susceptible group there is recruitment of infants who are born everyday, represented by  $\mu$  and they add the number population in a susceptible class. Also, those people from outside the country were quarantined directly for the same period of 7 days to 14 days and then tested to see if they are infected or not. This group is represented by  $\phi$  in this *SEQIHR* model. The portion tested positive was considered as infected and they are grouped as infected class  $(1 - \omega)$ . It should be noted that  $0 \leq \theta + (1 - \omega) \leq 1$  under the portion of the quarantined class.

The quarantine class of populations, where the stress factor  $\eta_1$  affects the immune system of the quarantined and infected individual, as well as the  $\alpha$  are the individuals becomes susceptible to the disease after the quarantine time. Because of the fear of being hospitalized due to the disease, the stress factor  $\eta_2$  affects the immune system of the patient to be diagnosed from  $I$  to  $H$ . In the hospitalized and infected group there were deaths caused by the disease among the patients which is represented by  $\delta$ . The parameters  $\lambda$  and  $\nu$  are the recovered rates of the infected population  $I$ , and the recovered rate of the hospitalized class  $H$  respectively. The recovered population can also be susceptible as represented by  $\rho$ . As denoted by  $b$ , natural death is assumed to be common to all compartments of the *SEQIHR* model, and then a recovered individual has a chance to become infected again. Therefore, the recovered population is assumed to move back to the susceptible class. To control the disease the government should control stress among the society and the patients so as to help them in building their body immunity. The study focused mostly on stress factors to control the disease from the infected population and to insist on a health education to reduce stress within the communities among individuals. After introducing a stress parameter, the *SEQIHR* model (3) of COVID-19 disease was introduced.



### 3.2.1 Model Assumptions

Presenting an infectious disease with a mathematical model, the following assumptions for the *SEQIHR* model were taken into account based on the characteristics of COVID-19 disease in this study:

- (i) All members of the population can have an equal chance of getting a COVID-19 disease.
- (ii) Stress in a quarantined class is higher than in an infectious class.
- (iii) Population from outside the country taken directly to quarantine class.
- (iv) All compartments have an equal natural death rate.
- (v) The death due to the disease may be only in two variables (infectious and hospitalized).
- (vi) Recruitment rates (Newborns) are assumed to be susceptible.
- (vii) Individuals are equally likely to be infectious to the infected individuals when coming into contact.
- (viii) Infected individuals are identified early and isolated (hospitalized) immediately for treatment.
- (ix) There are only two options, either a patient recovers or dies, which means no treatment failure.
- (x) The population differs within a given time step where recruitment and leaving rates differ.
- (xi) Recovered individuals are not permanently immune against COVID-19 disease.

### 3.2.2 Model Compartments and Dynamics

From the model Assumption (3.2.1), the variable and parameter descriptions are presented by the following *SEQIHR* model compartmental diagram:

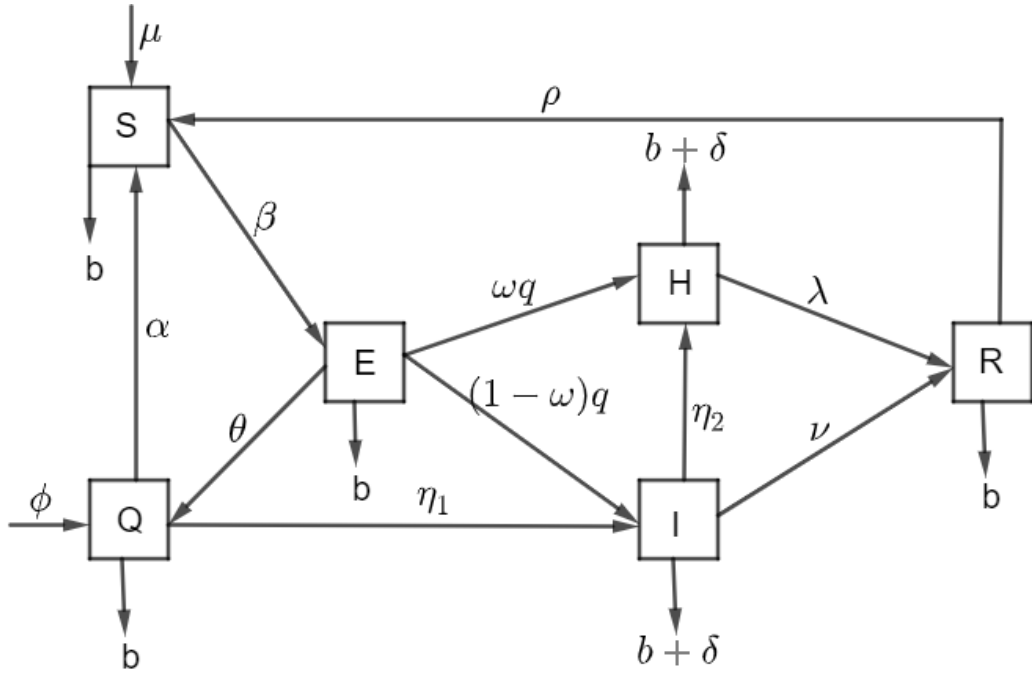


**Figure 3: Schematic flow diagram showing dynamics of COVID-19**

The transmission dynamics of COVID-19 disease in a population are shown in Fig. 4 and Table 1, with the variables and their descriptions:

**Table 1: Description of state model variables**

Variables	Description
$S(t)$	Number of susceptible population at time $t$
$Q(t)$	Number of quarantined population at time $t$
$E(t)$	Number of exposed population at time $t$
$I(t)$	Number of infectious population at time $t$
$H(t)$	Number of hospitalized population at time $t$
$R(t)$	Number of recovered population at time $t$

The total population  $N(t)$  is calculated using Equation (3.1):

$$N(t) = S(t) + Q(t) + E(t) + I(t) + H(t) + R(t), \quad (3.1)$$

where  $t \in [0, t]$  and  $t > 0$ .

**Table 2: Model parameters description**

Parameters	Description
$\beta$	Contact rate (effective transmission rate)
$\mu$	Recruitment rate to the susceptible population
$b$	Human natural death rate
$\phi$	Quarantined population rate from infected countries
$\rho$	Recovered population rate back to susceptible class
$\alpha$	Rate of quarantined population with no infection to susceptible
$\nu$	Recovery rate from infected population
$\lambda$	Recovered rate from hospitalized population
$\omega$	Rate of exposed population with contradicting symptoms
$q$	Progression rate from exposed class to hospitalized and infectious classes
$\theta$	Rate of exposed population with no symptoms
$\eta_1$	Progression rate of stressed population to the infected class from quarantine
$\eta_2$	Progression rate of stressed population to be hospitalized from infected class
$\delta$	Rate of death due to COVID-19 disease in infectious and hospitalized classes

Where,  $\eta_1 > \eta_2$ .

The model parameters found in Equation (3.2) are described in Table 2. By considering the *SEQIHR* model with six compartments in Fig. 4, the following are the transmission phases:

The susceptible class  $S(t)$ , increases by the addition of a recruitment rate,  $\mu$  and decreases when individuals contact the disease,  $\beta$  and move to the exposed compartment together with natural death,  $b$ .

The exposed class,  $E(t)$  increases after the individuals in susceptible class comes into contact with a disease from the infected individual and also decreases by the leaving rates to the infected, hospitalized, quarantined and natural death of individuals.

Individuals with no clear symptoms move from exposed class at the rate  $\theta$  and the individuals from infected countries  $\phi$  to the quarantined class and then decreases by the leaving rates,  $\alpha$ ,  $\eta_1$  and natural death,  $b$ .

The infected class increases due to the population moving from exposed class and quarantined class with the rate of stressed individuals,  $\eta_1$  and decreases with the rates of  $\eta_2$ , recovered rate,  $\nu$ , natural death,  $b$  and death due to the COVID-19 disease,  $\delta$ .

The hospitalized class receive individuals from exposed class and infected class and diminished by the leaving rates, recovered rate  $\lambda$ , death due to disease,  $\delta$  and natural death,  $b$ .

The recovered class receive individuals from infected at the rate  $\nu$  and from hospitalized class at the rate  $\lambda$ , and then diminished by the rates,  $\delta$  and natural death,  $b$ .

### 3.2.3 The *SEQIHR* Model Equations

The assumptions made and the relationship between the variables shown in Fig. 4 were used to create a system of six ordinary differential equations:

$$\begin{aligned}
\frac{dS}{dt} &= \mu + \alpha Q + \rho R - \beta IS - bS, \\
\frac{dE}{dt} &= \beta IS - \theta E - qE - bE, \\
\frac{dQ}{dt} &= \phi + \theta E - \alpha Q - \eta_1 Q - bQ, \\
\frac{dI}{dt} &= (1 - \omega)qE + \eta_1 Q - \eta_2 I - \nu I - \delta I - bI, \\
\frac{dH}{dt} &= \omega qE + \eta_2 I - \lambda H - \delta H - bH, \\
\frac{dR}{dt} &= \lambda H + \nu I - \rho R - bR.
\end{aligned} \tag{3.2}$$

## 3.3 Model Analysis

In this section, positivity, boundedness, derived equilibrium states, basic reproduction number, and stability analysis are discussed.

### 3.3.1 Properties of the Model

When the invariant region is identified, the solution's positiveness is tested, and the model solutions are positive and bounded, the *SEQIHR* model is determined whether it is mathematically meaningful. The *SEQIHR* model has positive and bounded solutions, as shown in Fig. 4.

### 3.3.2 Model Positivity

For the epidemiologically model equations, the compartmental variables must be verified to be non-negative, for all  $t \geq 0$ .

**Theorem 3.1**

Let the initial data set be:  $(S, E, Q, I, H, R)(0) > 0$ . The solution set of the model system (3.2) is positive  $\forall t \geq 0$ .

*Proof.* From the system of model Equation (3.2), consider the first equation:

$$\frac{dS}{dt} = \mu + \alpha Q + \rho R - (\beta I + b)S, \quad (3.3)$$

By considering the negative term, by ignoring the rest, Equation (3.3) is reduced to:

$$\frac{dS}{dt} \geq -(\beta I + b)S.$$

This is the first-order linear differential inequality which can be solved by a separable method  $y' = f(x)g(y)$  (where  $S \geq 0$ ) resulting in:

$$\begin{aligned} \int_{S(0)}^{S(t)} \frac{dS}{S} &\geq - \int_0^t (\beta I + b) dt, \\ \implies S(t) &\geq S(0)e^{-(\beta I + b)t}. \end{aligned}$$

in the absence of COVID-19 disease,

$$S(t) \geq S(0)e^{-bt},$$

where  $S(0) \geq 0, \forall t > 0$ .

Then, from the second  $SEQIHR$  model equation

$$\begin{aligned} \frac{dE}{dt} &= \beta IS - \theta E - qE - bE, \\ \frac{dE}{dt} &\geq -(\theta + q + b)E, \end{aligned}$$

by separable method with the help of Maple software:

$$\int_{E(0)}^{E(t)} \frac{dE}{E} \geq - \int_0^t (\theta + q + b) dt,$$

$$\ln \frac{E(t)}{E(0)} \geq -(\theta + q + b)t,$$

$$\begin{aligned}\frac{E(t)}{E(0)} &\geq e^{-(\beta+q+b)t}, \\ E(t) &\geq E(0)e^{-(\beta+q+b)t}.\end{aligned}$$

Thus,

$$E(0) \geq 0, \forall t > 0.$$

The following findings are derived by applying the same approaches to the remaining equations:

$$\begin{aligned}Q(t) &\geq Q(0)e^{-(\alpha+\eta_1+b)t}, \\ I(t) &\geq I(0)e^{-(\eta_2+\nu+\delta+b)t}, \\ H(t) &\geq H(0)e^{-(\lambda+\delta+b)t}, \\ R(t) &\geq R(0)e^{-(\rho+b)t}.\end{aligned}$$

For any  $t > 0$ , the model (3.2) solutions  $S(t), E(t), Q(t), I(t), H(t), R(t)$  are all positive.  $\square$

### 3.3.3 Invariant (Boundedness) Region

The  $SEQIHR$  model was represented by differential equations in a system (3.2), which was examined in the invariant region  $\Omega$ , with all variables and parameters assumed to be positive  $\forall t \geq 0$ . Theorem 3.2 is used to find the bounded region.

#### Theorem 3.2

*Positively invariant, the set  $\Omega$  attracts all solutions in  $\mathbb{R}_+^6$ .*

*Proof.* Since  $N(t) = S(t) + Q(t) + E(t) + I(t) + H(t) + R(t)$ , then the derivative of  $N(t)$  is given as:

$$\frac{dN}{dt} = \frac{dS}{dt} + \frac{dE}{dt} + \frac{dQ}{dt} + \frac{dI}{dt} + \frac{dH}{dt} + \frac{dR}{dt}, \quad (3.4)$$

Substituting the equations from model (3.2) to Equation (3.4) and then obtain Equation (3.5):

$$\frac{dN}{dt} = \begin{cases} (\mu + \alpha Q + \rho R - \beta IS - bS) + (\beta IS - \theta E - qE - bE) \\ +(\phi + \theta E - \alpha Q - \eta_1 Q - bQ) + ((1 - \omega)qE + \eta_1 Q - \eta_2 I - \nu I - \delta I - bI) \\ +(\omega qE + \eta_2 I - \lambda H - \delta H - bH) + (\lambda H + \nu I - \rho R - bR), \end{cases} \quad (3.5)$$

For further simplification Equation (3.5) leads to Equation (3.6):

$$\frac{dN}{dt} = \mu + \phi - (S + E + Q + I + H + R)b - (\delta I + \delta R), \quad (3.6)$$

For disease-free,  $\delta I \implies 0$  and  $\delta R \implies 0$ ,

$$\frac{dN}{dt} = \mu + \phi - (S + E + Q + I + H + R)b, \quad (3.7)$$

then,

$$\frac{dN}{dt} \leq \mu + \phi - Nb. \quad (3.8)$$

By separable method with the help of Maple software:

$$\int_{N(0)}^{N(t)} \frac{dN}{(\mu + \phi - bN)} \leq \int_0^t dt,$$

$$-\frac{1}{b} \ln\left(\frac{\mu + \phi - bN(0)}{\mu + \phi - bN(t)}\right) \leq t,$$

$$-bN(t) \geq -(\mu + \phi) + (\mu + \phi - bN(0))e^{-bt},$$

$$N(t) \geq \frac{\mu + \phi}{b} - \left(\frac{\mu + \phi - bN(0)}{b}\right)e^{-bt},$$

Then

$$N(t) \geq \frac{\mu + \phi}{b}(1 - e^{-bt}) + N(0)e^{-bt}.$$

At  $t = 0$

$$N(0) \geq 0.$$

At  $t \rightarrow \infty$

$$N(\infty) \leq \frac{\mu + \phi}{b}.$$

As a result, the invariant region is defined in Equation (3.9):

$$\Omega = (S, E, Q, I, H, R) \in \mathbb{R}_+^6 : 0 \leq N(t) \leq \frac{\mu + \phi}{b}. \quad (3.9)$$

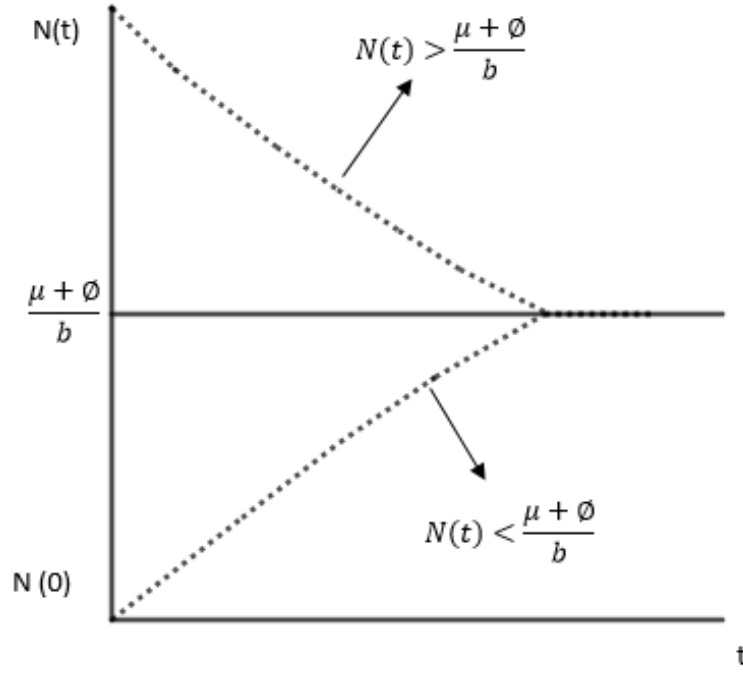


**Figure 4: Boundedness Region**

We can analyze the flow generated by the *SEQIHR* model because it is biologically and epidemiologically meaningful.  $\square$

### 3.3.4 The Existence and Uniqueness of the Solution

The first order ordinary differential equation as given in the Equation (3.10) used to prove the solution to be exist in order to have a unique solution.

$$y' = f(t, y), y(t_0) = y_0. \quad (3.10)$$

Consider the two Theorems (3.3) and (3.4) together with proofs.

#### Theorem 3.3

Uniqueness of Solution for the Proposed Model

*Proof.* Let consider  $D$  as a domain as proposed by Zhang *et al.* (2021) and considered in Equation (3.11).

$$|t - t_0| \leq a, ||y - y_0|| \leq b, y = (y_1, y_2, \dots, y_n), y_0 = (y_{10}, y_{20}, \dots, y_{n0}). \quad (3.11)$$

And suppose  $f(t, y)$  satisfy the Lipschitz condition (3.12) for which the pairs  $(t, y_1) \in D$  and  $(t, y_2) \in D$  where  $k$  represent a positive constant.

$$||f(t, y_2) - f(t, y_1)|| \leq k ||x_2 - x_1||. \quad (3.12)$$



Also, there exist a constant  $\sigma > 0$  where exist a unique continuous vector solution  $y(t)$  of system (3.2) for the interval  $|t - t_0| \leq \sigma$ . Hence, the condition (3.12) is satisfied in Equation (3.13) which shows to be continuous and bounded in domain  $D$ .

$$\frac{\partial f_i}{\partial y_j}, i, j = 1, 2, \dots, n \quad (3.13)$$

**Lemma 3.1**

If  $f(t, y)$  has a continuous partial derivative  $\frac{\partial f_i}{\partial y_j}$  to the bounded and convex domain  $\mathfrak{R}$ , then consider the domain (3.14).

$$1 \leq \epsilon \leq \mathfrak{R}. \quad (3.14)$$

From Equation (3.14), the condition (3.15) is obtained.

$$0 < \mathfrak{R} < \infty \quad (3.15)$$

□

**Theorem 3.4**

Existence Solution of the Proposed Model (3.2)

*Proof.* Let  $D$  denotes the domain which is defined in Equation (3.11), such that Equations (3.12) and (3.13) holds for the existence of model (3.2) which is bounded in domain  $D$ . Let consider Equation the equations:

$$f_1 = \mu + \alpha Q + \delta R - \beta IS - bS, \quad (3.16)$$

$$f_2 = \beta IS - \theta E - qE - bE, \quad (3.17)$$

$$f_3 = \phi + \theta E - (\alpha + \eta_1 + b)Q, \quad (3.18)$$

$$f_4 = (1 - \omega)qE + \eta_1 Q - (\eta_2 + \nu + \delta + b)I, \quad (3.19)$$

$$f_5 = \omega qE + \eta_2 I - (\lambda + \delta + b)H, \quad (3.20)$$

$$f_6 = \lambda H + \nu I - (\rho + b)R. \quad (3.21)$$

Let us prove that  $\frac{\partial f_i}{\partial y_j}$ ,  $j = 1, 2, 3, 4, 5, 6$  are continuous and bounded. Consider the following

partial derivatives for the equations of model (3.2).

$$\begin{aligned}
\frac{\partial f_1}{\partial S} &= -\beta I - b, & \left| \frac{\partial f_1}{\partial S} \right| &= |-\beta I - b| < \infty, \\
\frac{\partial f_1}{\partial E} &= 0, & \left| \frac{\partial f_1}{\partial E} \right| &= |0| < \infty, \\
\frac{\partial f_1}{\partial Q} &= \alpha, & \left| \frac{\partial f_1}{\partial Q} \right| &= |\alpha| < \infty, \\
\frac{\partial f_1}{\partial I} &= -\beta S, & \left| \frac{\partial f_1}{\partial I} \right| &= |-\beta S| < \infty, \\
\frac{\partial f_1}{\partial H} &= 0, & \left| \frac{\partial f_1}{\partial H} \right| &= |0| < \infty, \\
\frac{\partial f_1}{\partial R} &= \rho, & \left| \frac{\partial f_1}{\partial R} \right| &= |\rho| < \infty.
\end{aligned} \tag{3.22}$$

Similarly from the second equation of Equation (3.2) we obtain the following systems of equations:

$$\begin{aligned}
\frac{\partial f_2}{\partial S} &= \beta I, & \left| \frac{\partial f_2}{\partial S} \right| &= |\beta I| < \infty, \\
\frac{\partial f_2}{\partial E} &= -(\theta + q + b), & \left| \frac{\partial f_2}{\partial E} \right| &= |-(\theta + q + b)| < \infty, \\
\frac{\partial f_2}{\partial Q} &= 0, & \left| \frac{\partial f_2}{\partial Q} \right| &= |0| < \infty, \\
\frac{\partial f_2}{\partial I} &= \beta S, & \left| \frac{\partial f_2}{\partial I} \right| &= |\beta S| < \infty, \\
\frac{\partial f_2}{\partial H} &= 0, & \left| \frac{\partial f_2}{\partial H} \right| &= |0| < \infty, \\
\frac{\partial f_2}{\partial R} &= 0, & \left| \frac{\partial f_2}{\partial R} \right| &= |0| < \infty.
\end{aligned} \tag{3.23}$$

Also from the third equation of Equation (3.2) we obtain:

$$\begin{aligned}
\frac{\partial f_3}{\partial S} &= 0, & \left| \frac{\partial f_3}{\partial S} \right| &= |0| < \infty, \\
\frac{\partial f_3}{\partial E} &= \theta, & \left| \frac{\partial f_3}{\partial E} \right| &= |\theta| < \infty, \\
\frac{\partial f_3}{\partial Q} &= -(\alpha + \eta_1 = b), & \left| \frac{\partial f_3}{\partial Q} \right| &= |-(\alpha + \eta_1 = b)| < \infty, \\
\frac{\partial f_3}{\partial I} &= 0, & \left| \frac{\partial f_3}{\partial I} \right| &= |0| < \infty, \\
\frac{\partial f_3}{\partial H} &= 0, & \left| \frac{\partial f_3}{\partial H} \right| &= |0| < \infty, \\
\frac{\partial f_3}{\partial R} &= 0, & \left| \frac{\partial f_3}{\partial R} \right| &= |0| < \infty.
\end{aligned} \tag{3.24}$$

Not only that but also from the fourth equation of Equation (3.2) we obtain the following:

$$\begin{aligned}
\frac{\partial f_4}{\partial S} &= 0, & \left| \frac{\partial f_4}{\partial S} \right| &= |0| < \infty, \\
\frac{\partial f_4}{\partial E} &= (1 - \omega)q, & \left| \frac{\partial f_4}{\partial E} \right| &= |(1 - \omega)q| < \infty, \\
\frac{\partial f_4}{\partial Q} &= \eta_1, & \left| \frac{\partial f_4}{\partial Q} \right| &= |\eta_1| < \infty, \\
\frac{\partial f_4}{\partial I} &= -(\eta_2 + \nu + \delta + b), & \left| \frac{\partial f_4}{\partial I} \right| &= |-(\eta_2 + \nu + \delta + b)| < \infty, \\
\frac{\partial f_4}{\partial H} &= 0, & \left| \frac{\partial f_4}{\partial H} \right| &= |0| < \infty, \\
\frac{\partial f_4}{\partial R} &= 0, & \left| \frac{\partial f_4}{\partial R} \right| &= |0| < \infty.
\end{aligned} \tag{3.25}$$

Then for the fifth equation of Equation (3.2) we obtain:

$$\begin{aligned}
\frac{\partial f_5}{\partial S} &= 0, & \left| \frac{\partial f_5}{\partial S} \right| &= |0| < \infty, \\
\frac{\partial f_5}{\partial E} &= \omega q, & \left| \frac{\partial f_5}{\partial E} \right| &= |\omega q| < \infty, \\
\frac{\partial f_5}{\partial Q} &= 0, & \left| \frac{\partial f_5}{\partial Q} \right| &= |0| < \infty, \\
\frac{\partial f_5}{\partial I} &= \eta_2, & \left| \frac{\partial f_5}{\partial I} \right| &= |\eta_2| < \infty, \\
\frac{\partial f_5}{\partial H} &= -(\lambda + \delta + b), & \left| \frac{\partial f_5}{\partial H} \right| &= |-(\lambda + \delta + b)| < \infty, \\
\frac{\partial f_5}{\partial R} &= 0, & \left| \frac{\partial f_5}{\partial R} \right| &= |0| < \infty.
\end{aligned} \tag{3.26}$$

From the sixth equation of Equation (3.2) we obtain the following systems of equations:

$$\begin{aligned}
\frac{\partial f_6}{\partial S} &= 0, & \left| \frac{\partial f_6}{\partial S} \right| &= |0| < \infty, \\
\frac{\partial f_6}{\partial E} &= 0, & \left| \frac{\partial f_6}{\partial E} \right| &= |0| < \infty, \\
\frac{\partial f_6}{\partial Q} &= 0, & \left| \frac{\partial f_6}{\partial Q} \right| &= |0| < \infty, \\
\frac{\partial f_6}{\partial I} &= \nu, & \left| \frac{\partial f_6}{\partial I} \right| &= |\nu| < \infty, \\
\frac{\partial f_6}{\partial H} &= \lambda, & \left| \frac{\partial f_6}{\partial H} \right| &= |\lambda| < \infty, \\
\frac{\partial f_6}{\partial R} &= -(\rho + b), & \left| \frac{\partial f_6}{\partial R} \right| &= |-(\rho + b)| < \infty.
\end{aligned} \tag{3.27}$$

All partial derivatives are continuous and bounded, hence there exists a unique solution of the model in Equation (3.2). □

### 3.3.5 The Existence of Disease-Free Equilibrium Point ( $E_0$ )

When the infected components are zero, the  $E_0$  obtained by setting the right-hand side of the equation equal to zero, as in Equation (3.28).

$$\frac{dS}{dt} = \frac{dE}{dt} = \frac{dQ}{dt} = \frac{dI}{dt} = \frac{dH}{dt} = \frac{dR}{dt} = 0. \quad (3.28)$$

When there is no disease, then:

$$E = 0, \quad Q = 0, \quad I = 0, \quad H = 0, \quad R = 0.$$

By considering model (3.2) equations:

$$\mu + \alpha Q + \rho R - \beta IS - bS = 0, \quad (3.29)$$

gives;

$$\mu - bS = 0,$$

then,

$$S = \frac{\mu}{b}.$$

In addition to the second model (3.2) equation:

$$\beta IS = (\theta + q + b) E = 0, \quad (3.30)$$

gives,

$$E = \frac{\beta IS}{\theta + q + b},$$

but  $\beta = 0$ , then,

$$E = 0. \quad (3.31)$$

Similarly from the third model equation

$$\phi + \theta E - \alpha Q - \eta_1 Q - bQ = 0, \quad (3.32)$$

gives,

$$Q = \frac{\phi + \theta E}{\alpha + \eta_1 + b},$$

but  $E = 0$  then,

$$Q = \frac{\phi}{\alpha + \eta_1 + b}. \quad (3.33)$$

From the fourth equation of the model

$$(1 - \omega)qE + \eta_1 Q - \eta_2 I - \nu I - \delta I - bI = 0, \quad (3.34)$$

gives,

$$I = \frac{(1 - \omega)qE + \eta_1 Q}{\eta_2 + \nu + \delta + b},$$

but  $E = 0$  and  $Q = 0$  then,

$$I = 0. \quad (3.35)$$

Similarly from the fifth model equation:

$$\omega qE + \eta_2 I - \lambda H - \delta H - bH = 0, \quad (3.36)$$

gives,

$$H = \frac{\omega qE + \eta_2 I}{\lambda + \delta + b},$$

but  $E = 0$  and  $I = 0$  therefore,

$$H = 0. \quad (3.37)$$

Then, from the sixth model equation:

$$\lambda H + \nu I - \rho R - bR = 0, \quad (3.38)$$

gives,

$$R = \frac{\lambda H + \nu I}{\rho + b},$$

but  $H = 0$  and  $I = 0$  thus,

$$R = 0. \quad (3.39)$$

Therefore,

$$E_0 = (S^0, E^0, Q^0, I^0, H^0, R^0) = \left(\frac{\mu}{b}, 0, \frac{\phi}{\alpha + \eta_1 + b}, 0, 0, 0\right)^T. \quad (3.40)$$

The state where there is no infection is the disease-free equilibrium point  $E_0$ , which is given in Equation (3.40).

### 3.3.6 The Basic Reproduction Number ( $R_0$ )

The midpoint number of infections caused by an infectious individual for the entire time of infectiousness is the basic reproduction number  $R_0$  (Dieckmann & Heesterbeek, 2000). The basic

reproduction number is a non-dimensional variable used in epidemiology studies to determine the threshold for both predicting outbreaks and evaluating control strategies. Furthermore,  $R_0$  examines the equilibrium stability  $R_0 < 1$ , which indicates that infectious individuals produce fewer secondary infections and eventually die off. When  $R_0 > 1$ , each infectious individual transmits the disease to the rest of the population by infecting several secondary infections. In the *SEQUIHR* model,  $R_0$  is computed using the next-generation matrix method as presented by Van den Driessche (2002) and the dominant eigenvalues (Spectral radius) are then obtained. Let the rate of new infection in compartment  $i$  be  $F_i(x)$ , and the rate of individuals being transferred into compartment  $i$  be  $V_i$  as it is essential to find the disease-free equilibrium point  $E_0$ . Thus, the computed matrices  $F$  and  $V$  which are  $n \times n$  matrices, where  $n$  represents the infected classes, defined by Equations (4.1) and (3.42).

$$F = \left( \frac{\partial F_i}{\partial x_j} (E_0) \right), \quad (3.41)$$

and

$$V = \left( \frac{\partial V_i}{\partial x_j} (E_0) \right), \quad (3.42)$$

where  $1 \leq i, j \leq n$ ,  $F$  are non-negative, and  $V$  is a non-singular  $n$ -matrix (the matrix with inverse belongs to the class of positive matrices). Since  $F$  is non-negative and  $V$  is a non-singular matrix, then  $V^{-1}$  and  $FV^{-1}$  are non-negative. As a result, the next-generation matrix  $FV^{-1}$  is computed according to Diekmann *et al.* (1990).

**Note that:** the basic reproduction number is defined as the spectral radius (dominant eigenvalue) of the matrix  $FV^{-1}$  as in Castillo-Chavez *et al.* (2002), and the following equations represents the spectral radius ( $R_0$ ) and the next-generation matrix  $FV^{-1}$  respectively:

$$R_0 = \rho(FV^{-1}), \quad (3.43)$$

and

$$FV^{-1} = \left[ \frac{\partial F_i}{\partial x_j} (E_0) \right] \left[ \frac{\partial V_i}{\partial x_j} (E_0) \right]^{-1}. \quad (3.44)$$

Where,  $F$  is the rate of new infection in compartment  $I$ . The new forces of infection are:

$$\begin{aligned}
\frac{dE}{dt} &= \beta IS - (\theta + q + b)E, \\
\frac{dQ}{dt} &= \phi + \theta E - (\alpha + \eta_1 + b)Q, \\
\frac{dI}{dt} &= (1 - \omega)qE + \eta_1 Q - (\eta_2 + \nu + \delta + b)I, \\
\frac{dH}{dt} &= \omega qE + \eta_2 I - (\lambda + \delta + b)H.
\end{aligned} \tag{3.45}$$

Equation (3.46) is obtained when  $I$  and  $S$  meet in Equation (3.45).

$$F_i = \begin{pmatrix} f_1 \\ f_2 \\ f_3 \\ f_4 \end{pmatrix} = \begin{pmatrix} \beta IS \\ 0 \\ 0 \\ 0 \end{pmatrix}. \tag{3.46}$$

Jacobian partial derivatives of  $E_0$  is presented in Equation (3.47).

$$F_J = \begin{pmatrix} \frac{\partial F_1}{\partial E}(E_0) & \frac{\partial F_1}{\partial Q}(E_0) & \frac{\partial F_1}{\partial I}(E_0) & \frac{\partial F_1}{\partial H}(E_0) \\ \frac{\partial F_2}{\partial E}(E_0) & \frac{\partial F_2}{\partial Q}(E_0) & \frac{\partial F_2}{\partial I}(E_0) & \frac{\partial F_2}{\partial H}(E_0) \\ \frac{\partial F_3}{\partial E}(E_0) & \frac{\partial F_3}{\partial Q}(E_0) & \frac{\partial F_3}{\partial I}(E_0) & \frac{\partial F_3}{\partial H}(E_0) \\ \frac{\partial F_4}{\partial E}(E_0) & \frac{\partial F_4}{\partial Q}(E_0) & \frac{\partial F_4}{\partial I}(E_0) & \frac{\partial F_4}{\partial H}(E_0) \end{pmatrix}. \tag{3.47}$$

From Equation (3.46), the Jacobian matrix of  $E_0$  is given by Equation (3.48).

$$F_j = \begin{pmatrix} 0 & 0 & \beta S & 0 \\ 0 & 0 & 0 & 0 \\ 0 & 0 & 0 & 0 \\ 0 & 0 & 0 & 0 \end{pmatrix}. \tag{3.48}$$



Also, consider the Jacobian matrix  $V_i$  as presented in Equation (3.49).

$$V_i = \begin{pmatrix} \theta E + qE + bE \\ -\phi - \theta E + \alpha Q + \eta_1 Q + bQ \\ (\omega - 1)qE - \eta_1 Q + \eta_2 I + \nu I + \delta I + bI \\ -\omega qE - \eta_2 I + \lambda H + \delta H + bH \end{pmatrix}. \quad (3.49)$$

The partial derivatives with respect to transmitting compartments  $E$ ,  $Q$ ,  $I$  and  $H$  evaluated at  $E_0$  as presented in Equation (3.50).

$$V = \begin{pmatrix} \frac{\partial V_1}{\partial E}(E_0) & \frac{\partial V_1}{\partial Q}(E_0) & \frac{\partial V_1}{\partial I}(E_0) & \frac{\partial V_1}{\partial H}(E_0) \\ \frac{\partial V_2}{\partial E}(E_0) & \frac{\partial V_2}{\partial Q}(E_0) & \frac{\partial V_2}{\partial I}(E_0) & \frac{\partial V_2}{\partial H}(E_0) \\ \frac{\partial V_3}{\partial E}(E_0) & \frac{\partial V_3}{\partial Q}(E_0) & \frac{\partial V_3}{\partial I}(E_0) & \frac{\partial V_3}{\partial H}(E_0) \\ \frac{\partial V_4}{\partial E}(E_0) & \frac{\partial V_4}{\partial Q}(E_0) & \frac{\partial V_4}{\partial I}(E_0) & \frac{\partial V_4}{\partial H}(E_0) \end{pmatrix}. \quad (3.50)$$

The Jacobian matrix  $V$  for the new infestation terms and the remaining transfer terms with  $4 \times 4$  dimension is given in Equation (3.51).

$$V = \begin{pmatrix} b + \theta + q & 0 & 0 & 0 \\ -\theta & \alpha + b + \eta_1 & 0 & 0 \\ (\omega - 1)q & -\eta_1 & b + \delta + \eta_2 + \nu & 0 \\ -\omega & 0 & -\eta_2 & b + \delta + \lambda \end{pmatrix}. \quad (3.51)$$

Let the values of  $A_1$  and  $A_2$  be presented by Equation (3.52) and (3.53) respectively.

$$A_1 = b + \alpha + \eta_1, \quad (3.52)$$

$$A_2 = b + \delta + \eta_2 + \nu. \quad (3.53)$$

The inverse of the Jacobian matrix  $V$  from Equation (3.51) is given by the Equation (3.54).

$$V^{-1} = \begin{pmatrix} \frac{1}{b+\theta+q} & 0 & 0 & 0 \\ \frac{\theta}{A_1(b+\theta+q)} & \frac{1}{A_1} & 0 & 0 \\ \frac{-\alpha\omega+\alpha+b(-\omega)+b+\eta_1\theta-\eta_1\omega+\eta_1}{A_1A_2(b+\theta+q)} & \frac{\eta_1}{A_1A_2} & \frac{1}{A_2} & 0 \\ \frac{A_1A_2\omega+\eta_2(-\alpha\omega+\alpha+b(-\omega)+b+\eta_1\theta-\eta_1\omega+\eta_1)}{A_1A_2(b+\delta+\lambda)(b+\theta+q)} & \frac{\eta_1\eta_2}{A_1A_2(b+\delta+\lambda)} & \frac{\eta_2}{A_2(b+\delta+\lambda)} & \frac{1}{b+\delta+\lambda} \end{pmatrix}. \quad (3.54)$$

The product of two Jacobian matrices  $FV^{-1}$  from Equation (3.48) and Equation (3.54) after computation of the two equations, Equation (3.55) was obtained:

$$FV^{-1} = \begin{pmatrix} \frac{\beta\mu(\eta_1\theta-q(\omega-1)(\alpha+b+\eta_1))}{b(\alpha+b+\eta_1)(b+\theta+q)(b+\delta+\eta_2+\nu)} & \frac{\beta\eta_1\mu}{b(\alpha+b+\eta_1)(b+\delta+\eta_2+\nu)} & \frac{\beta\mu}{b(b+\delta+\eta_2+\nu)} & 0 \\ 0 & 0 & 0 & 0 \\ 0 & 0 & 0 & 0 \\ 0 & 0 & 0 & 0 \end{pmatrix}. \quad (3.55)$$

From Equation (3.55) by using maple software four eigenvalues of the next-generation matrix ( $FV^{-1}$ ) are obtained and presented in Equation (3.56).

$$\text{Eigenvalues} = \left\{ 0, 0, 0, \frac{\beta\mu(-bq\omega + bq + \eta_1\theta - \alpha q\omega + \alpha q - \eta_1 q\omega + \eta_1 q)}{b(\alpha + b + \eta_1)(b + \theta + q)(b + \delta + \eta_2 + \nu)} \right\}. \quad (3.56)$$

From Equation (3.56) the four eigenvalues were obtained as presented herewith:

$$\lambda_1 = 0,$$

$$\lambda_2 = 0,$$

$$\lambda_3 = 0,$$

$$\lambda_4 = \frac{\beta\mu(\eta_1(\theta + q(-\omega) + q) - q(\omega - 1)(\alpha + b))}{b(\alpha + b + \eta_1)(b + \theta + q)(b + \delta + \eta_2 + \nu)},$$

whereby  $\lambda_4$  is the most dominant eigenvalue and  $R_0$  is given by the spectral radius (the most dominant eigenvalue) thus, the basic reproduction number,  $R_0$  is given in Equation (3.57).

$$R_0 = \frac{\beta\mu(\eta_1(\theta - \omega q + q) + q(1 - \omega)(\alpha + b))}{b(\alpha + b + \eta_1)(b + \theta + q)(b + \delta + \eta_2 + \nu)}. \quad (3.57)$$

The results shows that the basic reproductive number  $R_0$  depends on contact rate between susceptible class and exposed class  $\beta$ , recruitment rate  $\mu$ , stress factor of the people quarantined to

infected class  $\eta_1$ , exposed population to be quarantined  $\theta$ , population to be hospitalized between exposed class and hospitalized class  $\omega$  and  $q$ , population rate from quarantine class to susceptible class  $\alpha$ , rate of population from infected class to hospitalized class  $\eta_2$ , rate of population recovered from infected class  $\nu$ , death due to the disease from hospital and infected class  $\delta$  and natural death  $b$  from all classes. Therefore,  $\beta$ ,  $\mu$ ,  $\eta_1$  and  $\theta$  when they are increased also, increase basic reproduction number  $R_0$ . Other parameters are inversely proportional to  $R_0$ .

### 3.4 Stability Analysis

The stability conditions for the disease-free equilibrium point,  $E_0$  and endemic equilibrium point,  $E_*$  for the model system (3.2) were determined in this section. The global stability of  $E_*$  was determined using the eigenvalues criterion for stability, Metzler matrix stability theory for global stability of  $E_0$ , and Lyapunov function for the stability approach.

#### 3.4.1 Local Stability of the Disease-Free Equilibrium ( $E_0$ )

The eigenvalues, which are derived by finding the partial derivatives of the vector-valued function, which are used to determine the local stability of the  $E_0$ . The equilibrium point is asymptotically stable if the Jacobian matrix assessed at that point has negative eigenvalues. The Routh–Hurwitz criterion was employed in local stability demonstration as presented by Patil (2021) and Barbastefano *et al.* (2020).

#### Theorem 3.5

*For the system (3.2), the disease-free equilibrium point  $E_0$  is locally asymptotically stable if  $R_0 < 1$ , and unstable when  $R_0 > 1$ .*

*Proof.* The linearization of model system (3.2) was done by Jacobian matrix computation to prove the Theorem (3.5). For state variables  $S, E, Q, I, H, R$ , which are used to produce the Jacobian

matrix  $J_{E_0}$  as in Equation (3.58), at  $E_0$  each equation has zero partial derivative.

$$J_{E_0} = \begin{pmatrix} -b & 0 & \alpha & -\beta S & 0 & \rho \\ 0 & -b - \theta - q & 0 & \beta S & 0 & 0 \\ 0 & \theta & -\alpha - b - \eta_1 & 0 & 0 & 0 \\ 0 & q(1 - \omega) & \eta_1 & -b - \delta - \eta_2 - \nu & 0 & 0 \\ 0 & \omega q & 0 & \eta_2 & -b - \delta - \lambda & 0 \\ 0 & 0 & 0 & \nu & \lambda & -b - \rho \end{pmatrix}. \quad (3.58)$$

At a disease-free equilibrium point,  $E_0$

$$S = \frac{\mu}{b}, \quad \text{and} \quad I = 0.$$

The  $E_0$  is asymptotically stable if the eigenvalues of  $J_{E_0} < 0$ . then:

$$\begin{vmatrix} -b & 0 & \alpha & -\frac{\beta\mu}{b} & 0 & \rho \\ 0 & -b - \theta - q & 0 & \frac{\beta\mu}{b} & 0 & 0 \\ 0 & \theta & -\alpha - b - \eta_1 & 0 & 0 & 0 \\ 0 & q(1 - \omega) & \eta_1 & -b - \delta - \eta_2 - \nu & 0 & 0 \\ 0 & \omega q & 0 & \eta_2 & -b - \delta - \lambda & 0 \\ 0 & 0 & 0 & \nu & \lambda & -b - \rho \end{vmatrix} = 0. \quad (3.59)$$

From matrix (3.59), it is clear that the first, second, and third eigenvalues are:

$$\lambda_1 = -b,$$

$$\lambda_2 = -b - \rho,$$

$$\lambda_3 = -b - \delta - \lambda.$$

After canceling the relevant rows and columns that are needed to derive the first, second, and third

eigenvalues, matrix (3.59) is reduced to a  $3 \times 3$  matrix as shown in Equation (3.60):

$$J_{E_0} = \begin{pmatrix} -b - \theta - q & 0 & \frac{\beta\mu}{b} \\ \theta & -\alpha - b - \eta_1 & 0 \\ q(1 - \omega) & \eta_1 & -b - \delta - \eta_2 - \nu \end{pmatrix}. \quad (3.60)$$

The characteristic polynomial of matrix (3.60) is given in the form of Equation (3.61).

$$Z(\lambda) = \lambda^3 + a_1\lambda^2 + a_2\lambda + a_3, \quad (3.61)$$

where

$$\begin{aligned} a_1 &= \alpha + 3b + \delta + \eta_1 + \eta_2 + \theta + \nu + q. \\ a_2 &= \begin{cases} \alpha\delta + \alpha\eta_2 + \alpha\theta + \alpha\nu + 3b^2 + 2\alpha b + 2b\delta + 2b\eta_1 + 2b\eta_2 + 2b\theta + 2b\nu - \frac{\beta\mu q}{b} \\ + 2bq + \delta\eta_1 + \delta\theta + \eta_1\theta + \eta_2\theta + \eta_1\nu + \eta_1\eta_2 + \theta\nu + \alpha q + \delta q + \eta_1 q + \eta_2 q + \nu q. \end{cases} \\ a_3 &= \begin{cases} \alpha\delta\theta + \alpha\eta_2\theta + \alpha\theta\nu + b^3 + \alpha b^2 + b^2\delta + b^2\eta_1 + b^2\eta_2 + b^2\theta + b^2\nu + b^2q + \alpha b\delta \\ + \alpha b\eta_2 + \alpha b\theta + \alpha b\nu - \frac{\beta\eta_1\theta\mu}{b} + b\delta\eta_1 + b\delta\theta + b\eta_1\theta + b\eta_2\theta + b\eta_1\nu + b\eta_1\eta_2 \\ + b\theta\nu + \frac{\alpha\beta\mu q\omega}{b} - \frac{\alpha\beta\mu q}{b} + \alpha b q + \frac{\beta\eta_1\mu q\omega}{b} - \frac{\beta\eta_1\mu q}{b} + b\delta q + b\eta_1 q + b\eta_2 q + b\nu q + \delta\eta_1\theta \\ + \eta_1\theta\nu + \eta_1\eta_2\theta + \alpha\delta q + \alpha\eta_2 q + \alpha\nu q + \beta\mu q\omega - \beta\mu q + \delta\eta_1 q + \eta_1\nu q + \eta_1\eta_2 q. \end{cases} \end{aligned}$$

However,  $a_1 > 0$ ,  $a_2 > 0$ , and  $a_3 > 0$  for the condition presented in Equation (3.62)

$$a_1 a_2 - a_3 > 0. \quad (3.62)$$

$$a_1 a_2 - a_3 = \left\{ \frac{-\beta\mu q\omega(\alpha+b) + M_1(M_2 - \beta\mu q) + M_3 + \eta_2(M_4 + M_5 - \beta\mu q) + \eta_1(M_6 + M_7 + \beta\mu(\theta - q\omega))}{b} \right\}. \quad (3.63)$$

$$\frac{M_1 M_2 + M_3 + \eta_2(M_4 + M_5) + \eta_1(\beta\theta\mu + M_6 + M_7)}{b} > \frac{\beta\mu q\omega(\alpha+b) + \beta\mu\eta_2 q + \beta\mu M_1 q + \mu q\omega\beta}{b},$$

where,

$$M_1 = 2b + \delta + \theta + \nu + q,$$

$$\begin{aligned}
M_2 &= 4b^3 + 2b^2(2\alpha + \delta + \theta + \nu + q) + b(\alpha + \delta + \nu)(\alpha + \theta + q), \\
M_3 &= b\eta_1^2(2b + \delta + \eta_2 + \theta + \nu + q), \\
M_4 &= 8b^3 + b(\alpha + \theta + q)(\alpha + 2\delta + \theta + 2\nu + q), \\
M_5 &= b^2(6\alpha + 4\delta + 6\theta + 4\nu + 6q) + b\eta_2(\alpha + 2b + \theta + q), \\
M_6 &= 8b^3 + b^2(4\alpha + 6(\delta + \theta + \nu) + 6q) + b(\delta + \theta + \nu + q)(2\alpha + \delta + \theta + \nu + q), \\
M_7 &= b\eta_2(2(\alpha + 3b + \delta + \theta + \nu + q) + \eta_2).
\end{aligned}$$

Hence the condition  $a_1a_2 - a_3 > 0$  is satisfied.

The Routh–Hurwitz criterion states that all elements of a system’s characteristic polynomial must be negative in order for the system to be stable (Agmour *et al.*, 2018). The disease is asymptotically stable because the Routh-Hurwitz requirements are satisfied for the condition  $a_1a_2 - a_3 > 0$ .  $\square$

### 3.4.2 Existence of Endemic Equilibrium Point

Endemic equilibrium points are the steady-state solutions whereby the disease persists in the population (Chitnis *et al.*, 2008). It refers to the solution at which the disease persists in the population. The stability analysis of the endemic equilibrium point describes the long-term dynamics of COVID-19 in the population (Collins, 2016). By solving all systems of differential equations from the model Equation (3.2), all derivatives are equal to zero (solve for all variables simultaneously).

#### Theorem 3.6

*The endemic equilibrium point of model Equation (3.2) is locally asymptotically stable in the region  $\Omega$  if  $R_0 < 1$  and unstable if  $R_0 > 1$ .*

*Proof.* At the endemic equilibrium point  $S = S^*$ ,  $E = E^*$ ,  $Q = Q^*$ ,  $I = I^*$ ,  $H = H^*$  and  $R = R^*$ . The variables for the  $SEQIHR$  model are given by the equations from Equation (3.64) to (3.68).

$$S^* = \frac{\mu + \alpha Q + \rho R}{b + \beta I}, \quad (3.64)$$

$$E^* = \frac{\beta IS}{b + \theta + q}, \quad (3.65)$$

$$Q^* = \frac{\phi + \theta E}{b + \alpha + \eta_1}, \quad (3.66)$$

$$H^* = \frac{E\omega q + \eta_2 I}{b + \delta + \lambda}, \quad (3.67)$$

$$R^* = \frac{H\lambda + \nu I}{b + \rho}, \quad (3.68)$$

By substituting the values of  $A_1$  and  $A_2$  from the Equations (3.52) and (3.53), the value of  $I^*$  is given by Equation (3.69).

$$I^* = \frac{\mu (\phi\eta_1 + A_1 A_2 (R_0 - 1)) + R_0 (\alpha Q^* + \rho R^*) A_1 A_2}{\beta\mu (A_1 A_2 - \phi\eta_1)}. \quad (3.69)$$

We have shown that  $S = S^*, E = E^*, Q = Q^*, I = I^*, H = H^*$  and  $R = R^*$  are all positives. Therefore,  $\tau^* = (S = S^*, E = E^*, Q = Q^*, I = I^*, H = H^*, R = R^*) > 0$ .  $\square$

### 3.4.3 The Global Stability of Disease-Free Equilibrium Point ( $E_0$ )

The  $SEQIHR$  model's global stability around the  $E_0$  was demonstrated. If  $R_0 < 1$ , the  $E_0$  stability result in epidemiological implications, that is minimizing COVID-19 infection cases did not result in an infection. The  $E_0$  must be proven to be globally asymptotically stable to ensure that the disease is independent of the initial size of the model's sub-population as presented by Link and Phelan (2001) and Castillo-Chavez *et al.* (2002) in their studies as considered in Theorem 3.7.

#### Theorem 3.7

*If  $R_0 < 1$ , the disease-free equilibrium point  $E_0$  for the model system (3.2) is globally asymptotically stable, while if  $R_0 > 1$  is unstable.*

*Proof.* Consider the Lyapunov function  $L$  chosen with non-negative coefficients  $A_1, A_2, A_3$  and  $A_4$  for the initial equilibrium point  $E_0$  as given by Equation (3.70).

$$L = \left( S - S^0 - S^0 \ln \frac{S}{S^0} \right) + A_1 E + \left( Q - Q^0 - Q^0 \ln \frac{Q}{Q^0} \right) + A_2 I + A_3 H + A_4 R \quad (3.70)$$

The derivatives of Equation (3.70) with respect to time is given in Equation (3.71)

$$\frac{dL}{dt} = \left( 1 - \frac{S^0}{S} \right) \frac{dS}{dt} + A_1 \frac{dE}{dt} + \left( 1 - \frac{Q^0}{Q} \right) \frac{dQ}{dt} + A_2 \frac{dI}{dt} + A_3 \frac{dH}{dt} + A_4 \frac{dR}{dt} \quad (3.71)$$

From system (3.2), the values of  $\frac{dS}{dt}, \frac{dE}{dt}, \frac{dQ}{dt}, \frac{dI}{dt}, \frac{dH}{dt}$  and  $\frac{dR}{dt}$  are substituted in Equation (3.71) so as to obtain Equation (3.72).

$$\begin{aligned}
\frac{dL}{dt} = & \left(1 - \frac{S^0}{S}\right) (\mu + \alpha Q + \rho R - (\beta I + b) S) + A_1 (\beta I S - (\theta + q + b) E) \\
& + \left(1 - \frac{Q^0}{Q}\right) (\phi + \theta E - (\alpha + \eta_1 + b) Q) + A_2 ((1 - \omega)qE + \eta_1 Q - (\eta_2 + \nu + \delta + b) I) \\
& + A_3 (\omega q E + \eta_2 I - (\lambda + \delta + b) H) + A_4 (\lambda H + \nu I - (\rho + b) R) \quad (3.72)
\end{aligned}$$

Suppose  $S \leq S^0$ ,  $Q \leq Q^0$  then by substituting to the Equation (3.72) the following results in Equation (3.73) were obtained.

$$\begin{aligned}
\frac{dL}{dt} \leq & A_1 (\beta I S - (\theta + q + b) E) + A_2 ((1 - \omega)qE + \eta_1 Q - (\eta_2 + \nu + \delta + b) I) \\
& + A_3 (\omega q E + \eta_2 I - (\lambda + \delta + b) H) + A_4 (\lambda H + \nu I - (\rho + b) R) \quad (3.73)
\end{aligned}$$

By collecting similar terms of  $E, I, H, R$  to simplify Equation (3.73) and at  $E_0 = E^0 = I^0 = H^0 = R^0 = 0$ , then by calculating the coefficients  $A_1, A_2, A_3$  and  $A_4$  the results gives Equation (3.74).

$$\frac{dL}{dt} \leq A_2 (\eta_1 Q) \quad (3.74)$$

By considering Equations (3.40) and (3.57) by substituting in Equation (3.73), gives Equation (3.75) and finally Equation (3.76) as simplified form.

$$\frac{dL}{dt} \leq A_2 \left( \frac{\phi b (b + \theta + q) (b + \delta + \eta_2 + \nu) R_0}{\beta \mu (\theta - \omega q + q)} - \frac{q (1 - \omega) (\alpha + b)}{(\theta - \omega q + q)} \right) \quad (3.75)$$

$$\frac{dL}{dt} \leq A_2 [R_0 - 1] \quad (3.76)$$

The largest invariant non-negative set in  $(S, E, Q, I, H, R) \in \Psi$  where  $\frac{dL}{dt} \leq 0$  is the singleton set of  $E_0$  for  $R_0 \leq 1$  for the system (3.2) as presented by the LaSalle's invariant principle LaSalle (1976) whereby  $E_0$  is globally asymptotically stable if  $R_0 < 1$  and unstable when  $R_0 > 1$ .  $\square$

### 3.4.4 The Global Stability of Endemic Equilibrium Point, $E_*$

The Lyapunov method and LaSalle's invariance principle are used to analyze the global stability of endemic equilibrium point ( $E_*$ ). The first integral, often known as the Lyapunov function, is well-known among ecologists and has been successfully applied in epidemiological models. Also, the Lyapunov function is a useful tool for analyzing the stability of autonomously differential equation systems. For compartmental epidemic models with any number of compartments, this strategy has been found to be useful by the studies done by Korobeinikov (2002), Vargas-De-León (2009) and Safi (2019) as used to prove the global stability of endemic equilibrium for  $SIS, SIR$ ,



and *SIRS* models. The logarithmic Lyapunov function is used to analyze the stability of the endemic equilibrium. For the derivation of Lyapunov function  $W$  consider Theorem 3.8 and its proof.

**Theorem 3.8**

If  $R_0 > 1$ , the global endemic equilibrium point  $E_*$  is asymptotically stable, while when  $R_0 < 1$  the  $E_*$  is unstable.

*Proof.* To determine the global stability of the system (3.2) for which  $E_*$  exists and  $R_0 > 1$ , the Lyapunov function  $W$  is defined and derived as follows:

$$W(x_1, \dots, x_n) = \sum_{i=1}^n \frac{1}{2} [x_i - x_i^*]^2. \quad (3.77)$$

Where

$n$  = Number of compartments (in this study there are 6 compartments, then  $n = 6$ ),

$X_i$  = Disease-free compartment, and

$x_i^*$  = Endemic compartment.

$$W(S, E, Q, I, H, R) = \frac{1}{2} [(S - S^*) + (E - E^*) + (Q - Q^*) + (I - I^*) + (H - H^*) + (R - R^*)]^2 \quad (3.78)$$

Consider the derivative of function  $W$  in Equation (3.78) with respect to time corresponding to system (3.2), the following solution in Equation (3.79) obtained.

$$\frac{dW}{dt} = [(S - S^*) + (E - E^*) + (Q - Q^*) + (I - I^*) + (H - H^*) + (R - R^*)] \frac{d}{dt} (S + E + Q + I + H + R) \quad (3.79)$$

From Equation (3.7) which is given as

$$\frac{dN}{dt} = \frac{d}{dt} (S + E + Q + I + H + R) \quad (3.80)$$

Then, by using Equation (3.8) therefore Equation (3.80) gives

$$\frac{dN}{dt} = \mu + \phi - Nb \quad (3.81)$$

But from Equation (3.7) given that

$$[S^* + E^* + Q^* + I^* + H^* + R^*] = \frac{\mu + \phi}{b} \quad (3.82)$$

Consider the substitute of Equations (3.81) and (3.82) into Equation (3.79), gives Equation (3.83).

$$\frac{dW}{dt} = \left[ N - \frac{\mu + \phi}{b} \right] [\mu + \phi - Nb] \quad (3.83)$$

Then,

$$\frac{dW}{dt} = -\frac{1}{b} [(\mu + \phi)^2 - 2N(\mu + \phi) + N^2b^2] \quad (3.84)$$

The simplification of Equation (3.84) is given in Equation (3.85).

$$\frac{dW}{dt} = -\frac{1}{b} [\mu + \phi - Nb]^2 \quad (3.85)$$

$\frac{dW}{dt} < 0$  is a strictly Lyapunov function as presented in Equation (3.85), which shows that the endemic equilibrium point  $E_*$  is globally asymptotically stable when  $R_0 > 1$  in the region  $\Delta$  as presented by LaSalle (1976) invariant principle.

From Equation (3.85),  $\frac{dW}{dt} = 0$  if and only if we set  $S = S^*, E = E^*, Q = Q^*, I = I^*, H = H^*, R = R^*$  and then,  $\frac{dW}{dt}$  converges in positive region  $\Delta$  as  $t \rightarrow \infty$ .  $\square$

### 3.5 Conclusion

In this chapter, the *SEQIHR* mathematical model was developed and the qualitative analysis was done well. From the qualitative analysis results, the model is positive, continuous and bounded, showing that it is biologically and epidemiologically meaningful. The next-generation matrix used to compute  $R_0$  which is the key of the study to show that the disease is persisting in the community if  $R_0 > 1$  and die if  $R_0 < 1$ . Moreover, the disease-free and endemic equilibrium points discussed. When  $R_0 < 1$ , the disease-free equilibrium point is locally and globally asymptotically stable, while the endemic equilibrium point is asymptotically stable if  $R_0 > 1$ , according to the LaSalle (1976) invariant principle.

## CHAPTER FOUR

### RESULTS AND DISCUSSION

#### 4.1 Introduction

The data is simulated in this study using the fourth-order Runge-Kutta method with Gaussian noise. The Partial Rank Correlation Coefficient (PRCC) was used to study the sensitivity analysis of model parameters in  $R_0$ , and it helped to discover the most sensitive and least sensitive parameter. The graphical presentations in this chapter are in compliance with the model theoretical solutions, where parameter values for  $R_0$  and susceptibility vary. The least square and Markov Chain Monte Carlo (MCMC) methods were used to determine parameter identifiability. The  $SI$  Units for the parameters are per day, as shown in Table 3, however the proportional parameters are unitless.

#### 4.2 Numerical Simulation

The series of numerical simulation results for the system (3.2) of the model equations are presented. The explicit Runge-Kutta fourth-order method was used to solve the first-order ordinary differential equations of the  $SEQIHR$  model with a given initial condition. The PRCC used to show the sensitivity analysis of the parameters and basic reproduction number. Parameter values from the literature were used and some were assumed as shown in Table 3. The sensitivity index of each partial basic reproduction number  $R_0$  for its parameters.

#### 4.3 Sensitivity Analysis and Uncertainty

In this section, sensitivity analysis of the basic reproduction number is conducted in order to investigate the most sensitive model parameters and then perform numerical simulation to investigate their effects on the basic reproduction number. Sensitivity analysis shows the impact of each parameter to the COVID-19 disease transmission through which each parameter is investigated with respect to  $R_0$ . The  $SEQIHR$  model's stability was determined through a sensitivity analysis of parameter values. The data collected and the assumed initial values for the parameters as discussed in Carvalho *et al.* (2020) are often with errors. The values for the parameters were taken from the literature, with some being assumed.

**Definition 4.1** The normalized forward sensitivity index on the differentiable model parameter of the  $R_0$  is defined as:

$$\Gamma_L^{R_0} = \frac{\partial R_0}{\partial L} \times \frac{L}{R_0}. \quad (4.1)$$

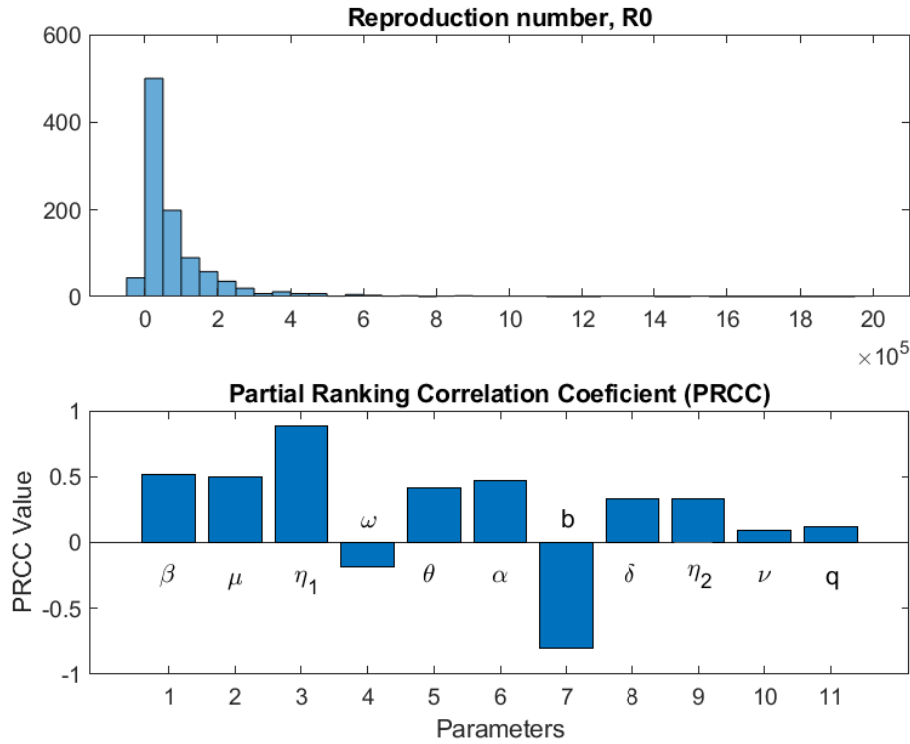
By making the use of the formula in Equation (4.1) the sensitivity index of each partial reproduction number  $R_0$  with respect to its parameters are given as in Table 3:

**Table 3: Sensitivity indices for  $R_0$  parameters**

Parameter	Values	Sources	Sensitivity index
$\beta$	$0.45 \text{ day}^{-1}$	Ojiambo <i>et al.</i> (2020)	1.0000
$\mu$	$50 \text{ day}^{-1}$	Mandal <i>et al.</i> (2020)	1.0000
$\omega$	$0.083 \text{ day}^{-1}$	Assumed	-0.0388
$b$	$0.0104 \text{ day}^{-1}$	Djaoue <i>et al.</i> (2020)	-0.9483
$\alpha$	$0.85 \text{ day}^{-1}$	Assumed	0.7100
$\nu$	$0.07 \text{ day}^{-1}$	Agaba (2020)	0.090
$\theta$	$0.2435 \text{ day}^{-1}$	Aldila <i>et al.</i> (2020)	1.2614
$\eta_1$	$0.85 \text{ day}^{-1}$	Assumed	1.2813
$\eta_2$	$0.65 \text{ day}^{-1}$	Assumed	0.8448
$\delta$	$0.039 \text{ day}^{-1}$	Serhani and Labbardi (2020)	0.0507
$q$	$0.099 \text{ day}^{-1}$	Assumed	0.7092

From Table 3, it is observed that the  $\eta_1$  parameter is more sensitive since it increases the basic reproduction number by  $\Gamma_L^{R_0} = 1.2813$ . The increase of this parameter means that in quarantine, people are more stressed such that the immune system decreases in its efficiency, so the virus spreads within the body. The virus causes blood clotting because the virus fights the respiratory system and enters the bloodstream through lung capillaries that are adjacent to the alveolus (Janardhan *et al.*, 2020). The Partial Rank Correlation Coefficient (PRCC) supported graphically in Fig. 6 shows that  $\eta_1$  has an impact on COVID-19 transmission. *SEQIHR* model shows that

hospitalized patients from the infected class are less stressed than those in quarantine, although it also increases the basic reproduction number by ( $\Gamma_L^{R_0} = 0.8448$ ), then  $\eta_1 > \eta_2$ . Other positive sensitive parameters are  $\theta$  with  $\Gamma_L^{R_0} = 1.2614$ ,  $\beta$  and  $\mu$  which both have  $\Gamma_L^{R_0} = 1$ , and also  $b$  is the most negative sensitive parameter with value  $-0.9483$ . Parameters with least sensitivity are  $\nu$ ,  $\delta$  and  $\omega$  with values 0.090, 0.0507, and  $-0.0388$  respectively. It shows that if most of the patients are hospitalized, the disease decreases, and subsequently, no more transmission within the community. Despite the fact that the other parameters have small values, they still increase  $R_0$  by their respective percentages. From PRCC, consider the following results from Fig. 5:



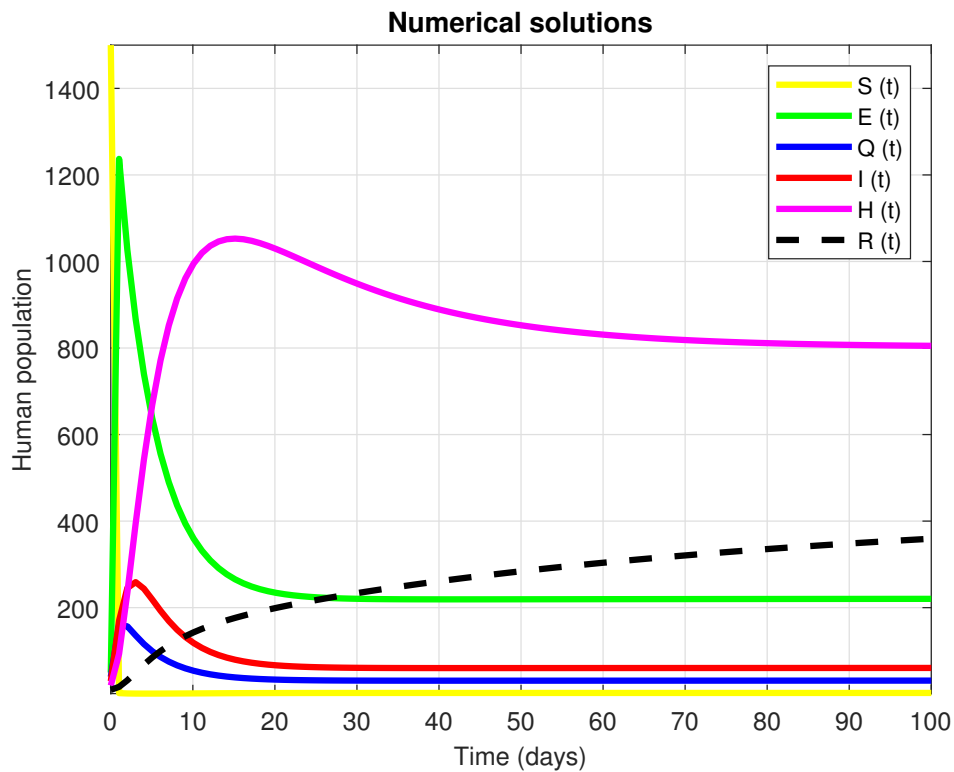
**Figure 5: Sensitivity analysis and PRCC results for  $R_0$**

Figure 5, shows that  $\eta_1$  is positively and highly correlated with  $R_0$  as the absolute value of its PRCC value is higher than the corresponding value of other parameters. Furthermore, natural death ( $b$ ) is highly negatively correlated with  $R_0$ .

#### 4.4 Dynamic Population simulation on a *SEQIHR* Model

The numerical simulation of the *SEQIHR* model variables is shown in Fig. 6. We observe that the susceptible class declines to obtain the endemic equilibrium point as individuals move to the exposed class and other individuals die naturally. The exposed class increases due to individuals

from the susceptible class and decreases as individuals move to quarantine, hospitalized, infected classes and others die naturally. The quarantined class decreases as individuals move to susceptible and infected classes and others die naturally. Furthermore, the infected and hospitalized classes decrease as individuals recovered, and others die from COVID-19 disease and also die naturally. the recovered class increases as individuals move from infected and hospitalized classes and later decreases as individuals move back to the susceptible class.



**Figure 6:** *SEQIHR* Model dynamic simulation

#### 4.5 Relationship between Parameters and $R_0$

In this section, the basic model simulation and how COVID-19 dynamic behavior when an endemic equilibrium point exists was observed. In addition, the impacts of each parameter on the basic reproduction number were displayed so that the sensitivity of  $R_0$  could be predicted. The variation of the parameters magnitude tends to change the magnitude of  $R_0$ . By looking at the graphs from Fig. 7 to Fig. 12, you can see how the most sensitive and moderate positive indices, as well as the most sensitive and moderate negative indices, affect  $R_0$ . From the Fig. 7, parameter  $\eta_1$  is the most positive sensitive parameter, and that increasing the contact rate ( $\beta$ ) leads to a rise in  $R_0$  quickly. This suggests that the interaction between infected people and the COVID-19 virus

could have a big impact on the people who are vulnerable. Similarly, as shown in Fig. 11a, natural death  $b$  is the most negative sensitive parameter, implying that any decrease in it (not dying) results in a significant exponential retardation in the  $R_0$ . In other words, if and only if there is no infection, the susceptible population remains constant. From Fig. 7, 8a, 9, 10, 11b and 12, a significant steep slope increase in the basic reproduction number for any increment of each of these parameters that leads to further positive increments.

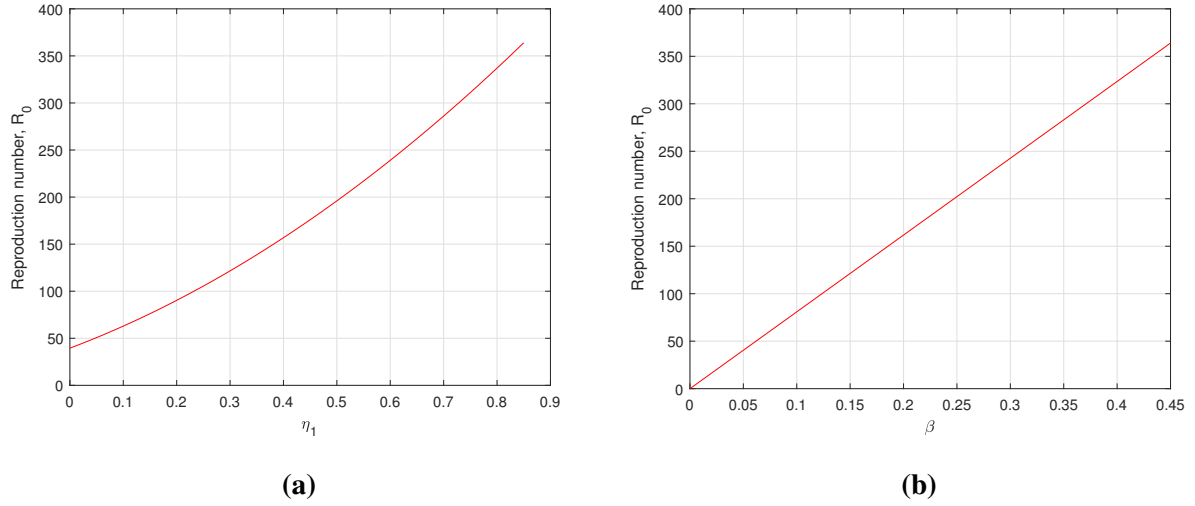


**Figure 7: Effect of stress  $\eta_1$  and contact rate  $\beta$  on  $R_0$**

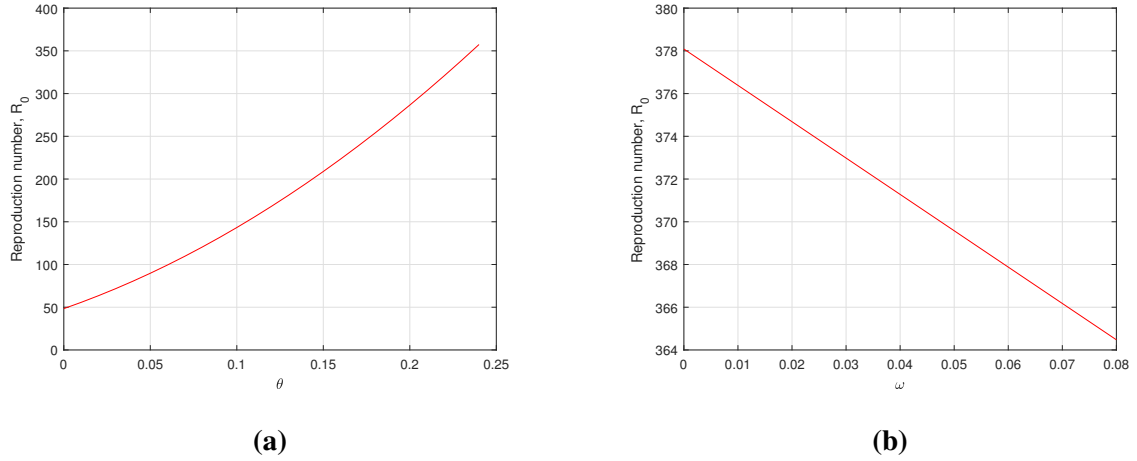
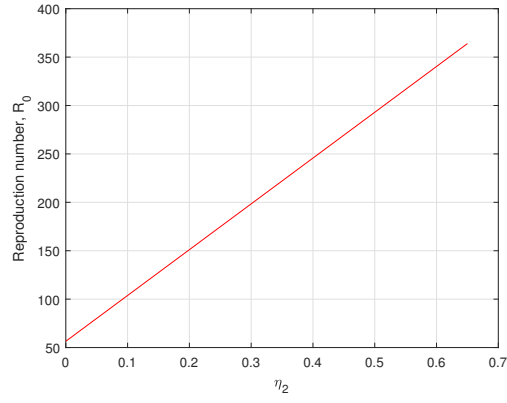
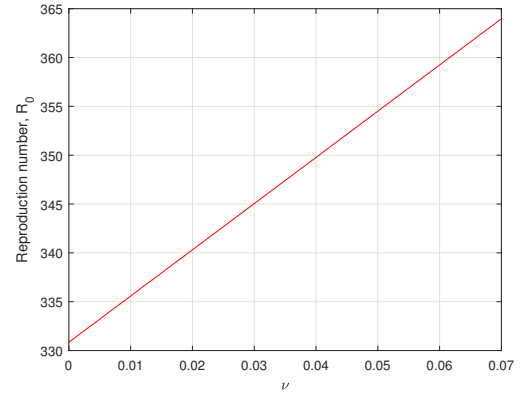


**Figure 8: Effect of quarantined rate  $\theta$  and hospitalized rate  $\omega$  on  $R_0$**

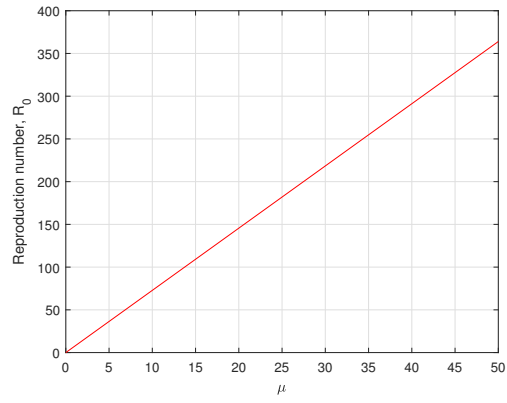


(a)

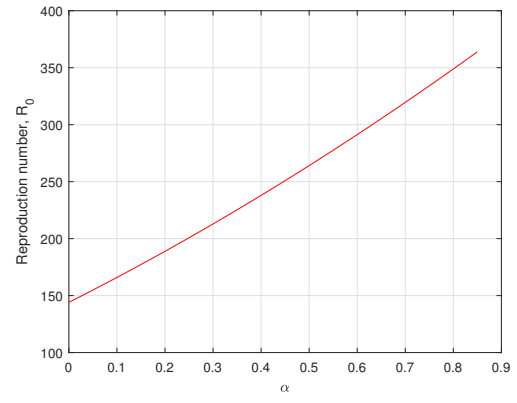


(b)

**Figure 9: Effect of infected rate  $\eta_2$  and recovered rate  $\nu$  on  $R_0$**

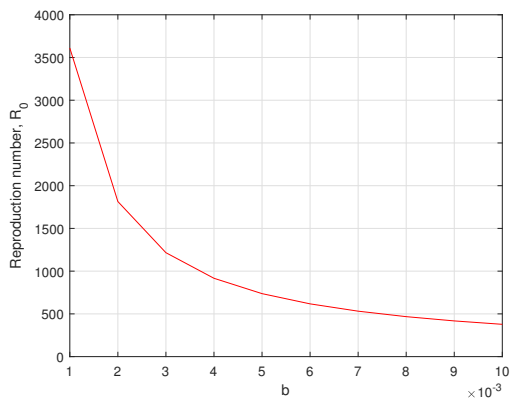


(a)

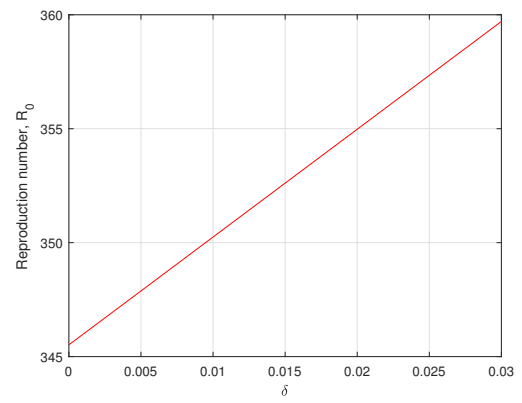


(b)

**Figure 10: Effect of recruitment rate  $\mu$  and uninfected rate  $\alpha$  on  $R_0$**



(a)



(b)

**Figure 11: Effect of natural death  $b$  and death due to disease  $\delta$  on  $R_0$**



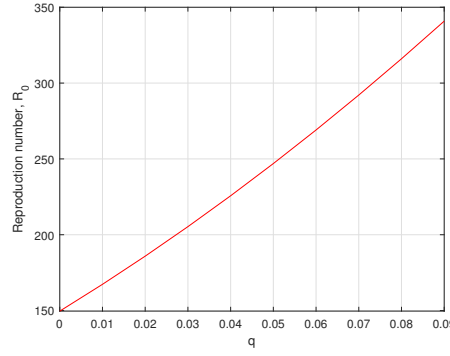


**Figure 12: Effect of  $q$  on  $R_0$  from exposed class to hospitalized and infected class**

#### 4.6 Simulation of Stability Analysis for Endemic Equilibrium Point of $SEQIHR$ Model

Numerical simulations are performed on the model's analytical results for the stability analysis. The model trajectories for the state variables should originate from different initial values and occasionally converge to a single point to maintain an endemic equilibrium point for any equilibrium point to be globally asymptomatic stable. The equilibrium point is globally stable if the model trajectories for state variables remain near the equilibrium point and move together in the long run. The six trajectories in each class are represented by different colors as shown by a legend as time approaches infinity converging towards equilibrium point. The model variables  $S$ ,  $E$ ,  $Q$ ,  $I$ ,  $H$ , and  $R$  varied by considering Figures; 13a, 13b, 14a, 14b, 15a, and 15b respectively are illustrated as follows:

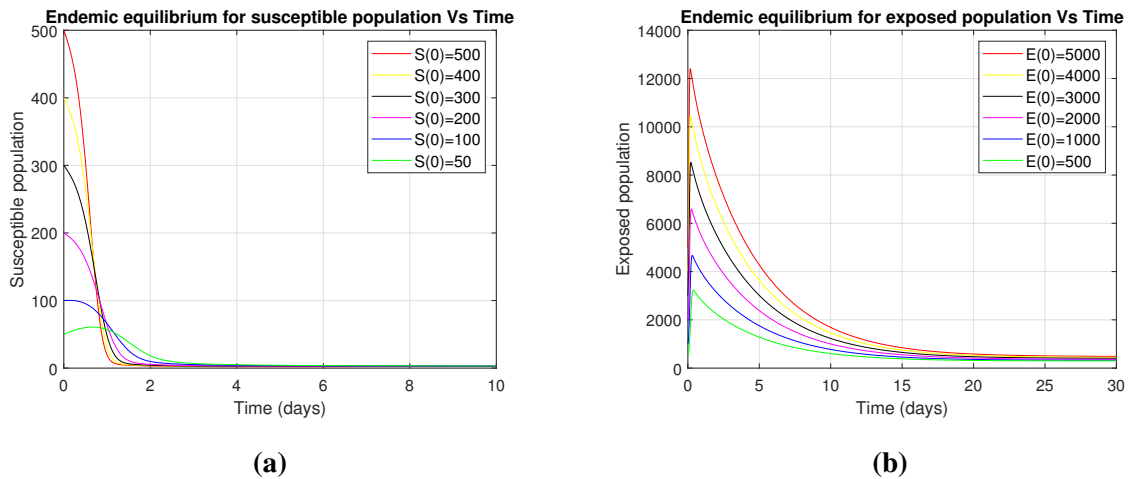


**Figure 13: Endemic equilibrium for susceptible and exposed human population**

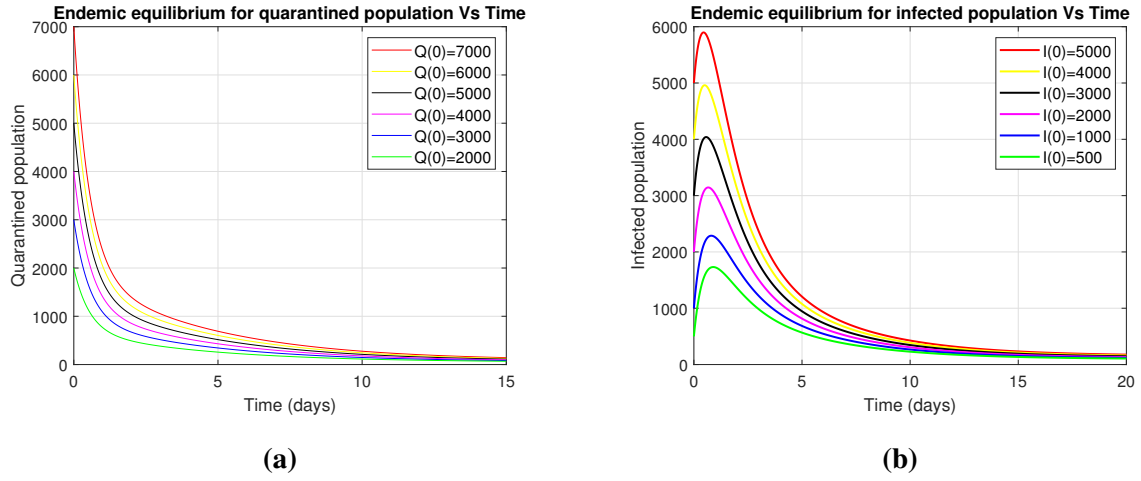


**Figure 14: Endemic equilibrium for quarantined and infected human population**

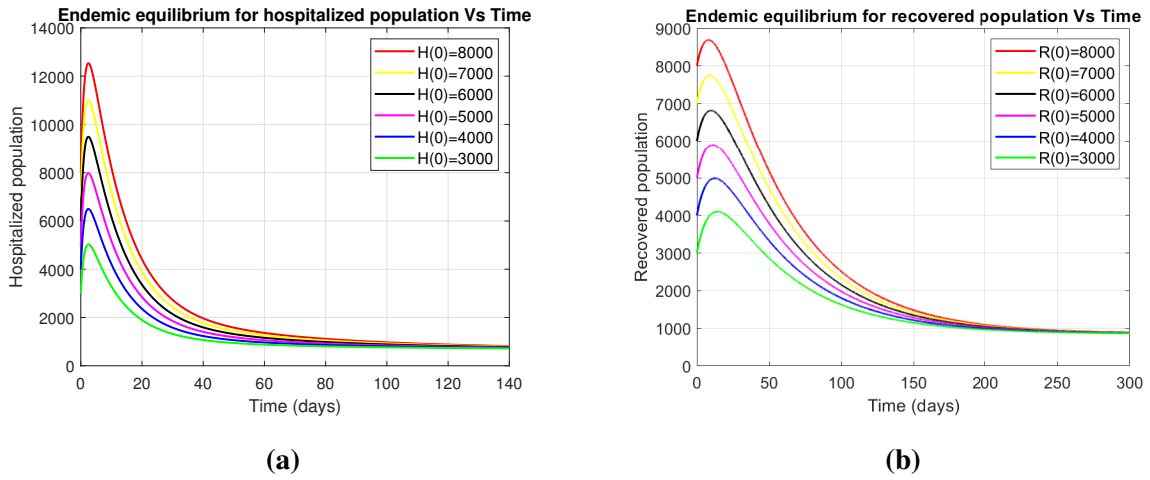


**Figure 15: Endemic equilibrium for hospitalized and recovered human population**

#### 4.7 Control Parameters

Considering the variation of some control parameters; from Fig. 16a, when the contact rate ( $\beta$ ) increases, the decaying population rate also increases, but when the contact rate decreases, the decaying rate also decreases. From Fig. 16b, when the contact rate increases, the infections also increase, and apply the same when the contact rate decreases and the infections decrease. When stress increases in the susceptible class, the rate of decaying increases, and if the stress decreases, the decaying rate decreases, as shown in Fig. 17a. From Fig. 17b, when stress ( $\eta_1$ ) increases, the rate of infection increases, and when  $\eta_1$  decreases, then the rate of infection decreases. Moreover, when  $\eta_2$  increases the rate of infection and hospitalization increases, and then decreases when  $\eta_2$  decreases as in Fig. 18a and 18b. Furthermore, the rate of infectious decreases when the rate of

recovered  $\nu$  increases, as presented in Fig. 19a and 19b respectively.

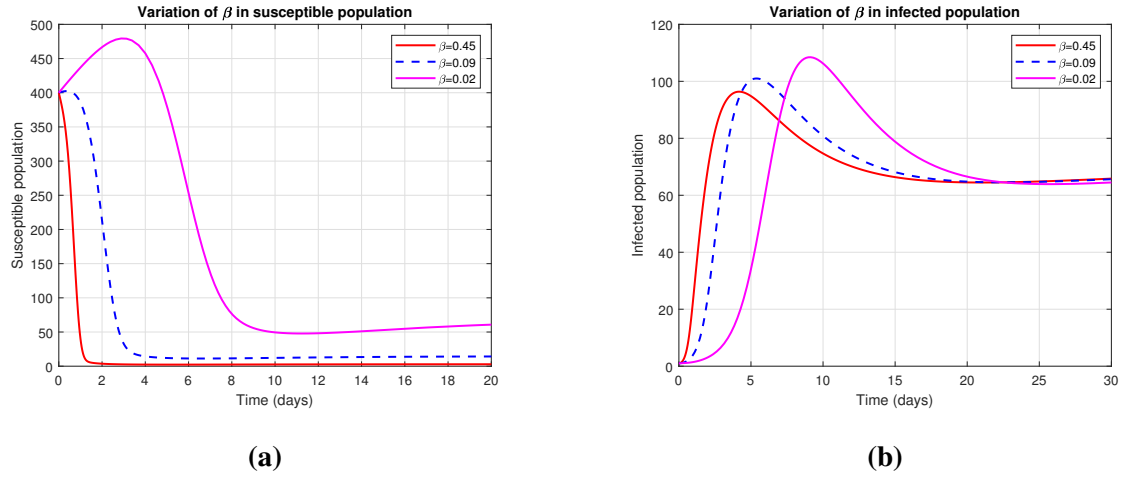


**Figure 16: Variation of contact rate  $\beta$  in susceptible and infected population**

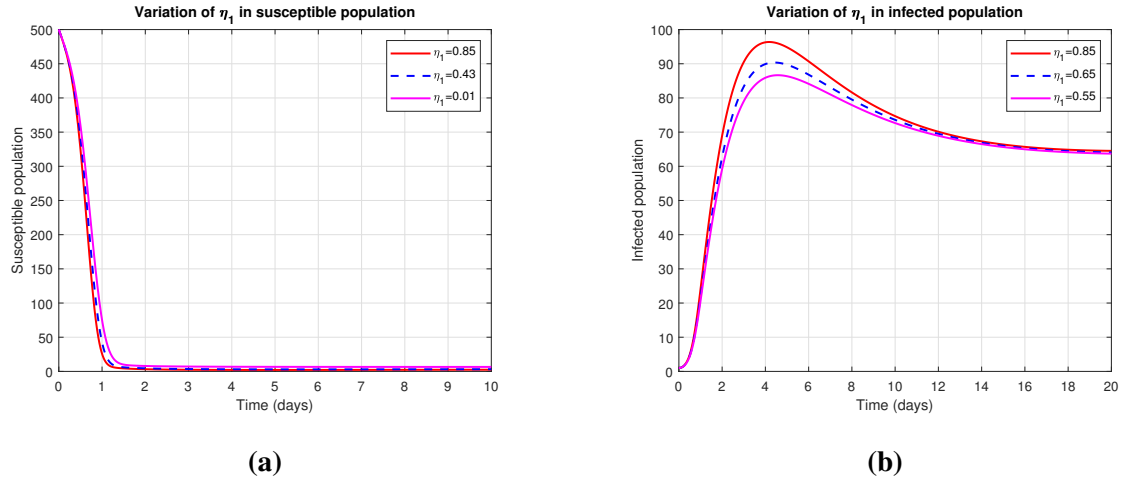


**Figure 17: Variation of  $\eta_1$  in susceptible and infected population**

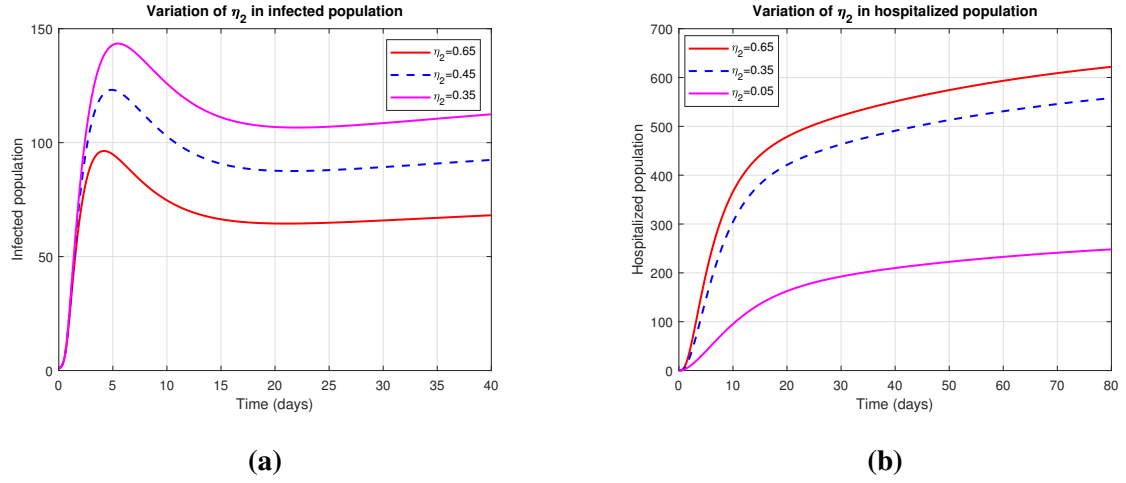


**Figure 18: Variation of  $\eta_2$  in infected and hospitalized population**

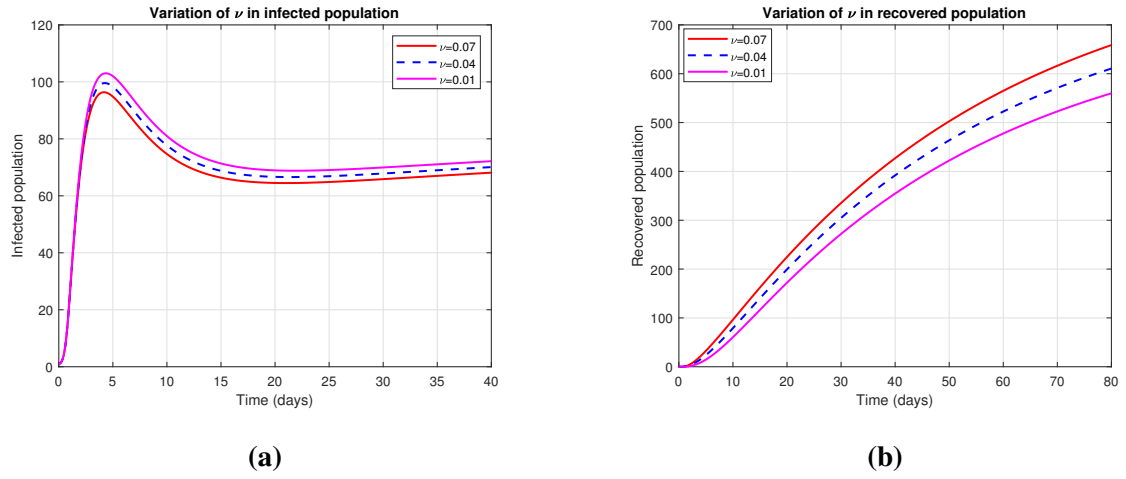


**Figure 19: Variation of  $\nu$  in infected and recovered population**

#### 4.8 Parameter identifiability and model fitting by least square method

The proposed *SEQIHR* model relies on the identifiability of parameters. Then,  $\beta$ ,  $\mu$ ,  $\omega$ ,  $\alpha$ ,  $\eta_1$ , and  $\eta_2$  are the parameters in concern. The sum of squared differences between the *SEQIHR* model and observations was minimized using the least square approach, obtaining the parameter identifiability Solonen *et al.* (2012), which is defined as:

$$SS(y) = \sum_{i=1}^n [y_i - f(x_i, y)]^2 \quad (4.2)$$

where  $y_i$  are the observed data of all compartments,  $i$  is the number of compartments (i.e.  $i = 1, 2, \dots, n$ ), and  $f(x_i, y)$  is the solution for all compartments of the *SEQIHR* model. With the

initial values of the parameters given as  $\beta$ ,  $\mu$ ,  $\omega$ ,  $\alpha$ ,  $\eta_1$ , and  $\eta_2$ , the least squares identifiabilities are obtained as shown in Table 4.

**Table 4: Parameter identifiability**

Parameter	Initial values	Estimated values
$\beta$	0.45	0.4541
$\mu$	50	50.2436
$\omega$	0.083	0.8562
$b$	0.0104	0.0848
$\alpha$	0.85	0.2446
$\nu$	0.07	0.8555
$\theta$	0.2435	0.0110
$\eta_1$	0.85	0.0394
$\eta_2$	0.65	0.6511
$\delta$	0.039	0.0705
$q$	0.099	0.0986
$\rho$	0.003	0.0028
$\lambda$	0.002	0.0020
$\phi$	0.001	0.0010

The initial values before adding noise,  $\sigma$ .

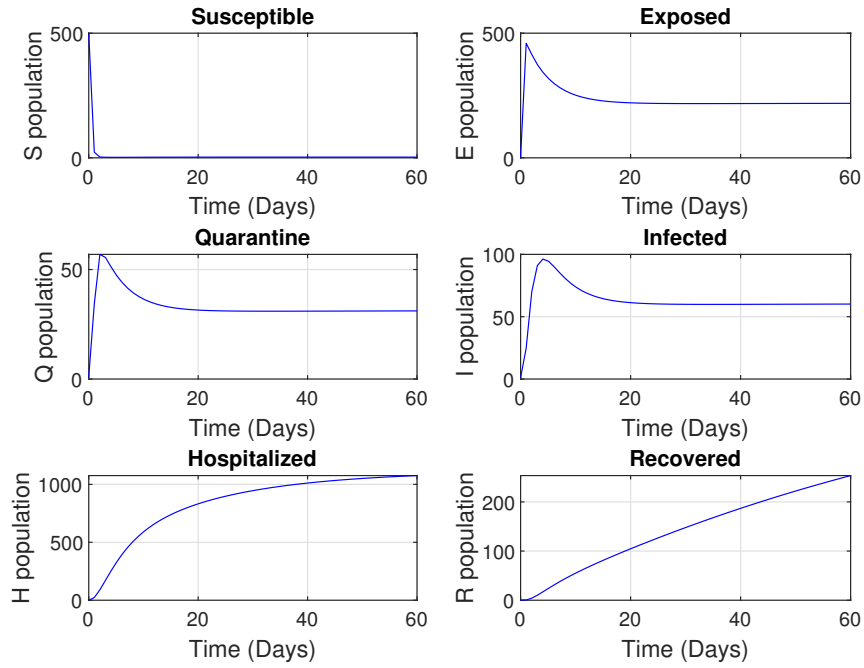


**Figure 20: Parameter estimations**

Then the initial values and estimated values are used to fit the simulated data as shown in Fig. 21 after adding noise  $\sigma = 0.01$ .

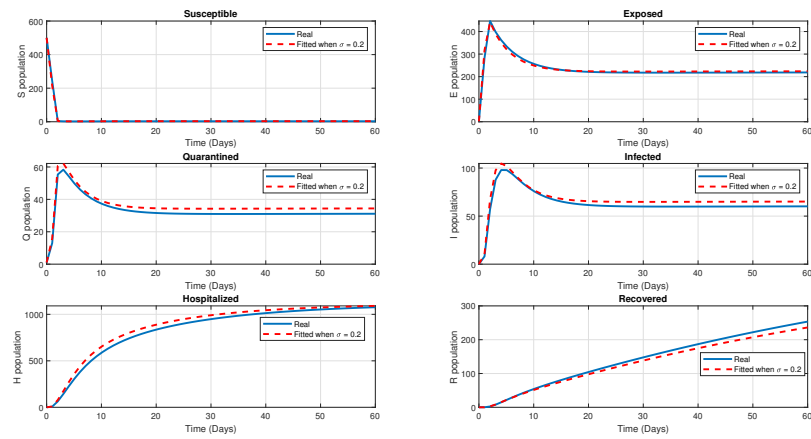


**Figure 21: Model Fitting**

The relationship of initial parameter values and the identifiable values from the least square method is very close.

#### 4.9 Parameter identifiability by Markov Chain Monte Carlo (MCMC)

The Markov Chain Monte Carlo (MCMC) method is a statistical and Bayesian method for determining the parameters of complex ordinary differential equations that fit the dynamical systems. There are fourteen parameters to be estimated in this study, and a sampling of  $100,000 \times 14$  parameters has been generated during simulations, with the technique being adapted 200 times. The initial values for parameters are obtained from least square estimates and the model parameters' identifiability is mostly determined by the MCMC's convergence. For the MCMC approaches, there are numerous statistical and graphical convergence tests (Rannala, 2002; Muhirwa *et al.*, 2021). The covariance matrix of MCMC is given by:

$$\sum_0 = \frac{10^{-4} I_j}{\sqrt{j}}, \quad (4.3)$$

where  $j$  is the length of model's parameters to be estimated, thus  $I_j = I_{j \times j}$  which is an  $j \times j$  identity matrix.

Table 5 shows that nearly all parameters converge to their initial values, and posterior means are within reasonable intervals with the posterior means and posterior medians being practically equal. Furthermore, the Markov Chain errors (MCerr) and the standard deviation of the model parameters are both quite small, indicating that the method worked well in determining the most accurate estimates. The computed autocorrelation time (tau) values are small, indicating the importance of sampling the subsequent posteriors independently as well as the method's convergence. Except for  $\phi = 0.0151$ , all geweke values are close to 1. The Gaussian distribution's skewness and kurtosis values are approximately to be 0 and 3, respectively. As a result, the acquired samples' skewness and kurtosis values demonstrate that only parameter  $\omega$  value is slightly skewed right and parameter  $\phi$  value highly skewed in the right hand side and do not incorporate the exact properties of the Gaussian distribution.

**Table 5: Estimated parameters using least square and MCMC methods**

Parameter	Value	LSQE	MMean	MMed	Std	MCerr	tau	geweke	Kurtosis	Skewness
$\beta$	0.4500	0.4541	0.4486	0.4489	20.0037	0.00014463	66.124	0.99658	3.2854	-0.0431
$\mu$	50.0000	50.2436	49.951	49.9628	0.0566	0.0060406	3928.6	0.99828	3.2976	-0.7268
$\eta_1$	0.8500	0.8562	0.8499	0.8500	0.0038	8.5757e-05	57.6290	0.9999	3.3715	0.0097
$\omega$	0.0830	0.0848	0.0817	0.0828	0.0067	0.0004	90.1350	0.96075	3.4261	-0.2351
$\theta$	0.2435	0.2446	0.2429	0.2430	0.0011	7.298e-05	79.525	0.9952	3.3919	-0.2964
$\alpha$	0.8500	0.8555	0.8469	0.8475	0.0045	0.0004	139.2100	0.9936	3.3871	-0.3061
$b$	0.0104	0.0110	0.0104	0.0104	5.3841e-05	2.2236e-06	76.2170	0.99802	3.2830	0.0547
$\delta$	0.0390	0.0394	0.0389	0.0390	5.9908e-05	2.6025e-06	63.6400	0.9992	3.0441	-0.0808
$\eta_2$	0.6500	0.6511	0.6504	0.6501	0.0021	0.0001	92.2610	0.9984	3.3909	0.2300
$\nu$	0.0700	0.0705	0.0699	0.0700	7.3615e-05	3.4535e-06	54.9780	0.9994	3.0098	-0.0638
$q$	0.0990	0.0986	0.0990	0.0990	0.0006	1.4153e-05	58.8590	0.9999	3.3773	0.0047
$\lambda$	0.0020	0.0028	0.0030	0.0030	5.1147e-05	1.9499e-06	79.3910	0.99852	3.4466	0.0883
$\rho$	0.0030	0.0020	0.0020	0.0020	1.2941e-05	7.2516e-07	61.6660	0.9946	2.9655	0.0745
$\phi$	0.0010	0.0010	0.0527	0.0397	0.0502	0.0057	4436.9000	0.0151	4.3919	1.2072

Where; LSQE = Least Square Estimates, MMean = MCMC Mean, MMed = MCMC Median, std = Standard deviation, MCerr = MCMC error.

Trace plots as one of the techniques to assess the MCMC's convergence can be used to examine the mixing of the generated sample of posteriors. If the created chain of posteriors becomes stationary for numerous beginning values with no noticeable spikes, it indicates that the mixing is good, which is a sign of convergence. In Fig. 22 we can see that the sample mixing is excellent, therefore the chain converges, and the 14 sampled posterior values are the samples' means (centers).



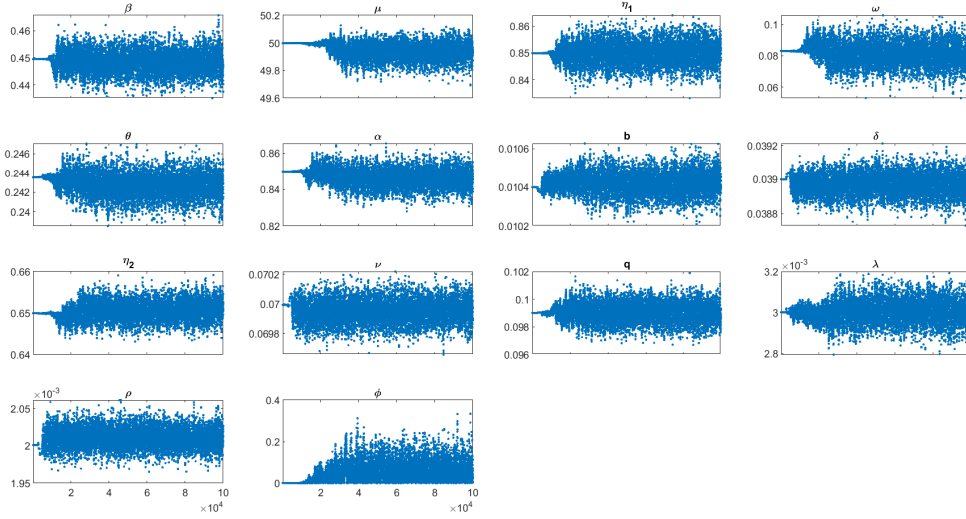


**Figure 22: Trace plots**

Inventively, a low convergence of the MCMC approach results in a strong correlation between estimated parameters. Because there are 14 parameters to identify, we'll need to look at 91 scatter plots to see if there are any major correlations between them. Figure 23 presents the scatter plots for the first 10 sampled parameters, which equates to 45 scatter plots, as well as how these posterior samples relate to one another. It shows that there is no strong association between the pairs of estimated parameters, indicating that the *SEQUIHR* model's parameters are well identified.

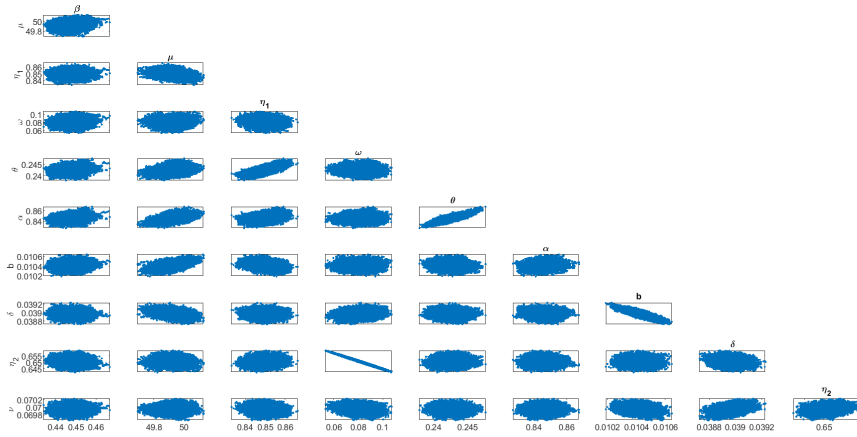


**Figure 23: Scatter plots**

Figure 24 shows that practically all parameter values are distributed normally. For  $\phi$ , the convergence of the MCMC is usually bad. The remaining 13 parameters, on the other hand, are perfect. This could be due to a variety of factors, all of which are difficult to predict. It could be due to lack

of information regarding their mean values, or the approach has failed to sample the  $\phi$  parameter from the specified distribution.

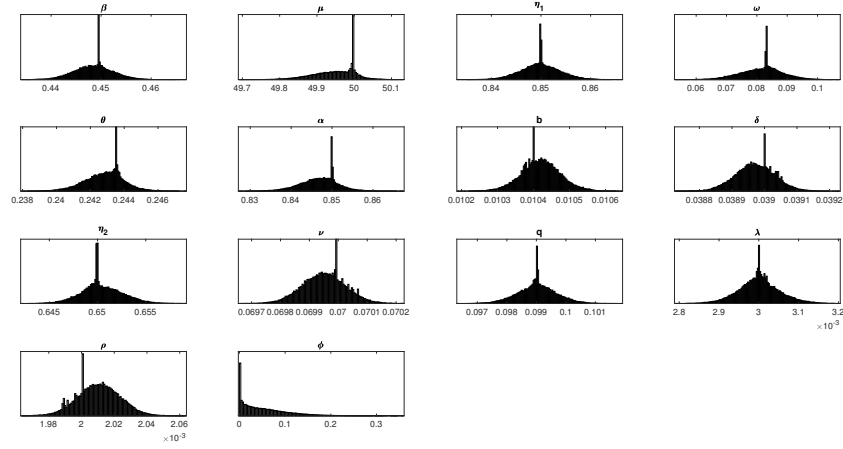


**Figure 24: Histograms**

Plotting the posterior density distributions is another diagnostic test. Normally, the result expects the distributions of all density estimations to follow a Gaussian distribution for better mixing. Figure 25 shows how the density distributions of all calculated parameters follow a Gaussian pattern, with their values serving as distribution means.

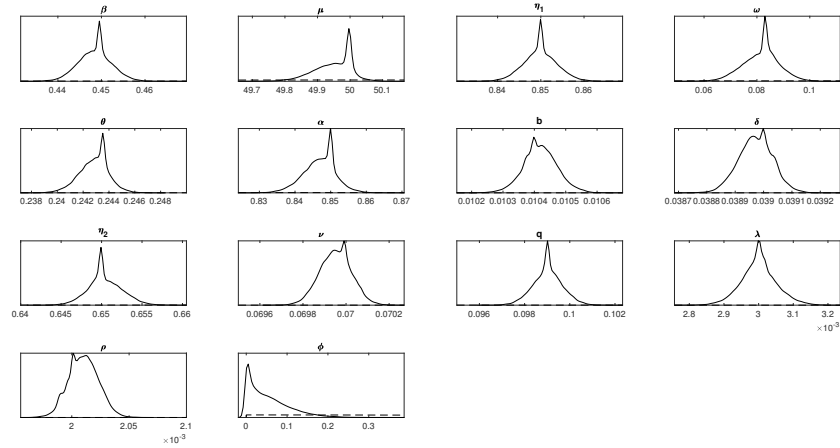


**Figure 25: Distribution density**

#### 4.10 Discussion

In this chapter, the numerical simulation on the deterministic model *SEQIHR* was discussed and the results were obtained. The model numerical results are shown in Fig. 6 where the trajectories

are in sinusoidal form. The control parameters show good results on the minimization of infections. The basic reproduction number for this study is 2.1692. From PRCC, the most sensitive parameter was  $\eta_1$  which increases the basic reproduction number by  $\Gamma_L^{R_0} = 1.2813$ , which means in quarantine people are more stressed which reduces the efficiency of the body immune system. As the numerical results validate the theoretical results, in controlling the disease when stress is decreased also the rate of infection decreases as shown in the control parameters from Fig. 16a to Fig. 19b. The endemic stability results were good, showing that the model trajectories for the state variables should be originated from distinct initial values and occasionally converge to a common point, preserving an endemic equilibrium point, as illustrated in Fig. 13 to Fig. 15. Parameter identifiability was done by using least square and Markov Chain Monte Carlo (MCMC) methods where by the parameters converge to their initial values and their posterior means are within reasonable intervals and all  $R_0$  parameters are normally distributed but for the parameters out of  $R_0$  only  $\phi$  the convergence is bad.

## CHAPTER FIVE

### CONCLUSION AND RECOMMENDATIONS

#### 5.1 Conclusion

The COVID-19 epidemic spread quickly throughout the world, causing a significant human and socioeconomic impact. A mathematical model for COVID-19 transmission when a human is stressed was established in this study, with six compartments: susceptible ( $S$ ), exposed ( $E$ ), quarantined ( $Q$ ), infected ( $I$ ), hospitalized ( $H$ ), and recovered ( $R$ ). For the disease-free equilibrium, a model was developed and some mathematical analysis was presented, including positivity, invariant region, existence, uniqueness of the solution, and stability results. The disease-free equilibrium for both local and global is stable when  $R_0 < 1$  was proved. This exploration suggests that the COVID-19 disease can enter and spread to the human population if  $R_0 > 1$  provided that the initial human population is close to the infested region. But also, die out when few initial human populations are infected and  $R_0 < 1$ . The basic reproduction number obtained from this study was 2.1692, which shows that the disease is endemic and unique. The most sensitivity indices are summarized in Table 3 and the least positive and negative sensitive parameters are crucial for the transmission of COVID-19. The numerical results in this study showed that stress affects many quarantined people whereby their immune system is disturbed by the COVID-19 and this is most likely because during quarantine, people are isolated from their families and community members, so they develop fear, and later the body becomes stressed which affects their immune system. When the immune system is disturbed, it fails to fight against the intruders, which leads to the fast spread of COVID-19 throughout the body. The graphical presentation demonstrated that the control parameters were very successful in reducing COVID-19 transmission in the population.

#### 5.2 Recommendations

COVID-19 is the world pandemic, which affected millions of human lives in which leads to the change of ways of living among the communities. This is the time for humility, the COVID-19 has humbled the world down to the knees because nowadays shaking hands has become a cause. Several mathematical modeling studies have been undertaken to meet the WHO goals on eliminating the disease. However these studies did not look at the modeling of stress. In this study, the mathematical model was proposed to assess the effects of stress in a quarantined

people towards COVID-19 elimination. Our research objectives are accomplished. Based on the outcomes of this study the following recommendations are made:

- (i) From this study, it was observed that most quarantined people are more stressed which leads to the ineffectiveness of their immune systems. This study recommends that people should not be quarantined for long or should not be separated from their families but they should be encouraged to follow precautions proposed by the WHO.
- (ii) The government and service providers should provide education about COVID-19 and its precautions to those individuals in quarantine to reduce stress.

### **5.2.1 Future Work**

Adding the important information to the model to study and understand more about the transmission of COVID-19. From the formulated model we intend to:

- (i) Use more detailed data when having access to COVID-19 data which will be employed in the *SEQIHR* model.
- (ii) Add a vaccination compartment in our model to implement optimal control strategies.
- (iii) Extend to stochastic model.

### **5.2.2 Study Limitations**

- (i) The assumption on an equal death in all compartments while in real situation the infected population has a higher death rate than the susceptible population.
- (ii) We assumed that the total population was uniformly distributed.
- (iii) Difficult in getting real data for numerical simulation.

## REFERENCES

- Agaba, G. O. (2020), Modelling the Spread of COVID-19 with Impact of Awareness and Medical Assistance. *Mathematical Theory and Modeling*, **10**(4), 21–28.
- Agmour, I., Achtaich, N., & Foutayeni, Y. E. (2018), Stability analysis of a competing fish populations model with the presence of a predator. *International Journal of Nonlinear Sciences*, **26**(2), 108.
- Ahmad, W., Abbas, M., & Baleanu, M. R. . D. (2021), Mathematical analysis for the effect of voluntary vaccination on the propagation of Corona virus pandemic. *Results in Physics*, **31**, 104917. <https://doi.org/10.1016/j.rinp.2021.104917>
- Aldila, D., Ndi, M. Z., & Samiadji, B. M. (2020), Optimal control on COVID-19 eradication program in Indonesia under the effect of community awareness. *Mathematical Biosciences and Engineering*, **17**, 6355–6389. <https://doi.org/10.3934/mbe.2020335>
- Ali, M., Imran, M., & Khan, A. (2020), Can medication mitigate the need for a strict lock down?: A mathematical study of control strategies for COVID-19 infection. *MedRxiv*. <https://doi.org/10.21203/rs.3.rs-35440/v1>
- Anderson, R. M., & May, R. M. (1992), Infectious diseases of humans: dynamics and control. *Oxford University Press*.
- Ashcroft, P., Lehtinen, S., Angst, D. C., Low, N., & Bonhoeffer, S. (2021), Quantifying the impact of quarantine duration on COVID-19 transmission. *Elife*, **10**, e63704. <https://doi.org/10.7554/eLife.63704>
- Baba, I. A., Yusuf, A., Nisar, K. S., Abdel-Aty, A.-H., & Nofal, T. A. (2021), Mathematical model to assess the imposition of lockdown during COVID-19 pandemic. *Results in Physics*, **20**, 103716. <https://doi.org/10.1016/j.rinp.2020.103716>
- Balkhair, A. A. (2020), COVID-19 pandemic: a new chapter in the history of infectious diseases. *Oman Medical Journal*, **35**(2), e123. <https://doi.org/10.5001/omj.2020.41>

- Barbastefano, R., Carvalho, D., Lippi, M. C., & Pastore, D. H. (2020), A novel predictive mathematical model for COVID-19 pandemic with quarantine, contagion dynamics, and environmentally mediated transmission. *MedRxiv*. <https://doi.org/10.1101/2020.07.27.20163063>
- Bernoulli, D., & Blower, S. (2004), An attempt at a new analysis of the mortality caused by smallpox and of the advantages of inoculation to prevent it. *Reviews in Medical Virology*, **14**(5), 275. <https://doi.org/10.1002/rmv.443>
- Brooks, S. K., Webster, R. K., Smith, L. E., Woodland, L., Wessely, S., Greenberg, N., & Rubin, G. J. (2020), The psychological impact of quarantine and how to reduce it: rapid review of the evidence. *The Lancet*, **395**(10227), 912–920. [https://doi.org/10.1016/S0140-6736\(20\)30460-8](https://doi.org/10.1016/S0140-6736(20)30460-8)
- Carvalho, D., Barbastefano, R., Pastore, D., & Lippi, M. C. (2020), A novel predictive mathematical model for COVID-19 pandemic with quarantine, contagion dynamics, and environmentally mediated transmission. *MedRxiv*. <https://doi.org/10.1101/2020.07.27.20163063>
- Castillo-Chavez, C., Feng, Z., & Huang, W. (2002), On the computation of  $R_0$  and its role in global stability. *IMA Volumes in Mathematics and Its Applications*, **125**, 229–250.
- Chitnis, N., Hyman, J. M., & Cushing, J. M. (2008), Determining important parameters in the spread of malaria through the sensitivity analysis of a mathematical model. *Bulletin of Mathematical Biology*, **70**(5), 1272. <https://doi.org/10.1007/s11538-008-9299-0>
- Chowdhury, M. A., Hossain, N., Kashem, M. A., Shahid, M. A., & Alam, A. (2020), Immune response in COVID-19: A review. *Journal of Infection and Public Health*. <https://doi.org/10.1016/j.jiph.2020.07.001>
- Cilli, A., Ergen, K., & Akat, E. (2019), Some mathematical models and applications used in epidemics. *SIGMA Journal of Engineering and Natural Sciences*, **37**(1), 17–23.
- Collins, Obiora C., & Duffy, K. J. (2016), Optimal control of maize foliar diseases using the plants population dynamics. *Acta Agriculturae Scandinavica, Section B—Soil & Plant Science*, **66**(1), 20–26. <https://doi.org/10.1080/09064710.2015.1061588>

- Cullen, W., Gulati, G., & Kelly, B. D. (2020), Mental health in the COVID-19 pandemic. *QJM: An International Journal of Medicine*, **113**(5), 311–312. <https://doi.org/10.1093/qjmed/hcaa110>
- Dagnino, P., Anguita, V., Escobar, K., & Cifuentes, S. (2020), Psychological effects of social isolation due to quarantine in chile: an exploratory study. *Frontiers in Psychiatry*, **11**. <https://doi.org/10.3389/fpsy.2020.591142>
- Daks, J. S., Peltz, J. S., & Rogge, R. D. (2020), Psychological flexibility and inflexibility as sources of resiliency and risk during a pandemic: Modeling the cascade of COVID-19 stress on family systems with a contextual behavioral science lens. *Journal of Contextual Behavioral Science*, **18**, 16–27. <https://doi.org/10.1016/j.jcbs.2020.08.003>
- Dhanwant, J. N., & Ramanathan, V. (2020), Forecasting covid 19 growth in india using susceptible-infected-recovered (sir) model. *ArXiv Preprint ArXiv:2004.00696*. <https://doi.org/10.48550/arXiv.2004.00696>
- Di Fronso, S., Costa, S., Montesano, C., Di Gruttola, F., Ciofi, E. G., Morgilli, L., Robazza, C., & Bertollo, M. (2020), The effects of COVID-19 pandemic on perceived stress and psychobiosocial states in Italian athletes. *International Journal of Sport and Exercise Psychology*, pp. 1–13. <https://doi.org/10.1080/1612197X.2020.1802612>
- Dieckmann, O., & Heesterbeek, J. (2000), Mathematical epidemiology of infectious diseases: model building, analysis and interpretation (Vol.5). *John Wiley & Sons*.
- Diekmann, O., Heesterbeek, J. A. P., & Metz, J. A. J. (1990), On the definition and the computation of the basic reproduction ratio  $R_0$  in models for infectious diseases in heterogeneous populations. *Journal of Mathematical Biology*, **28**(4), 365–382. <https://doi.org/10.1007/BF00178324>
- Djaoue, S., Kolaye, G. G., Abboubakar, H., Ari, A. A. A., & Damakoa, I. (2020), Mathematical modeling, analysis and numerical simulation of the COVID-19 transmission with mitigation of control strategies used in Cameroon. *Chaos, Solitons & Fractals*, **139**, 110281. <https://doi.org/10.1016/j.chaos.2020.110281>



- Dos Santos, R. M. (2020), Isolation, social stress, low socioeconomic status and its relationship to immune response in Covid-19 pandemic context. *Brain, Behavior, & Immunity-Health*, p. 100103. <https://doi.org/10.1016/j.bbih.2020.100103>
- Fitzpatrick, K. M., Harris, C., & Drawve, G. (2020), Fear of COVID-19 and the mental health consequences in America.. *Psychological Trauma: Theory, Research, Practice, and Policy*, **12**(S1), S17. <https://doi.org/10.1037/tra0000924>
- Garba, S. M., Lubuma, J. M.-S., & Tsanou, B. (2020), Modeling the transmission dynamics of the COVID-19 Pandemic in South Africa. *Mathematical Biosciences*, **328**, 108441. <https://doi.org/10.1016/j.mbs.2020.108441>
- Giordano, G., Blanchini, F., Bruno, R., Colaneri, P., Di Filippo, A., Di Matteo, A., & Colaneri, M. (2020), Modelling the COVID-19 epidemic and implementation of population-wide interventions in Italy. *Nature Medicine*, pp. 1–6. <https://doi.org/10.1038/s41591-020-0883-7>
- Girona, T. (2020), Confinement time required to avoid a quick rebound of Covid-19: Predictions from a Monte Carlo stochastic model. *Frontiers in Physics*, **8**, 186. <https://doi.org/10.3389/fphy.2020.00186>
- Gostic, K., Gomez, A. C. R., Mummah, R. O., Kucharski, A. J., & Lloyd-Smith, J. O. (2020), Estimated effectiveness of symptom and risk screening to prevent the spread of COVID-19. *Elife*, **9**, e55570. <https://doi.org/10.7554/eLife.55570>
- Harapan, H., Itoh, N., Yufika, A., Winardi, W., Keam, S., Te, H., Megawati, D., Hayati, Z., Wagner, A. L., & Mudatsir, M. (2020), Coronavirus disease 2019 (COVID-19): A literature review. *Journal of Infection and Public Health*, **13**(5), 667–673. <https://doi.org/10.1016/j.jiph.2020.03.019>
- He, S., Peng, Y., & Sun, K. (2020), SEIR modeling of the COVID-19 and its dynamics. *Nonlinear Dynamics*, **101**(3), 1667–1680. <https://doi.org/10.1007/s11071-020-05743-y>
- Henssler, J., Stock, F., van Bohemen, J., Walter, H., Heinz, A., & Brandt, L. (2021), Mental health effects of infection containment strategies: quarantine and isolation—a systematic

- review and meta-analysis. *European Archives of Psychiatry and Clinical Neuroscience*, **271**(2), 223–234. <https://doi.org/10.1007/s00406-020-01196-x>
- Hethcote, H. W. (1994), A thousand and one epidemic models, in *Frontiers in mathematical biology*. Springer, pp. 504–515. [https://doi.org/10.1007/978-3-642-50124-1\\_29](https://doi.org/10.1007/978-3-642-50124-1_29)
- Hui, D. S., Zumla, A., & Tang, J. W. (2021), Lethal zoonotic coronavirus infections of humans—comparative phylogenetics, epidemiology, transmission, and clinical features of coronavirus disease 2019, The Middle East respiratory syndrome and severe acute respiratory syndrome. *Current Opinion in Pulmonary Medicine*, **27**(3), 146–154. <https://doi.org/10.1097/MCP.0000000000000774>
- Huy, N. T., Nguyen Tran, M. D., Mohammed Alhady, S. T., Luu, M. N., Hassan, A. K., Giang, T. V., Truong, L. V., Ravikulan, R., Raut, A. P., & Dayyab, F. M. (2021), Perceived Stress of Quarantine and Isolation During COVID-19 Pandemic: A Global Survey. *Frontiers in Psychiatry*, **12**, 651. <https://doi.org/10.3389/fpsy.2021.656664>
- Islam, S. M. D.-U., Bodrud-Doza, M., Khan, R. M., Haque, M. A., & Mamun, M. A. (2020), Exploring COVID-19 stress and its factors in Bangladesh: a perception-based study. *Heliyon*, **6**(7), e04399. <https://doi.org/10.1016/j.heliyon.2020.e04399>
- Ivorra, B., Ferrández, M. R., Vela-Pérez, Maria., & Ramos, A. M. (2020), Mathematical modeling of the spread of the coronavirus disease 2019 (COVID-19) taking into account the undetected infections. The case of China. *Communications in Nonlinear Science and Numerical Simulation*, **88**, 105303. <https://doi.org/10.1016/j.cnsns.2020.105303>
- Janardhan, V., Janardhan, V., & Kalousek, V. (2020), COVID-19 as a Blood Clotting Disorder Masquerading as a Respiratory Illness: A Cerebrovascular Perspective and Therapeutic Implications for Stroke Thrombectomy. *Journal of Neuroimaging*, **30**(5), 555–561. <https://doi.org/10.1111/jon.12770>
- Jurblum, M., Ng, C. H., & Castle, D. J. (2020), Psychological consequences of social isolation and quarantine: Issues related to COVID-19 restrictions. *Australian Journal of General*

- Practice*, **49**(12), 778–783. <https://search.informit.org/doi/10.3316/informit.638701007415032>
- Kateman, B. (2020), /www.forbes.com/sites/briankateman/2020/03/11/want-to-boost-your-immune-system-a-healthy-diet-is-an-important-start/?sh=1453668f78ae. *March 11, 2020*, **16**, 2020.
- Khan, A. H., Sultana, M. S., Hossain, S., Hasan, M. T., Ahmed, H. U., & Sikder, M. T. (2020), The impact of COVID-19 pandemic on mental health & wellbeing among home-quarantined Bangladeshi students: A cross-sectional pilot study. *Journal of Affective Disorders*, **277**, 121–128. <https://doi.org/10.1016/j.jad.2020.07.135>
- Khan, M., Adil, S. F., Alkhathlan, H. Z., Tahir, M. N., Saif, S., Khan, M., & Khan, S. T. (2021), COVID-19: a global challenge with old history, epidemiology and progress so far. *Molecules*, **26**(1), 39. <https://doi.org/10.3390/molecules26010039>
- Khan, Muhammad Altaf., & Atangana, A. (2020), Modeling the dynamics of novel coronavirus (2019-nCov) with fractional derivative. *Alexandria Engineering Journal*, **59**(4), 2379–2389. <https://doi.org/10.1016/j.aej.2020.02.033>
- Koh, D., Lim, M. K., Chia, S. E., Ko, S. M., Qian, F., Ng, V., Tan, B. H., Wong, K. S., Chew, Wuen M., & Tang, H. K. (2005), Risk perception and impact of severe acute respiratory syndrome (SARS) on work and personal lives of healthcare Workers in Singapore What can we Learn? *Medical Care*, pp. 676–682. <https://www.jstor.org/stable/3768367>
- Korobeinikov, A., & Wake, G. C. (2002), Lyapunov functions and global stability for SIR, SIRS, and SIS epidemiological models. *Applied Mathematics Letters*, **15**(8), 955–960. [https://doi.org/10.1016/S0893-9659\(02\)00069-1](https://doi.org/10.1016/S0893-9659(02)00069-1)
- Kouidere, A., Youssoufi, L. E. L., Ferjouchia, H., Balatif, O., & Rachik, M. (2021), Optimal Control of Mathematical modeling of the spread of the COVID-19 pandemic with highlighting the negative impact of quarantine on diabetics people with Cost-effectiveness. *Chaos, Solitons & Fractals*, **145**, 110777. <https://doi.org/10.1016/j.chaos.2021.110777>

- LaSalle, J. P. (1976), Stability theory and invariance principles, in 'Dynamical systems. Elsevier, pp. 211–222. <https://doi.org/10.1016/B978-0-12-164901-2.50021-0>
- Lengiteng'i, L., Kajunguri, D., & Nkansah-Gyekye, Y. (2016), Modeling the Effect of Stress and Stigma on the Transmission and Control of Tuberculosis Infection. *American Scientific Research Journal for Engineering, Technology, and Sciences (ASRJETS)*, **24**(1), 26–50.
- Lin, Q., Zhao, S., Gao, D., Lou, Y., Yang, S., Musa, S. S., Wang, M. H., Cai, Y., Wang, W., & Yang, L. (2020), A conceptual model for the coronavirus disease 2019 (COVID-19) outbreak in Wuhan, China with individual reaction and governmental action. *International Journal of Infectious Diseases*, **93**, 211–216. <https://doi.org/10.1016/j.ijid.2020.02.058>
- Link, B. G., & Phelan, J. C. (2001), Conceptualizing stigma. *Annual Review of Sociology*, **27**(1), 363–385. <https://doi.org/10.1146/annurev.soc.27.1.363>
- López Steinmetz, L. C., Dutto Florio, M. A., Leyes, C. A., Fong, S. B., Rigalli, A., & Godoy, J. C. (2020), Levels and predictors of depression, anxiety, and suicidal risk during COVID-19 pandemic in Argentina: the impacts of quarantine extensions on mental health state. *Psychology, Health & Medicine*, pp. 1–17. <https://doi.org/10.1080/13548506.2020.1867318>
- Macdonald, G. (1950), The analysis of infection rates in diseases in which super infection occurs. *Tropical Diseases Bulletin*, **47**, 907–915. <https://www.cabdirect.org/cabdirect/abstract/19512202350>
- Mahamid, F. A., Veronese, G., & Bdier, D. (2021), Fear of coronavirus (COVID-19) and mental health outcomes in Palestine: The mediating role of social support. *Current Psychology*, pp. 1–10. <https://doi.org/10.1007/s12144-021-02395-y>
- Maier, B. F., & Brockmann, D. (2020), Effective containment explains subexponential growth in recent confirmed COVID-19 cases in China. *Science*, **368**(6492), 742–746. <https://doi.org/10.1126/science.abb4557>
- Mandal, M., Jana, S., Nandi, S. K., Khatua, A., Adak, S., & Kar, T. K. (2020), A model based

- study on the dynamics of COVID-19: Prediction and control. *Chaos, Solitons & Fractals*, **136**, 109889. <https://doi.org/10.1016/j.chaos.2020.109889>
- Mbogo, Rachel W., & Odhiambo, J. W. (2021), COVID-19 outbreak, social distancing and mass testing in Kenya-insights from a mathematical model. *Afrika Matematika*, pp. 1–16. <https://doi.org/10.1007/s13370-020-00859-1>
- Meacci, L. & Primicerio, M. (2021), Pandemic fatigue impact on COVID-19 spread: A mathematical modelling answer to the Italian scenario. *Results in Physics*, p. 104895. <https://doi.org/10.1016/j.rinp.2021.104895>
- Morato, M. M., Bastos, S. B., Cajueiro, D. O., & Normey-Rico, J. E. (2020), An optimal predictive control strategy for COVID-19 (SARS-CoV-2) social distancing policies in Brazil. *Annual Reviews in Control*, **50**, 417–431. <https://doi.org/10.1016/j.arcontrol.2020.07.001>
- Mpeshe, Saul C., & Nyerere, N. (2021), Modeling the dynamics of coronavirus disease pandemic coupled with fear epidemics. *Computational and Mathematical Methods in Medicine*, **2021**. <https://doi.org/10.1155/2021/6647425>
- Muhirwa, J. P., Mbalawata, S. I., & Masanja, V. G. (2021), Markov Chain Monte Carlo Analysis of the Variable-Volume Exothermic Model for a Continuously Stirred Tank Reactor. *Engineering, Technology & Applied Science Research*, **11**(2), 6919–6929. <https://doi.org/10.48084/etasr.3962>
- Nemawejje, H., Shaban, N., & Hove-Musekwa, S. (2011), Modeling the effect of stress on the dynamics and treatment of Tuberculosis, PhD thesis, MSc. Thesis, UDSM, Dar Es Salaam.
- Ojiambo, V. N., Kimathi, M., Mwalili, S., Gathungu, D., & Mbogo, R. (2020), A Human-Pathogen SEIR-P Model for COVID-19 Outbreak under different intervention scenarios in Kenya. *MedRxiv*. <https://doi.org/10.1101/2020.05.15.20102954>
- Okuonghae, D., & Oname, A. (2020), Analysis of a mathematical model for COVID-19 population dynamics in Lagos, Nigeria. *Chaos, Solitons & Fractals*, **139**, 110032. <https://doi.org/10.1016/j.chaos.2020.110032>

- Organization, W. Health. (2020), Considerations for quarantine of individuals in the context of containment for coronavirus disease (COVID-19): interim guidance, 19 March 2020. *Technical report*. <https://iris.paho.org/handle/10665.2/51961>
- Ornell, F., Schuch, J. B., Sordi, A. O., & Kessler, F. H. P. (2020), “Pandemic fear” and COVID-19: mental health burden and strategies. *Brazilian Journal of Psychiatry*, **42**(3), 232–235. <https://doi.org/10.1590/1516-4446-2020-0008>
- Pancani, L., Marinucci, M., Aureli, N., & Riva, P. (2021), Forced Social Isolation and Mental Health: A Study on 1,006 Italians Under COVID-19 Lockdown. *Frontiers in Psychology*, **12**, 1540. <https://doi.org/10.3389/fpsyg.2021.663799>
- Patil, A. (2021), Routh-Hurwitz criterion for stability: an overview and its implementation on characteristic equation vectors using MATLAB. *Emerging Technologies in Data Mining and Information Security*, pp. 319–329. [https://doi.org/10.1007/978-981-15-9927-9\\_32](https://doi.org/10.1007/978-981-15-9927-9_32)
- Peiris, J. S. M., Lai, S. T., Poon, L. L. M., Guan, Y., Yam, L. Y. C., Lim, W., Nicholls, J., Yee, W. K. S., Yan, W. W., & Cheung, M. T. (2003), Coronavirus as a possible cause of severe acute respiratory syndrome. *The Lancet*, **361**(9366), 1319–1325. [https://doi.org/10.1016/S0140-6736\(03\)13077-2](https://doi.org/10.1016/S0140-6736(03)13077-2)
- Peter, O. J., Qureshi, S., Yusuf, A., Al-Shomrani, M., & Idowu, A. A. (2021), A new mathematical model of COVID-19 using real data from Pakistan. *Results in Physics*, **24**, 104098. <https://doi.org/10.1016/j.rinp.2021.104098>
- Pfefferbaum, B., & North, C. S. (2020), Mental health and the Covid-19 pandemic. *New England Journal of Medicine*, **383**(6), 510–512. <https://doi.org/10.1056/NEJMp2008017>
- Poudel, K. & Subedi, P. (2020), Impact of COVID-19 pandemic on socioeconomic and mental health aspects in Nepal. *International Journal of Social Psychiatry*, **66**(8), 748–755. <https://doi.org/10.1177/0020764020942247>
- Prati, G. (2021), Mental health and its psychosocial predictors during national quarantine in Italy against the coronavirus disease 2019 (COVID-19). *Anxiety, Stress, & Coping*, **34**(2), 145–156. <https://doi.org/10.1080/10615806.2020.1861253>

- Prem, K., Liu, Y., Russell, T. W., Kucharski, A. J., Eggo, R. M., Davies, N., Flasche, S., Clifford, S., Pearson, C. A. B., & Munday, J. D. (2020), The effect of control strategies to reduce social mixing on outcomes of the COVID-19 epidemic in Wuhan, China: a modelling study. *The Lancet Public Health*. [https://doi.org/10.1016/S2468-2667\(20\)30073-6](https://doi.org/10.1016/S2468-2667(20)30073-6)
- Rannala, B. (2002), Identifiability of parameters in MCMC Bayesian inference of phylogeny. *Systematic Biology*, **51**(5), 754–760. <https://doi.org/10.1080/10635150290102429>
- Safi, M. A. (2019), Global stability analysis of two-stage quarantine-isolation model with Holling type II incidence function. *Mathematics*, **7**(4), 350. <https://doi.org/10.3390/math7040350>
- Saltzman, L. Y., Hansel, Tonya C., & Bordnick, P. S. (2020), Loneliness, isolation, and social support factors in post-COVID-19 mental health., *Psychological Trauma: Theory, Research, Practice, and Policy*, **12**(S1), S55. <https://doi.org/10.1037/tra0000703>
- Savi, P. V., Savi, M. A., & Borges, B. (2020), A mathematical description of the dynamics of coronavirus disease 2019 (COVID-19): a case study of Brazil. *Computational and Mathematical Methods in Medicine*, **2020**. <https://doi.org/10.1155/2020/9017157>
- Serafini, G., Parmigiani, B., Amerio, A., Aguglia, A., Sher, L., & Amore, M. (2020), The psychological impact of COVID-19 on the mental health in the general population. *QJM: An International Journal of Medicine*, **113**(8), 531–537. <https://doi.org/10.1093/qjmed/hcaa201>
- Serhani, M., & Labbardi, H. (2020), Mathematical modeling of COVID-19 spreading with asymptomatic infected and interacting peoples. *Journal of Applied Mathematics and Computing*, pp. 1–20. <https://doi.org/10.1007/s12190-020-01421-9>
- Siettos, C. I., & Russo, L. (2013), Mathematical modeling of infectious disease dynamics. *Virulence*, **4**(4), 295–306. <https://doi.org/10.4161/viru.24041>
- Singh, R., & Subedi, M. (2020), COVID-19 and stigma: Social discrimination towards front-line healthcare providers and COVID-19 recovered patients in Nepal. *Asian Journal of Psychiatry*. <https://doi.org/10.1016/j.ajp.2020.102222>

- Smith, D. G. (2020), <https://elemental.medium.com/coronavirus-may-be-a-blood-vessel-disease-which-explains-everything-2c4032481ab2>. May 29, 2020, **16**, 2020. <https://doi.org/10.1109/ICCICT50803.2021.9510051>
- Solonen, A., Ollinaho, P., Laine, M., Haario, H., Tamminen, J., & Järvinen, H. (2012), Efficient MCMC for climate model parameter estimation: Parallel adaptive chains and early rejection. *Bayesian Analysis*, **7**(3), 715–736. <https://doi.org/10.1214/12-BA724>
- Steardo, L., Steardo Jr, L., Zorec, R., & Verkhatsky, A. (2020), Neuroinfection may contribute to pathophysiology and clinical manifestations of COVID-19. *Acta Physiologica (Oxford, England)*. <https://doi.org/10.1111/apha.13473>
- Torales, J., Ríos-González, C., Barrios, I., O'Higgins, M., González, I., García, O., Castaldelli-Maia, João M., & Ventriglio, A. (2020), Self-perceived stress during the quarantine of COVID-19 pandemic in Paraguay: an exploratory survey. *Frontiers in Psychiatry*, **11**, 1155. <https://doi.org/10.3389/fpsy.2020.558691>
- Tsang, K. W., Ho, P. L., Ooi, G. C., Yee, W. K., Wang, T., Chan-Yeung, M., Lam, W. K., Seto, W. H., Yam, Loretta Y., & Cheung, T. M. (2003), A cluster of cases of severe acute respiratory syndrome in Hong Kong. *New England Journal of Medicine*, **348**(20), 1977–1985. <https://doi.org/10.1056/NEJMoa030666>
- Ullah, S., & Khan, M. A. (2020), Modeling the impact of non-pharmaceutical interventions on the dynamics of novel coronavirus with optimal control analysis with a case study. *Chaos, Solitons & Fractals*, **139**, 110075. <https://doi.org/10.1016/j.chaos.2020.110075>
- Usher, K., Durkin, J., & Bhullar, N. (2020), The COVID-19 pandemic and mental health impacts. *International Journal of Mental Health Nursing*, **29**(3), 315. <https://doi.org/10.1111/inm.12726>
- Van den Driessche, P., & Watmough, J. (2002), Reproduction numbers and sub-threshold endemic equilibria for compartmental models of disease transmission. *Mathematical Biosciences*, **180**(1-2), 29–48. [https://doi.org/10.1016/S0025-5564\(02\)00108-6](https://doi.org/10.1016/S0025-5564(02)00108-6)
- Vargas-De-León, C. (2009), Constructions of Lyapunov functions for classic SIS, SIR and SIRS



epidemic models with variable population size. *Foro-Red-Mat: Revista Electrónica de Contenido Matemático*, **26**, 1–12.

Velavan, Thirumalaisamy P., & Meyer, C. G. (2020), The COVID-19 epidemic. *Tropical Medicine & International Health*, **25**(3), 278. <https://doi.org/10.1111/tmi.13383>

Zaki, A. M., Van Boheemen, S., Bestebroer, T. M., Osterhaus, Albert D. M. E., & Fouchier, R. A. M. (2012), Isolation of a novel coronavirus from a man with pneumonia in Saudi Arabia. *New England Journal of Medicine*, **367**(19), 1814–1820. <https://doi.org/10.1056/NEJMoa1211721>

Zhang, Z., Gul, R., & Zeb, A. (2021), Global sensitivity analysis of COVID-19 mathematical model. *Alexandria Engineering Journal*, **60**(1), 565–572. <https://doi.org/10.1016/j.aej.2020.09.035>

Zhou, J., Liu, L., Xue, P., Yang, X., & Tang, X. (2020), Mental health response to the COVID-19 outbreak in China. *American Journal of Psychiatry*, **177**(7), 574–575. <https://doi.org/10.1176/appi.ajp.2020.20030304>

## APPENDICES

### MATLAB CODES

```
% MODEL
function ds = Jamesmodel(t,y,par)
S = y(1);
E = y(2);
Q = y(3);
I = y(4);
H = y(5);
R = y(6);

N = S+E+Q+I+H+R;

function dy = mymodel(~,y,par)

beta=par(1);
mu=par(2);
eta_1=par(3);
omega=par(4);
theta=par(5);
alpha=par(6);
b=par(7);
delta=par(8);
eta_2=par(9);
nu=par(10);
rho=par(11);
lambda=par(12);
phi=par(13);

%N = sum(y);
```

```

x = y;

dy = [mu+alpha*x(3)+rho*x(6)-beta*x(4)*x(1)-b*x(1);
beta*x(4)*x(1)-theta*x(2)-omega*x(2)-(1-omega)*x(2)-b*x(2);
phi + theta*x(2)-alpha*x(3)-eta_1*x(3)-b*x(3);
(1-omega)*x(2)+eta_1*x(3)-(eta_2+nu+delta+b)*x(4);
omega*x(2)+eta_2*x(4)-(lambda+delta+b)*x(5);
lambda*x(5)+nu*x(4)-(rho+b)*x(6)];

ds = [dSdt;dEdt;dQdt; dIdt; dHdt; dRdt];

end

%Parameter values
N=1000;
beta=0:0.001:0.45;
mu=50;
eta_1=0.85;
omega=0.083;
theta=0.2435;
alpha=0.0015;
b=0.0104;
delta=0.039;
eta_2=0.65;
nu=0.07;
rho=0.03;
lambda=0.02;
phi=0.01;

%%%%%%%%%%%%%%%%%%%%%%%%%%%%%%%%%%%%%%%%%%%%%%%%%%%%%%%%%%%%%%%%%%%%%%%%%%%%%%

fx1 = @(t,x)[mu+alpha*x(3)+rho*x(6)-beta*x(4)*x(1)-b*x(1);

```

```

beta*x(4)*x(1)-theta*x(2)-omega*x(2)-(1-omega)*x(2)-b*x(2);
phi+theta*x(2)-alpha*x(3)-eta_1*x(3)-b*x(3);
(1-omega)*x(2)+eta_1*x(3)-(eta_2+nu+delta+b)*x(4);
omega*x(2)+eta_2*x(4)-(lambda+delta+b)*x(5);
lambda*x(5)+nu*x(4)-(rho+b)*x(6)];

```

```

[t,x1]=ode45(fx1,[0 20],[500,0,0,0,0,0]);
figure (1)
plot(t,x1(:,1),'y','LineWidth',1.5)
grid on
title('Susceptible Population at disease free')
xlabel('Time (Days)')
ylabel('Susceptible population')

```

%%%

```

fx2=@(t,x)[mu+alpha*x(3)+rho*x(6)-beta*x(4)*x(1)-b*x(1);
beta*x(4)*x(1)-theta*x(2)-omega*x(2)-(1-omega)*x(2)-b*x(2);
phi+theta*x(2)-alpha*x(3)-eta_1*x(3)-b*x(3);
(1-omega)*x(2)+eta_1*x(3)-(eta_2+nu+delta+b)*x(4);
omega*x(2)+eta_2*x(4)-(lambda+delta+b)*x(5);
lambda*x(5)+nu*x(4)-(rho+b)*x(6)];

```

```

[t,x2]=ode45(fx2,[0 20],[500,200,100,50,30,20]);
figure (2)
plot(t,x2(:,2),'g','LineWidth',0.5)
grid on
title('Exposed Population')
xlabel('Time (Days)')
ylabel('Exposed population')

```

%%%

```
fx3= @(t,x)[mu+alpha*x(3)+rho*x(6)-beta*x(4)*x(1)-b*x(1);
beta*x(4)*x(1)-theta*x(2)-omega*x(2)-(1-omega)*x(2)-b*x(2);
phi+theta*x(2)-alpha*x(3)-eta_1*x(3)-b*x(3);
(1-omega)*x(2)+eta_1*x(3)-(eta_2+nu+delta+b)*x(4);
omega*x(2)+eta_2*x(4)-(lambda+delta+b)*x(5);
lambda*x(5)+nu*x(4)-(rho+b)*x(6)];
```

```
[t,x3]=ode45(fx3,[0 20],[500,200,100,50,30,20]);
figure (3)
plot(t,x3(:,3),'b','LineWidth',1.5)
grid on
title ('Quarantined Population ')
xlabel('Time (Days)')
ylabel('Quarantined population')
```

%%%

```
fx4= @(t,x)[mu+alpha*x(3)+rho*x(6)-beta*x(4)*x(1)-b*x(1);
beta*x(4)*x(1)-theta*x(2)-omega*x(2)-(1-omega)*x(2)-b*x(2);
phi+theta*x(2)-alpha*x(3)-eta_1*x(3)-b*x(3);
(1-omega)*x(2)+eta_1*x(3)-(eta_2+nu+delta+b)*x(4);
omega*x(2)+eta_2*x(4)-(lambda+delta+b)*x(5);
lambda*x(5)+nu*x(4)-(rho+b)*x(6)];
```

```
[t,x4]=ode45(fx4,[0 20],[500,200,100,50,30,20]);
figure (4)
plot(t,x4(:,4),'r','LineWidth',1.5)
grid on
title ('Infected Population ')
xlabel('Time (Days)')
```

```
ylabel('Infected population')
```

```
%%%%%%%%%%%%%%%%%%%%%%%%%%%%%%%%%%%%%%%%%%%%%%%%%%%%%%%%%%%%%%%%%%%%%%%%%%
```

```
fx5= @(t,x)[mu+alpha*x(3)+rho*x(6)-beta*x(4)*x(1)-b*x(1);
beta*x(4)*x(1)-theta*x(2)-omega*x(2)-(1-omega)*x(2)-b*x(2);
phi+theta*x(2)-alpha*x(3)-eta_1*x(3)-b*x(3);
(1-omega)*x(2)+eta_1*x(3)-(eta_2+nu+delta+b)*x(4);
omega*x(2)+eta_2*x(4)-(lambda+delta+b)*x(5);
lambda*x(5)+nu*x(4)-(rho+b)*x(6)];
```

```
[t,x5]=ode45(fx5,[0 20],[500,200,100,50,30,20]);
```

```
figure (5)
```

```
plot(t,x5(:,5),'m','LineWidth',1.5)
```

```
grid on
```

```
title('Hospitalized Population')
```

```
xlabel('Time (Days)')
```

```
ylabel('Hospitalized population')
```

```
%%%%%%%%%%%%%%%%%%%%%%%%%%%%%%%%%%%%%%%%%%%%%%%%%%%%%%%%%%%%%%%%%%%%%%%%%%
```

```
fx6= @(t,x)[mu+alpha*x(3)+rho*x(6)-beta*x(4)*x(1)-b*x(1);
beta*x(4)*x(1)-theta*x(2)-omega*x(2)-(1-omega)*x(2)-b*x(2);
phi+theta*x(2)-alpha*x(3)-eta_1*x(3)-b*x(3);
(1-omega)*x(2)+eta_1*x(3)-(eta_2+nu+delta+b)*x(4);
omega*x(2)+eta_2*x(4)-(lambda+delta+b)*x(5);
lambda*x(5)+nu*x(4)-(rho+b)*x(6)];
```

```
[t,x6]=ode45(fx6,[0 20],[500,200,100,50,30,20]);
```

```
figure (6)
```

```
plot(t,x6(:,6),'k','LineWidth',1.5)
```

```
grid on
```

```

title ( 'Recovered Population ' )
xlabel ( 'Time (Days)' )
ylabel ( 'Recovered population ' )

```

```

%%%%%%%%%%%%%%%%%%%%%%%%%%%%%%%%%%%%%%%%%%%%%%%%%%%%%%%%%%%%%%%%%%%%%%%%

```

```

%Total Population
fx= @(t , x) [mu+alpha*x(3)+rho*x(6)-beta*x(4)*x(1)-b*x(1);
beta*x(4)*x(1)-theta*x(2)-omega*x(2)-(1-omega)*x(2)-b*x(2);
phi+theta*x(2)-alpha*x(3)-eta_1*x(3)-b*x(3);
(1-omega)*x(2)+eta_1*x(3)-(eta_2+nu+delta+b)*x(4);
omega*x(2)+eta_2*x(4)-(lambda+delta+b)*x(5);
lambda*x(5)+nu*x(4)-(rho+b)*x(6)];

```

```

[t , x]=ode45 (fx , [0 20] , [500 , 200 , 100 , 50 , 30 , 20]);
figure (7)
plot (t , x(:,1) , 'y' , t , x(:,2) , 'g' , t , x(:,3) , 'b' , \
t , x(:,4) , 'r' , t , x(:,5) , 'm' , t , x(:,6) , 'k' , 'lineWidth' , 1.5)
legend ( 'S' , 'E' , 'Q' , 'I' , 'H' , 'R' );
grid on
title ( 'Total Population ' )
xlabel ( 'Time (Days)' )
ylabel ( 'Total population ' )

```

```

% R_0
function R0 = myR0New(par)

```

```

beta=par(1);
mu=par(2);
eta_1=par(3);
omega=par(4);
theta=par(5);

```

```

alpha=par(6);
b=par(7);
delta=par(8);
eta_2=par(9);
nu=par(10);
q=par(11);
% rho=par(12);
% lambda=par(13);
% phi=par(14);

R0 = beta*mu*(eta_1*(q-omega*q+theta)+q*(1-omega)...
*(alpha+b))./b*((b+theta+q)*(alpha+b+eta_1)...
*(b+delta+eta_2+nu));

```



## RESEARCH OUTPUTS

### 1. Publications

Paul, J. N., Mirau, S. S., & Mbalawata, I. S. (2022). Mathematical Approach to Investigate Stress due to Control Measures to Curb COVID-19. *Computational and Mathematical Methods in Medicine*, (2022). <https://doi.org/https://doi.org/10.1155/2022/7772263>

### 2. Poster Presentation

## Research Article

# Mathematical Approach to Investigate Stress due to Control Measures to Curb COVID-19

James Nicodemus Paul <sup>1</sup>, Silas Steven Mirau <sup>1</sup> and Isambi Sailon Mbalawata <sup>2</sup>

<sup>1</sup>*School of Computational and Communication Science and Engineering, The Nelson Mandela, African Institution of Science and Technology, P.O. Box 447, Arusha, Tanzania*

<sup>2</sup>*African Institute for Mathematical Sciences, NEI Global Secretariat, rue KG590 St., Kigali, Rwanda*

Correspondence should be addressed to James Nicodemus Paul; paulj@nm-aist.ac.tz

Received 14 July 2021; Revised 30 September 2021; Accepted 15 December 2021; Published 13 January 2022

Academic Editor: Murat Sari

Copyright © 2022 James Nicodemus Paul et al. This is an open access article distributed under the Creative Commons Attribution License, which permits unrestricted use, distribution, and reproduction in any medium, provided the original work is properly cited.

COVID-19 is a world pandemic that has affected and continues to affect the social lives of people. Due to its social and economic impact, different countries imposed preventive measures that are aimed at reducing the transmission of the disease. Such control measures include physical distancing, quarantine, hand-washing, travel and boarder restrictions, lockdown, and the use of hand sanitizers. Quarantine, out of the aforementioned control measures, is considered to be more stressful for people to manage. When people are stressed, their body immunity becomes weak, which leads to multiplying of coronavirus within the body. Therefore, a mathematical model consisting of six compartments, Susceptible-Exposed-Quarantine-Infectious-Hospitalized-Recovered (*SEQIHR*) was developed, aimed at showing the impact of stress on the transmission of COVID-19 disease. From the model formulated, the positivity, bounded region, existence, uniqueness of the solution, the model existence of free and endemic equilibrium points, and local and global stability were theoretically proved. The basic reproduction number ( $R_0$ ) was derived by using the next-generation matrix method, which shows that, when  $R_0 < 1$ , the disease-free equilibrium is globally asymptotically stable whereas when  $R_0 > 1$  the endemic equilibrium is globally asymptotically stable. Moreover, the Partial Rank Correlation Coefficient (PRCC) method was used to study the correlation between model parameters and  $R_0$ . Numerically, the *SEQIHR* model was solved by using the Rung-Kutta fourth-order method, while the least square method was used for parameter identifiability. Furthermore, graphical presentation revealed that when the mental health of an individual is good, the body immunity becomes strong and hence minimizes the infection. Conclusively, the control parameters have a significant impact in reducing the transmission of COVID-19.

## 1. Introduction

Coronavirus disease-2019 (COVID-19) is an infectious disease caused by a newly discovered coronavirus named severe acute respiratory syndrome coronavirus-2 (SARS-COV-2). This pandemic originated in Wuhan, China, with the first case reported in December 2019, and has spread to other parts of the world in early 2020 as discussed in [1, 2]. When the total confirmed cases globally were 125,260 and 4613 deaths in 24 hours, the World Health Organization (WHO), on 12th March 2020, announced COVID-19 disease as the World pandemic as presented in [3]. The global leaders were greatly bothered by this disease

due to its fast spread from one person to another and its social and economic impact on their respective countries. The WHO and country leaders focused on finding ways to reduce the transmission of the disease by introducing some measures such as lockdown, quarantine, closing borders, travel bans, and isolation centers [4–7].

Mathematical models are essential tools in evaluating various transmission and control intervention programs for infectious diseases. There are a number of mathematical models on COVID-19 pandemic developed from the start of this human disturbing disease [8]. The author discusses social isolation measures taken by the government in Brazil to fight COVID-19 disease, and also, the protection of health

workers was discussed by Masandawa et al. [9]. In their study, Khan et al. [10] discussed on isolation and quarantine as the best ways of fighting COVID-19 disease. At the beginning of the pandemic, many ways to fight the disease were introduced by many scientists. Ullah and Khan [11] explored several ways such as social distancing, self-isolation, quarantine, and hospitalization and concluded that these are the best ways to curb COVID-19. Dos Santos [12], in his review, studied on the effects of social distancing and social isolation measures as good ways to fight against the disease, although they lead to social stress which influences the spread of the disease. Early 2020, some mathematical models for COVID-19 were developed and published. Dhanwant and Ramanathan [13] explored how the social distancing in India during the pandemic helped to reduce the transmission of COVID-19 disease because the spread of the disease is by social contact. Khan and Atangana [14] discussed the interaction of bats and unknown hosts and then the interaction of people in the seafood market where there is enough source of infection. They presented their results graphically to show how they can minimize the infections.

Ashcroft et al. [15] discussed the impact of quarantine on the transmission of COVID-19 disease showing that many countries impose quarantine to ensure the exposed people and those from abroad are isolated for a specific period of time to prevent the spread of the disease. However, these measures took a larger economical toll and affected the health of the isolated individuals. Prati [16], from Italy, discussed the national impacts of quarantine psychologically. In their online survey of 1569 people living in Italy, they found that there are psychosocial factors that influence the disease, such as media exposure to COVID-19 outbreak, financial loss, higher worry, and negative attitude towards quarantine leading to psychological impacts. The mental health of public and healthcare professionals is affected by the pandemic, especially during quarantine time where hypervigilance arises because of fear and anxiety [17, 18].

Stress affects many quarantined people whereby their immune system is disturbed by the COVID-19, and this is most likely because during quarantine, people are isolated from their families and community members, so they develop fear, and later, the body becomes stressed which affects their immune system. When the immune system is disturbed, it fails to fight against the intruders, which leads to the fast spread of COVID-19 throughout the body. Therefore, this research is aimed at formulating a deterministic model to explore the impact of stress in quarantine to the human population. The model has six compartmental classes (Susceptible, Exposed, Quarantine, Infectious, Hospitalized, and Recovered). The model is extended from the model given in [19] by incorporating the hospitalized class and introducing a stress parameter in a quarantined and infected class.

The introduction of this work presented in Section 1. Model formulation, discussion of its compartments, and parameters are presented in Section 2. Section 3 contains the discussion of the model analysis theoretically, which includes positivity and bounded regions, the existence, uniqueness of the model, reproduction number, and local

and global stability of the COVID-19 disease. Section 4 deals with a discussion of numerical simulation for the model, including sensitivity analysis, numerical solutions, PRCC results, parameter identifiability, and model fitting by the least square method are presented. Section 5 concludes this work and contains the possible extension of this model.

## 2. Model Formulation

In this study, a mathematical model for COVID-19 was formulated based on realistic assumptions. The total population model  $N(t)$  is divided into six human subclasses, namely, susceptible  $S(t)$  (those who are at risk to contact COVID-19 infection), exposed  $E(t)$  (the population which is infected but not infectious), quarantined  $Q(t)$  (those who contacted a COVID-19-infected individual but did not develop any symptom), infectious  $I(t)$  (those who have COVID-19 symptoms and are capable of spreading the disease), hospitalized  $H(t)$  (infectious individuals admitted to a healthcare facility (active cases)), and recovered  $R(t)$  (those recovered from the COVID-19).

**2.1. Model Assumptions.** By presenting an infectious disease with a mathematical model, the following assumptions for the *SEQIHR* model are considered based on the characteristics of COVID-19 disease in this work.

- (i) All members of the population can have an equal chance of getting a COVID-19 disease
- (ii) Stress in a quarantined class is higher than that in an infectious class
- (iii) Population from outside the country were taken directly to quarantine class
- (iv) All compartments have an equal natural death rate
- (v) The death due to the disease may be only in two variables (infectious and hospitalized)
- (vi) Recruitment rates (Newborns) are assumed to be susceptible
- (vii) Individuals are equally likely to be infectious to the infected individuals when coming into contact
- (viii) Infected individuals are identified early and isolated (hospitalized) immediately for treatment
- (ix) There are only two options, a patient will either recover or die, which means no treatment failure
- (x) The population differs within a given time step where recruitment and leaving rates differ

**2.2. Model Compartments and Dynamics.** From Section 2.1, the variable and parameter descriptions are to be presented by the following *SEQIHR* model compartmental diagram:

Let  $N$  be the total population divided; the transmission dynamics of COVID-19 disease in a population are shown in Figure 1. Consider Table 1, showing the variables and their descriptions:

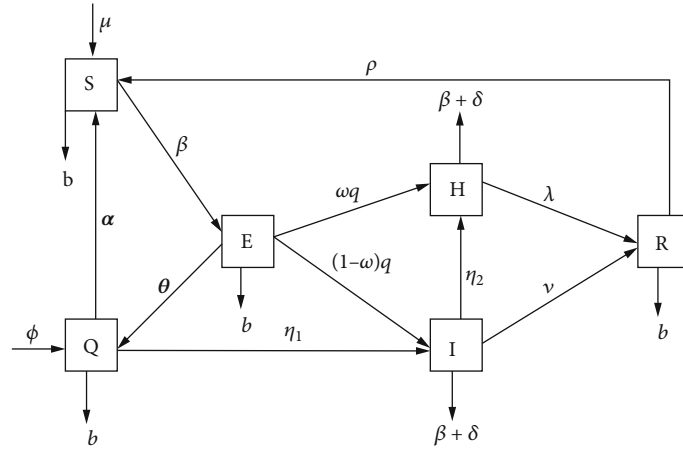


FIGURE 1: Schematic flow diagram showing dynamics of COVID-19.

The total population  $N(t)$  is given by the mathematical equation:

$$N(t) = S(t) + Q(t) + E(t) + I(t) + H(t) + R(t), \quad (1)$$

where  $t \in [0, t]$  and  $t > 0$ .

Table 2 shows the model parameters and their descriptions:

The model parameters found in Equation (2) are described in Table 2. By considering the *SEQIHR* model with six compartments in Figure 1, the following are the transmission phases:

The Susceptible class,  $S(t)$ , increases by the addition of a recruitment rate,  $\mu$ . It also decreases by infection, if contacted with an infected individual at the rate of  $\beta$  and natural death at the rate of  $b$ .

An individual enters the Exposed class,  $E(t)$ , after direct contact with an infected person, with an infection rate  $\beta$ . Furthermore, taking to hospital decreases the rate of  $\omega$  and  $q$  for individuals with multiple symptoms. Individuals with clear (direct) symptoms are presented by  $(1-\omega)$ , and those with no symptoms are represented by  $\theta$ , and then, the population in  $E(t)$  class is diminished by a leaving rate of natural death  $b$ .

The Quarantined class,  $Q(t)$ , was formed by individuals' progress from exposed,  $\theta$ , and population rate from outside the country,  $\phi$ , also decreased by individuals with no symptoms after being tested. Then, the individuals with no infections going back to the susceptible class are presented by  $\alpha$  and those infected individuals after being tested, going to the infectious class at the rate of  $\eta_1$  and diminishing by leaving a natural death rate of  $b$ .

The Infectious class,  $I(t)$ , are individuals who progress from exposed at the rate of  $(1-\omega)$  and then quarantine at the rate of  $\eta_1$ . Additionally, this class decreases with hospitalized individuals at the rate of  $\eta_2$  and recovered at the rate of  $\nu$ . Not only that but also it diminished by leaving the rate of natural death,  $b$ , and death due to the disease,  $\delta$ .

The Hospitalized class,  $H(t)$ , are individuals who progress from the exposed class at the rate of  $\omega$  and  $q$ , then from the infectious compartment at the rate of  $\eta_2$ . Individuals

TABLE 1: Model variable description.

Variables	Description
$S(t)$	Number of susceptible population at time $t$
$Q(t)$	Number of quarantined population at time $t$
$E(t)$	Number of exposed population at time $t$
$I(t)$	Number of infectious population at time $t$
$H(t)$	Number of hospitalized population at time $t$
$R(t)$	Number of recovered population at time $t$

recovered from hospitalized class at the rate of  $\lambda$  and diminished by leaving the rate of natural death,  $b$ , and death due to COVID-19 disease,  $\delta$ .

The Recovered class,  $R(t)$ , are individuals who progress from a hospitalized compartment at the rate of  $\lambda$  and infectious rate  $\nu$  and decrease by recovered individuals who are going back to the susceptible population  $\rho$  and then diminished by the leaving rate of  $b$ .

**2.3. Model Equations.** Based on the assumptions made and the relationship that exists between the variables shown in Figure 1, the system of six ordinary differential equations is formed as in

$$\frac{dS}{dt} = \mu + \alpha Q + \rho R - \beta IS - bS, \quad (2)$$

$$\frac{dE}{dt} = \beta IS - \theta E - qE - bE, \quad (3)$$

$$\frac{dQ}{dt} = \phi + \theta E - \alpha Q - \eta_1 Q - bQ, \quad (4)$$

$$\frac{dI}{dt} = (1-\omega)qE + \eta_1 Q - \eta_2 I - \nu I - \delta I - bI, \quad (5)$$

$$\frac{dH}{dt} = \omega qE + \eta_2 I - \lambda H - \delta H - bH, \quad (6)$$

TABLE 2: Model parameter description.

Parameters	Description
$\beta$	Contact rate (effective transmission rate)
$\mu$	Recruitment rate to the susceptible population
$b$	Human natural death rate
$\phi$	Quarantined population from infected countries
$\rho$	Recovered population rate back to susceptible class
$\alpha$	Population rate after the quarantined period to susceptible
$\nu$	Recovery rate from infected population
$\lambda$	Recovered rate from hospitalized population
$\omega$	Proportion of exposed population with contradicting symptoms
$q$	Progression rate from exposed to hospitalized and infectious classes
$\theta$	Proportion of exposed population with no symptoms
$\eta_1$	Stress to the infected population from quarantine
$\eta_2$	Stress to the hospitalized population from infectious class
$\delta$	Death due to the disease from infectious and hospitalized classes

$$\frac{dR}{dt} = \lambda H + \nu I - \rho R - bR. \quad (7)$$

$$S(t) \geq S(0)e^{-bt}, \quad S(0) \geq 0, \forall t > 0. \quad (11)$$

### 3. Model Analysis

□

In this section, positivity, boundedness, derived equilibrium states, basic reproduction number, and stability analysis are discussed.

**3.1. Positivity of the Model.** For the model equations to be epidemiologically, we need to prove that the state variables are nonnegative  $\forall t \geq 0$ .

**Theorem 1.** *Let the initial data set be  $(S, E, Q, I, H, R)(0) > 0$ . The solution set of the model system 2 is positive  $\forall t > 0$ .*

*Proof.* From the system of model Equation (2), consider the first equation:

$$\frac{dS}{dt} = \mu + \alpha Q + \rho R - (\beta I + b)S. \quad (8)$$

By considering the negative term, by ignoring the rest, Equation (8) is reduced to

$$\frac{dS}{dt} \geq -(\beta I + b)S. \quad (9)$$

This is the first-order linear differential inequality which can be solved by a separable method  $y' = f(x)g(y)$  (where  $S \geq 0$ ) resulting in

$$\int_{S(0)}^{S(t)} \frac{dS}{S} \geq - \int_0^t (\beta I + b) dt, \quad S(t) \geq S(0)e^{-(\beta I + b)t}, \quad (10)$$

in the absence of COVID-19 disease,

By applying the same procedure to the remaining equations, the results are  $E(0) \geq 0$ ,  $Q(0) \geq 0$ ,  $I(0) \geq 0$ ,  $H(0) \geq 0$ , and  $R(0) \geq 0$ . Therefore, the set of solutions  $S(t)$ ,  $E(t)$ ,  $Q(t)$ ,  $I(t)$ ,  $H(t)$ , and  $R(t)$  of the model is positive  $\forall t > 0$ .

**3.2. Invariant (Boundedness) Region.** The SEQIHR model is represented by differential equations in system 2, which is to be analyzed in a feasible region  $\Omega$ , and all state variables and parameters of the model are assumed to be positive  $\forall t \geq 0$ . The bounded region is obtained through the following theorem.

**Theorem 2.** *The set  $\Omega$  is positively invariant and attracts all solutions in  $\mathbb{R}_+^6$ .*

*Proof.* Since  $N(t) = S(t) + Q(t) + E(t) + I(t) + H(t) + R(t)$ , then the derivative of  $N(t)$  is given as

$$\frac{dN}{dt} = \frac{dS}{dt} + \frac{dE}{dt} + \frac{dQ}{dt} + \frac{dI}{dt} + \frac{dH}{dt} + \frac{dR}{dt}. \quad (12)$$

Substituting model Equation (2) to Equation (12) gives

$$\frac{dN}{dt} = \begin{cases} (\mu + \alpha Q + \rho R - \beta IS - bS) + (\beta IS - \theta E - qE - bE) \\ + (\phi + \theta E - \alpha Q - \eta_1 Q - bQ) + ((1 - \omega)qE + \eta_1 Q - \eta_2 I - \nu I - \delta I - bI) \\ + (\omega qE + \eta_2 I - \lambda H - \delta H - bH) + (\lambda H + \nu I - \rho R - bR). \end{cases} \quad (13)$$

Further simplification leads to

$$\frac{dN}{dt} = \mu + \phi - (S + E + Q + I + H + R)b - (\delta I + \delta R), \quad (14)$$

implying that

$$\frac{dN}{dt} = \mu + \phi - Nb - (\delta I + \delta R). \quad (15)$$

For disease-free,  $\delta I \implies 0$  and  $\delta R \implies 0$ , then  $(dN/dt) \leq \mu + \phi - Nb$ .

This is a first-order linear differential equation, by a separable method.

$$\int_{N(0)}^{N(t)} \frac{dN}{(\mu + \phi - bN)} \leq \int_0^t dt, \implies N(t) \geq \frac{\mu + \phi}{b} (1 - e^{-bt}) + N(0)e^{-bt}. \quad (16)$$

□

When  $t = 0$ ,  $N(0) \geq 0$ . When  $t \implies \infty$  then,  $N(\infty) \leq (\mu + \phi)/b$ .

The Invariant region is given by  $\Omega = (S, E, Q, I, H, R) \in \mathbb{R}_+^6 : 0 \leq N(t) \leq (\mu + \phi)/b$ . The SEQIHR model is biologically and epidemiologically meaningful; thus, we can consider the flow generated by the model for analysis.

**3.3. Existence and Uniqueness of the Solution.** From the first-order differential equation given in the form:  $y' = f(t, y)$ ,  $y(t_0) = y_0$ . The following questions will be of interest:

- (i) Under what conditions can we say that a solution to the equation  $y'$  exists?
- (ii) Under what conditions does a unique solution exist to the equation  $y'$ ?

Consider the following equations to answer the question.

$$f_1 = \mu + \alpha Q + \delta R - \beta IS - bS, \quad (17)$$

$$f_2 = \beta IS - \theta E - qE - bE, \quad (18)$$

$$f_3 = \phi + \theta E - (\alpha + \eta_1 + b)Q, \quad (19)$$

$$f_4 = (1 - \omega)qE + \eta_1 Q - (\eta_2 + \nu + \delta + b)I, \quad (20)$$

$$f_5 = \omega qE + \eta_2 I - (\lambda + \delta + b)H, \quad (21)$$

$$f_6 = \lambda H + \nu I - (\rho + b)R. \quad (22)$$

### 3.3.1. Uniqueness of Solution

**Theorem 3.** Let us use  $D$  to denote the domain:

$$|t - t_0| \leq a, \|y - y_0\| \leq b, y = (y_1, y_2, \dots, y_n), \quad y_0 = (y_1^0, y_2^0, \dots, y_n^0). \quad (23)$$

*Proof.* Suppose  $f(t, y)$  satisfies the Lipschitz condition; therefore,

$$\|f(t, y_2) - f(t, y_1)\| \leq k\|x_2 - x_1\|. \quad (24)$$

Whenever the points  $(t, x_1)$  and  $(t, x_2)$  belong to the domain  $D$  and  $k$  is used to represent the positive constant, then, there exist a constant  $\alpha > 0$  and a unique solution  $y(t)$  of system 11 in the interval  $|t - t_0| \leq \alpha$ . It is essential to note that condition (24) is satisfied by  $(\partial f_i / \partial y_j)$ ,  $i, j = 1, 2, 3, \dots, n$  to be continuous and bounded in domain  $D$ . □

If  $f(t, y)$  has a continuous partial derivative  $(\partial f_i / \partial y_j)$  on a bounded closed convex domain  $\mathbb{R}$  (i.e., the convex set of real numbers), where  $\mathbb{R}$  is used to denote real numbers; then it satisfies a Lipschitz condition in  $\mathbb{R}$ . Our interest is in the domain:

$$1 \leq \varepsilon \leq \mathbb{R}. \quad (25)$$

Therefore, we look for the bounded solution of the form  $0 < \mathbb{R} < \infty$ .

### 3.3.2. Existence of a Solution

**Theorem 4.** Let the domain be denoted by  $D$ , also defined in Equation (23), such that Equations (24) and (25) hold. Then, the existing solution of Equation (2) is bounded in the domain  $D$ .

*Proof.* From Equations (10)–(15), by showing that  $\{(\partial f_i / \partial y_j), i, j = 1, 2, 3, 4, 5, 6\}$ , then, Equations (1) and (2) are continuous and bounded. That means the partial derivatives are continuous and bound. Consider the exploration of the partial derivatives for all model equations.

From Equation (17), we obtain the following system of equations:

$$\begin{aligned} \frac{\partial f_1}{\partial S} &= -\beta I - b, \left| \frac{\partial f_1}{\partial S} \right| = |-\beta I - b| < \infty, \\ \frac{\partial f_1}{\partial E} &= 0, \left| \frac{\partial f_1}{\partial E} \right| = |0| < \infty, \\ \frac{\partial f_1}{\partial Q} &= \alpha, \left| \frac{\partial f_1}{\partial Q} \right| = |\alpha| < \infty, \\ \frac{\partial f_1}{\partial I} &= -\beta S, \left| \frac{\partial f_1}{\partial I} \right| = |-\beta S| < \infty, \\ \frac{\partial f_1}{\partial H} &= 0, \left| \frac{\partial f_1}{\partial H} \right| = |0| < \infty, \\ \frac{\partial f_1}{\partial R} &= \rho, \left| \frac{\partial f_1}{\partial R} \right| = |\rho| < \infty. \end{aligned} \quad (26)$$

Similarly, from Equation (18), we obtain the following system of equations:



$$\begin{aligned}
\frac{\partial f_2}{\partial S} &= \beta I, \left| \frac{\partial f_2}{\partial S} \right| = |\beta I| < \infty, \\
\frac{\partial f_2}{\partial E} &= -(\theta + q + b), \left| \frac{\partial f_2}{\partial E} \right| = |-(\theta + q + b)| < \infty, \\
\frac{\partial f_2}{\partial Q} &= 0, \left| \frac{\partial f_2}{\partial Q} \right| = |0| < \infty, \\
\frac{\partial f_2}{\partial I} &= \beta S, \left| \frac{\partial f_2}{\partial I} \right| = |\beta S| < \infty, \\
\frac{\partial f_2}{\partial H} &= 0, \left| \frac{\partial f_2}{\partial H} \right| = |0| < \infty, \\
\frac{\partial f_2}{\partial R} &= 0, \left| \frac{\partial f_2}{\partial R} \right| = |0| < \infty.
\end{aligned} \tag{27}$$

□

The same procedures are taken for Equations (19), (20), (21), and (22). Therefore, all partial derivatives are continuous and bounded; hence, from Theorem 4, it is concluded that there exists a unique solution of the model in Equation (2) in the domain region  $D$ .

**3.4. Existence of Disease-Free Equilibrium Point (DFE).** The disease-free equilibrium point, obtained when the infected components are zero, can be done by setting the right-hand side of the equation equal to zero, as in

$$\frac{dS}{dt} = \frac{dE}{dt} = \frac{dQ}{dt} = \frac{dI}{dt} = \frac{dH}{dt} = \frac{dR}{dt} = 0. \tag{28}$$

When there is no disease, then,  $E=0$ ,  $Q=0$ ,  $I=0$ ,  $H=0$ , and  $R=0$ .

By considering each model equation from Equation (2),

$$\mu + \alpha Q + \rho R - \beta IS - bS = 0 \text{ gives } \mu - bS = 0, \text{ then, } S = \frac{\mu}{b}. \tag{29}$$

In addition to the second model equation,

$$\beta IS = (\theta + q + b)E = 0 \text{ gives } E = \frac{\beta IS}{\theta + q + b}, \text{ but } \beta = 0, \text{ then, } E = 0. \tag{30}$$

Similarly, for the third model equation,

$$\phi + \theta E - \alpha Q - \eta_1 Q - bQ = 0 \text{ gives } Q = \frac{\phi + \theta E}{\alpha + \eta_1 + b}, \text{ but, } E = 0, \tag{31}$$

then,

$$Q = \frac{\phi}{\alpha + \eta_1 + b}. \tag{32}$$

By considering the same procedures for the fourth, fifth, and sixth model equations, the following is obtained:

$$I = 0, H = 0, R = 0. \tag{33}$$

Therefore,

$$E_0 = (S^0, E^0, Q^0, I^0, H^0, R^0) = \left( \frac{\mu}{b}, 0, \frac{\phi}{\alpha + \eta_1 + b}, 0, 0, 0 \right)^T. \tag{34}$$

Equation (34) represents the state in which there is no infection and is known as the disease-free equilibrium point.

**3.5. Basic Reproduction Number ( $R_0$ ).** The basic reproduction number  $R_0$  is the midpoint number of infections caused by an infectious individual during the entire period of infectiousness [20]. In an epidemiology study, the basic reproduction number is a nondimensional quantity that sets the threshold during the study, both for predicting the outbreak and for evaluating the control strategies. Additionally,  $R_0$  analyzes the equilibrium stability,  $R_0 < 1$ , which means that infectious individuals will cause less than one secondary infection and die out. Every infectious individual infects more than one secondary infection when  $R_0 > 1$ , and the disease spreads to the population. In the *SEQIHR* model, the basic reproduction number is computed by using the next-generation matrix approach [21] and then obtained by taking the dominant eigenvalues (Spectral radius). Let  $F_i(x)$  be the rate of new infection in compartment  $i$  and  $V_i$  be the rate of transfer of individuals into compartment  $i$  by all means other than the epidemic. The important thing is to obtain the disease-free equilibrium point  $E_0$ . Thus, the computed matrices  $F$  and  $V$  which are  $n \times n$  matrices, where  $n$  represents the infected classes, defined by:  $F = ((\partial F_i / \partial x_j)(E_0))$  and  $V = ((\partial V_i / \partial x_j)(E_0))$ , where  $1 \leq i, j \leq n$ ,  $F$  are non-negative, and  $V$  is a nonsingular  $n$ -matrix (the matrix with inverse belongs to the class of positive matrices). Since  $F$  is nonnegative and  $V$  is a nonsingular matrix, then  $V^{-1}$  and  $FV^{-1}$  are nonnegative. Therefore, the next-generation matrix  $FV^{-1}$  is computed as defined by [22].

Note that the basic reproduction number is defined as the spectral radius (dominant eigenvalue) of the matrix  $FV^{-1}$  [23], that is,

$$R_0 = \rho(FV^{-1}), \tag{35}$$

$$FV^{-1} = \left[ \frac{\partial F_i}{\partial x_j}(E_0) \right] \left[ \frac{\partial V_i}{\partial x_j}(E_0) \right]^{-1}.$$

where  $F$  is the rate of new infection in compartment  $I$ . The new forces of infection are

$$\begin{aligned}
\frac{dE}{dt} &= \beta IS - (\theta + q + b)E, \\
\frac{dQ}{dt} &= \phi + \theta E - (\alpha + \eta_1 + b)Q, \\
\frac{dI}{dt} &= (1 - \omega)qE + \eta_1 Q - (\eta_2 + \nu + \delta + b)I, \\
\frac{dH}{dt} &= \omega qE + \eta_2 I - (\lambda + \delta + b)H.
\end{aligned} \tag{36}$$

$$F_J = \begin{pmatrix} 0 & 0 & \beta S & 0 \\ 0 & 0 & 0 & 0 \\ 0 & 0 & 0 & 0 \\ 0 & 0 & 0 & 0 \end{pmatrix}. \tag{38}$$

The partial derivative of Equation (38) with respect to  $E, Q, I,$  and  $H$  is given as

From Equation (36), when  $I$  and  $S$  meet, we obtain the following:

$$F_i = \begin{pmatrix} f_1 \\ f_2 \\ f_3 \\ f_4 \end{pmatrix} = \begin{pmatrix} \beta IS \\ 0 \\ 0 \\ 0 \end{pmatrix}, \tag{37}$$

$$V = \begin{pmatrix} b + \theta + q & 0 & 0 & 0 \\ -\theta & \alpha + b + \eta_1 & 0 & 0 \\ (\omega - 1)q & -\eta_1 & b + \delta + \eta_2 + \nu & 0 \\ -\omega & 0 & -\eta_2 & b + \delta + \lambda \end{pmatrix}, \tag{39}$$

From Equation (37), the Jacobian matrix of disease-free equilibrium (DFE) is given by

Given that  $A_1 = b + \alpha + \eta_1$  and  $A_2 = b + \delta + \eta_2 + \nu$ . The inverse of  $V$  is

$$V^{-1} = \begin{pmatrix} \frac{1}{b + \theta + q} & 0 & 0 & 0 \\ \frac{\theta}{A_1(b + \theta + q)} & \frac{1}{A_1} & 0 & 0 \\ \frac{-\alpha\omega + \alpha + b(-\omega) + b + \eta_1\theta - \eta_1\omega + \eta_1}{A_1A_2(b + \theta + q)} & \frac{\eta_1}{A_1A_2} & \frac{1}{A_2} & 0 \\ \frac{A_1A_2\omega + \eta_2(-\alpha\omega + \alpha + b(-\omega) + b + \eta_1\theta - \eta_1\omega + \eta_1)}{A_1A_2(b + \delta + \lambda)(b + \theta + q)} & \frac{\eta_1\eta_2}{A_1A_2(b + \delta + \lambda)} & \frac{\eta_2}{A_2(b + \delta + \lambda)} & \frac{1}{b + \delta + \lambda} \end{pmatrix}. \tag{40}$$

The product matrix  $FV^{-1}$  is given by:

$$FV^{-1} = \begin{pmatrix} \frac{\beta\mu(\eta_1\theta - q(\omega - 1)(\alpha + b + \eta_1))}{b(\alpha + b + \eta_1)(b + \theta + q)(b + \delta + \eta_2 + \nu)} & \frac{\beta\eta_1\mu}{b(\alpha + b + \eta_1)(b + \delta + \eta_2 + \nu)} & \frac{\beta\mu}{b(b + \delta + \eta_2 + \nu)} & 0 \\ 0 & 0 & 0 & 0 \\ 0 & 0 & 0 & 0 \\ 0 & 0 & 0 & 0 \end{pmatrix}, \tag{41}$$

$$\text{Eigenvalues} = \left\{ 0, 0, 0, \frac{\beta\mu(-bq\omega + bq + \eta_1\theta - \alpha q\omega + \alpha q - \eta_1 q\omega + \eta_1 q)}{b(\alpha + b + \eta_1)(b + \theta + q)(b + \delta + \eta_2 + \nu)} \right\},$$

$$\lambda_1 = 0, \lambda_2 = 0, \lambda_3 = 0, \lambda_4 = \frac{\beta\mu(\eta_1(\theta + q(-\omega) + q) - q(\omega - 1)(\alpha + b))}{b(\alpha + b + \eta_1)(b + \theta + q)(b + \delta + \eta_2 + \nu)}.$$



Thus, the basic reproduction number becomes

$$R_0 = \frac{\beta\mu(\eta_1(\theta - \omega q + q) + q(1 - \omega)(\alpha + b))}{b(\alpha + b + \eta_1)(b + \theta + q)(b + \delta + \eta_2 + \nu)}. \quad (42)$$

**3.6. Existence of Endemic Equilibrium Point.** Endemic equilibrium points are the steady-state solutions whereby the disease persists in the population [24]. The stability analysis of the endemic equilibrium point describes the long-term dynamics of COVID-19 in the population [25]. By solving all systems of differential equations from the model Equation (2), all derivatives are equal to zero (solve for all variables simultaneously).

**Theorem 5.** *The endemic equilibrium point of model Equation (2) is locally asymptotically stable in the region  $\Omega$  if  $R_0 < 1$  and unstable if  $R_0 > 1$ .*

*Proof.* At the endemic equilibrium point  $S = S^*, E = E^*, Q = Q^*, I = I^*, H = H^*$ , and  $R = R^*$ . The variables are given as follows:

$$\begin{aligned} S^* &= \frac{\mu + \alpha Q + \rho R}{b + \beta I} E^* = \frac{\beta I S}{b + \theta + q} Q^* = \frac{\phi + \theta E}{b + \alpha + \eta_1} H^* \\ &= \frac{E\omega q + \eta_2 I}{b + \delta + \lambda} R^* = \frac{H\lambda + \nu I}{b + \rho}, \end{aligned} \quad (43)$$

$$I^* = \frac{\mu(\phi\eta_1 + A_1 A_2(R_0 - 1)) + R_0(\alpha Q^* + \rho R^*)A_1 A_2}{\beta\mu(A_1 A_2 - \phi\eta_1)}.$$

□

**3.7. Local Stability of the Disease-Free Equilibrium.** The eigenvalues, which are determined by finding the partial

derivatives of the vector-valued function, are used to study the local stability of the disease-free equilibrium. If the Jacobian matrix evaluated at that point has negative eigenvalues, the equilibrium point is asymptotically stable. The Routh-Hurwitz criterion in [26] will be utilized to demonstrate the local stability in this work.

**Theorem 6.** *The disease-free equilibrium point  $E_0$  is locally asymptotically stable if  $R_0 < 1$ , and it is unstable when  $R_0 > 1$ .*

*Proof.* The linearization of the system of model 2 is done by computing its Jacobian matrix to prove this theorem. At the disease-free equilibrium point, the partial derivatives of each equation in the system for state variables  $S, E, Q, I, H, R$ , which are used to generate the Jacobian matrix  $J_{E_0}$  as in 21.

$$J_{E_0} = \begin{pmatrix} -b & 0 & \alpha & -\beta S & 0 & \rho \\ 0 & -b - \theta - q & 0 & \beta S & 0 & 0 \\ 0 & \theta & -\alpha - b - \eta_1 & 0 & 0 & 0 \\ 0 & q(1 - \omega) & \eta_1 & -b - \delta - \eta_2 - \nu & 0 & 0 \\ 0 & \omega q & 0 & \eta_2 & -b - \delta - \lambda & 0 \\ 0 & 0 & 0 & \nu & \lambda & -b - \rho \end{pmatrix}. \quad (44)$$

At a disease-free equilibrium,

$$S = \frac{\mu}{b}, I = 0. \quad (45)$$

The disease-free equilibrium will be asymptotically stable if the eigenvalues of  $J_{E_0} < 0$ .

$$\begin{vmatrix} -b & 0 & \alpha & -\frac{\beta\mu}{b} & 0 & \rho \\ 0 & -b - \theta - q & 0 & \frac{\beta\mu}{b} & 0 & 0 \\ 0 & \theta & -\alpha - b - \eta_1 & 0 & 0 & 0 \\ 0 & q(1 - \omega) & \eta_1 & -b - \delta - \eta_2 - \nu & 0 & 0 \\ 0 & \omega q & 0 & \eta_2 & -b - \delta - \lambda & 0 \\ 0 & 0 & 0 & \nu & \lambda & -b - \rho \end{vmatrix} = 0. \quad (46)$$

From matrix (46), it is clear that the first, second, and third eigenvalues are

$$\lambda_1 = -b, \lambda_2 = -b - \rho, \text{ and } \lambda_3 = -b - \delta - \lambda. \quad (47)$$

Then matrix (46) reduces to a  $3 \times 3$  matrix after the cancellation of the respective rows and columns used to obtain the first, second, and third eigenvalues as shown in

$$J_{E_0} = \begin{pmatrix} -b - \theta - q & 0 & \frac{\beta\mu}{b} \\ \theta & -\alpha - b - \eta_1 & 0 \\ q(1 - \omega) & \eta_1 & -b - \delta - \eta_2 - \nu \end{pmatrix}. \quad (48)$$

The characteristic polynomial of matrix (48) is given in the form

$$Z(\lambda) = \lambda^3 + a_1\lambda^2 + a_2\lambda + a_3, \quad (49)$$

where

$$\begin{aligned} a_1 &= \alpha + 3b + \delta + \eta_1 + \eta_2 + \theta + \nu + q, \\ a_2 &= \alpha\delta + \alpha\eta_2 + \alpha\theta + \alpha\nu + 3b^2 + 2\alpha b + 2b\delta + 2b\eta_1 + 2b\eta_2 \\ &\quad + 2b\theta + 2b\nu - \frac{\beta\mu q}{b} + 2bq + \delta\eta_1 + \delta\theta + \eta_1\theta + \eta_2\theta + \eta_1\nu \\ &\quad + \eta_1\eta_2 + \theta\nu + \alpha q + \delta q + \eta_1 q + \eta_2 q + \nu q, \\ a_3 &= \alpha\delta\theta + \alpha\eta_2\theta + \alpha\theta\nu + b^3 + \alpha b^2 + b^2\delta + b^2\eta_1 + b^2\eta_2 + b^2\theta \\ &\quad + b^2\nu + b^2 q + \alpha b\delta + \alpha b\eta_2 + \alpha b\theta + \alpha b\nu - \frac{\beta\eta_1\theta\mu}{b} + b\delta\eta_1 \\ &\quad + b\delta\theta + b\eta_1\theta + b\eta_2\theta + b\eta_1\nu + b\eta_1\eta_2 + b\theta\nu + \frac{\alpha\beta\mu q\omega}{b} \\ &\quad - \frac{\alpha\beta\mu q}{b} + \alpha b q + \frac{\beta\eta_1\mu q\omega}{b} - \frac{\beta\eta_1\mu q}{b} + b\delta q + b\eta_1 q \\ &\quad + b\eta_2 q + b\nu q + \delta\eta_1\theta + \eta_1\theta\nu + \eta_1\eta_2\theta + \alpha\delta q + \alpha\eta_2 q \\ &\quad + \alpha\nu q + \beta\mu q\omega - \beta\mu q + \delta\eta_1 q + \eta_1\nu q + \eta_1\eta_2 q. \end{aligned} \quad (50)$$

However,  $a_1 > 0$ ,  $a_2 > 0$ , and  $a_3 > 0$ , condition  $a_1 a_2 - a_3 > 0$ .

$$\begin{aligned} a_1 a_2 - a_3 &= \frac{-\beta\mu q\omega(\alpha + b) + M_1(M_2 - \beta\mu q) + M_3 + \eta_2(M_4 + M_5 - \beta\mu q) + \eta_1(M_6 + M_7 + \beta\mu(\theta - q\omega))}{b}, \\ &\quad \frac{M_1 M_2 + M_3 + \eta_2(M_4 + M_5) + \eta_1(\beta\theta\mu + M_6 + M_7)}{b} > \frac{\beta\mu q\omega(\alpha + b) + \beta\mu\eta_2 q + \beta\mu M_1 q + \mu q\omega\beta}{b}, \end{aligned} \quad (51)$$

where

$$\begin{aligned} M_1 &= 2b + \delta + \theta + \nu + q, \\ M_2 &= 4b^3 + 2b^2(2\alpha + \delta + \theta + \nu + q) + b(\alpha + \delta + \nu)(\alpha + \theta + q), \\ M_3 &= b\eta_1^2(2b + \delta + \eta_2 + \theta + \nu + q), \\ M_4 &= 8b^3 + b(\alpha + \theta + q)(\alpha + 2\delta + \theta + 2\nu + q), \\ M_5 &= b^2(6\alpha + 4\delta + 6\theta + 4\nu + 6q) + b\eta_2(\alpha + 2b + \theta + q), \\ M_6 &= 8b^3 + b^2(4\alpha + 6(\delta + \theta + \nu) + 6q) \\ &\quad + b(\delta + \theta + \nu + q)(2\alpha + \delta + \theta + \nu + q), \\ M_7 &= b\eta_2(2(\alpha + 3b + \delta + \theta + \nu + q) + \eta_2). \end{aligned} \quad (52)$$

□

Hence, the condition  $a_1 a_2 - a_3 > 0$  is satisfied. The Routh-Hurwitz criterion states that all elements of a system's characteristic polynomial must be negative in order for the system to be stable [27]. The disease is asymptotically stable because the eigenvalues are negative, and the Routh-Hurwitz requirements are satisfied.

**3.8. Global Stability of Disease-Free Equilibrium Point (DFE).** The global stability of the SEQIHR model around the DFE will be proved. The stability result of DFE in epidemiological implication is that minimizing the COVID-19 infection cases will not generate an infection if  $R_0 < 1$ . Theorem 7 is considered.

**Theorem 7.** The DFE is globally asymptotically stable if  $R_0 < 1$ , and unstable if  $R_0 > 1$ .

*Proof.* Using the technique described in [23, 28], the studies examine the global stability of the model 1 disease-free equilibrium point. The format can be used to write the SEQIHR model as in

$$\begin{cases} \frac{dX_n}{dt} = A(X_n - X_{d_{fe}}) + A_1 X_i, \\ \frac{dX_i}{dt} = A_2 X_i. \end{cases} \quad (53)$$

By considering Equation (54),  $X_n$  is the vector of the nontransmitting compartment,  $X_i$  is the vector of transmitting compartment, and  $X_{d_{fe}}$  is the vector of disease-free equilibrium point.

TABLE 3: Parameter values and sensitivity indices.

Parameter	Values	Sources	Sensitivity index value
$\beta$	0.015	Assumed	1.0000
$\mu$	8.94	Assumed	1.0000
$\omega$	0.083	Assumed	-0.0388
$b$	0.0104	[31]	-0.9483
$\alpha$	0.85	Assumed	0.7100
$\nu$	0.07	[32]	0.090
$\theta$	0.2435	[33]	1.2614
$\eta_1$	0.85	Assumed	1.2813
$\eta_2$	0.65	Assumed	0.8448
$\delta$	0.039	[34]	0.0507
$q$	0.099	Assumed	0.7092

$$X_n = (S, R)^T, X_i = (E, Q, I, H)^T, X_{d_{fe}} = \left(\frac{1}{b}, 0\right), \quad (54)$$

$$X_n - X_{d_{fe}} = \begin{pmatrix} S - \frac{1}{b} \\ R \end{pmatrix}. \quad (55)$$

$$A_1 = \begin{pmatrix} 0 & \alpha & -\beta S & 0 \\ 0 & 0 & \nu & \lambda \end{pmatrix},$$

$$A_2 = \begin{pmatrix} -(\theta + q + b) & 0 & \beta S & 0 \\ \theta & -(\alpha + \eta_1 + b) & 0 & 0 \\ (1 - \omega)q & \eta_1 & -(\eta_2 + \nu + \delta + b) & 0 \\ \omega q & 0 & \eta_2 & -(\lambda + \delta + b) \end{pmatrix}. \quad (58)$$

We must show that the matrix  $A$  has real negative eigenvalues and  $A_2$  is a Metzler matrix in order for DFE to be globally stable (i.e., the off-diagonal elements of  $A_2$  are non-negative, symbolically denoted by  $A_2(X_{ij}) \geq \forall \neq j$ ). We can derive equations with and without transmission from model 1, as stated herewith.

$A_2$  represents a Metzler matrix where its diagonal elements are negatives while the off-diagonal elements are nonnegative.

$$\begin{pmatrix} \mu + \alpha Q + \rho R - \beta IS - bS \\ \lambda H + \nu I - \rho R - bR \end{pmatrix} = A \begin{pmatrix} S - \frac{1}{b} \\ R \end{pmatrix} + A_1 \begin{pmatrix} E \\ Q \\ I \\ H \end{pmatrix},$$

$$\begin{pmatrix} \beta IS - \theta E - qE - bE \\ \phi + \theta E - \alpha Q - \eta_1 Q - bQ \\ (1 - \omega)qE + \eta_1 Q - \eta_2 I - \nu I - \delta I - bI \\ \omega qE + \eta_2 I - \lambda H - \delta H - bH \end{pmatrix} = A_2 \begin{pmatrix} E \\ Q \\ I \\ H \end{pmatrix}, \quad (56)$$

$$\text{then, } A = \begin{pmatrix} -b & 0 \\ 0 & -b \end{pmatrix}. \quad (57)$$

The eigenvalues of the matrix  $A$  are located at the diagonal (-b and -b), and these eigenvalues are real, distinct, and negative. Moreover, matrices  $A_1$  and  $A_2$  are given by

**3.9. Global Stability of Endemic Equilibrium Point.** The stability analysis explains the behavior of epidemic near the equilibrium points. The logarithmic Lyapunov function was proposed by Korobeinikov and Wake [29] to prove the global stability of endemic equilibrium for SIS, SIR, and SIRS models.

**Theorem 8.** *The endemic equilibrium point  $W^*$  is asymptotically stable when  $R_0 > 1$  and unstable when  $R_0 < 1$ .*

*Proof.* The logarithmic Lyapunov function is used to analyze the stability of the endemic equilibrium and is given in the form

$$W = \sum_{i=1}^6 a_i (X_i - x_i^* \ln(X_i)), \quad (59)$$

where  $a_i$  represents a positive constant,  $X_i$  represents some free virus in compartment  $i$ , and  $X_i^*$  denotes the number of free viruses in compartment  $i$  at the equilibrium point. Then, model system (2) is now written as follows:

$$\begin{aligned}
W(S, E, Q, I, H, R) \\
= \{A_1(S - S^* \ln(S)) + A_2(E - E^* \ln(E)) \\
+ A_3(Q - Q^* \ln(Q)) + A_4(I - I^* \ln(I)) \\
+ A_5(H - H^* \ln(H)) + A_6(R - R^* \ln(R))\}
\end{aligned} \quad (60)$$

The constants  $A_1, A_2, A_3, A_4, A_5$ , and  $A_6$  are nonnegative constants and the function  $W$  which is continuous and differentiable. Consider the derivative with respect to each compartment

$$\begin{aligned}
\frac{dW}{dt} &= \left\{ A_1 \left(1 - \frac{S^*}{S}\right) \frac{dS}{dt} + A_2 \left(1 - \frac{E^*}{E}\right) \frac{dE}{dt} + A_3 \left(1 - \frac{Q^*}{Q}\right) \frac{dQ}{dt} + A_4 \left(1 - \frac{I^*}{I}\right) \frac{dI}{dt} \right. \\
&\quad \left. + A_5 \left(1 - \frac{H^*}{H}\right) \frac{dH}{dt} + A_6 \left(1 - \frac{R^*}{R}\right) \frac{dR}{dt} \right\}. \\
\frac{dW}{dt} &= \left\{ A_1 \left(1 - \frac{S^*}{S}\right) (\mu + \alpha Q + \rho R - \beta IS - bS) + A_2 \left(1 - \frac{E^*}{E}\right) (\beta IS - (\theta + q + b)E) \right. \\
&\quad + A_3 \left(1 - \frac{Q^*}{Q}\right) (\phi + \theta E - (\alpha + \eta_1 + b)Q) \\
&\quad + A_4 \left(1 - \frac{I^*}{I}\right) ((1 - \omega)qE + \eta_2 I - (\eta_2 + \nu + \delta + b)I) \\
&\quad + A_5 \left(1 - \frac{H^*}{H}\right) (\omega qE + \eta_2 I - (\lambda + \delta + b)H) \\
&\quad \left. + A_6 \left(1 - \frac{R^*}{R}\right) (\lambda H + \nu I - (\rho + b)R) \right\}.
\end{aligned} \quad (61)$$

At the endemic equilibrium point,

$$\begin{aligned}
\mu &= \beta IS + bS - \alpha Q - \rho R, \\
\beta IS &= (\theta + q + b)E^*, \\
\phi + \theta E &= (\alpha + \eta_1 + b)Q^*, \\
(1 - \omega)qE + \eta_1 Q &= (\eta_1 + \nu + \delta + b)I^*, \\
\omega qE + \eta_2 I &= (\lambda + \delta + b)H^*, \\
\lambda H + \nu I &= (\rho + b)R^*.
\end{aligned} \quad (62)$$

$$\begin{aligned}
\frac{dW}{dt} &= \left\{ A_1 \left(\frac{S - S^*}{S}\right) (bS^* - bS) + A_2 \left(\frac{E - E^*}{E}\right) (\theta + q + b)(E^* - E) \right. \\
&\quad + A_3 \left(\frac{Q - Q^*}{Q}\right) (\alpha + \eta_1 + b)(Q^* - Q) + A_4 \left(\frac{I - I^*}{I}\right) (\eta_1 + \nu + \delta + b)(I^* - I) \\
&\quad \left. + A_5 \left(\frac{H - H^*}{H}\right) (\lambda + \delta + b)(H^* - H) + A_6 \left(\frac{R - R^*}{R}\right) (\rho + b)(R^* - R) \right\},
\end{aligned} \quad (63)$$

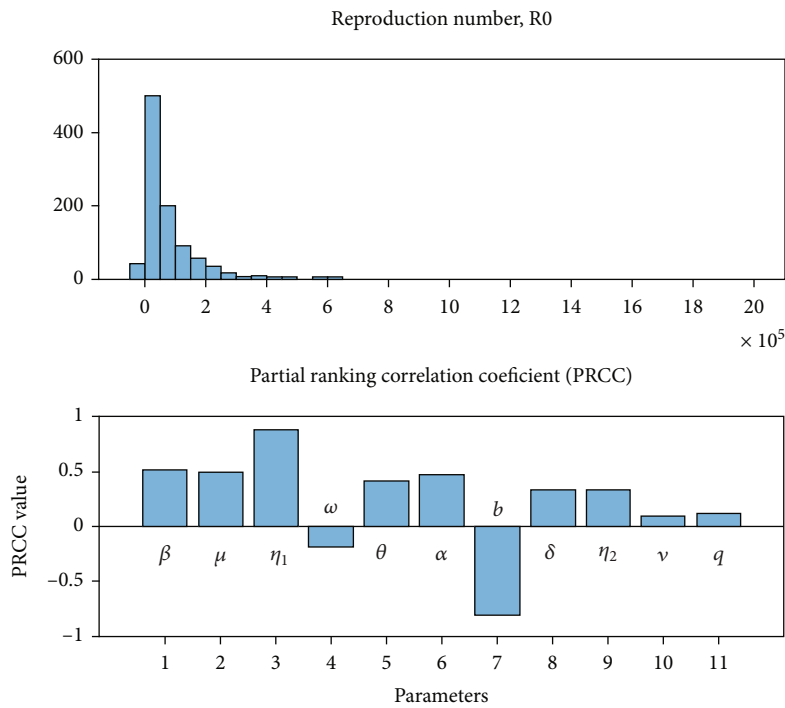


FIGURE 2: Global sensitivity analysis and PRCC results for  $R_0$ .

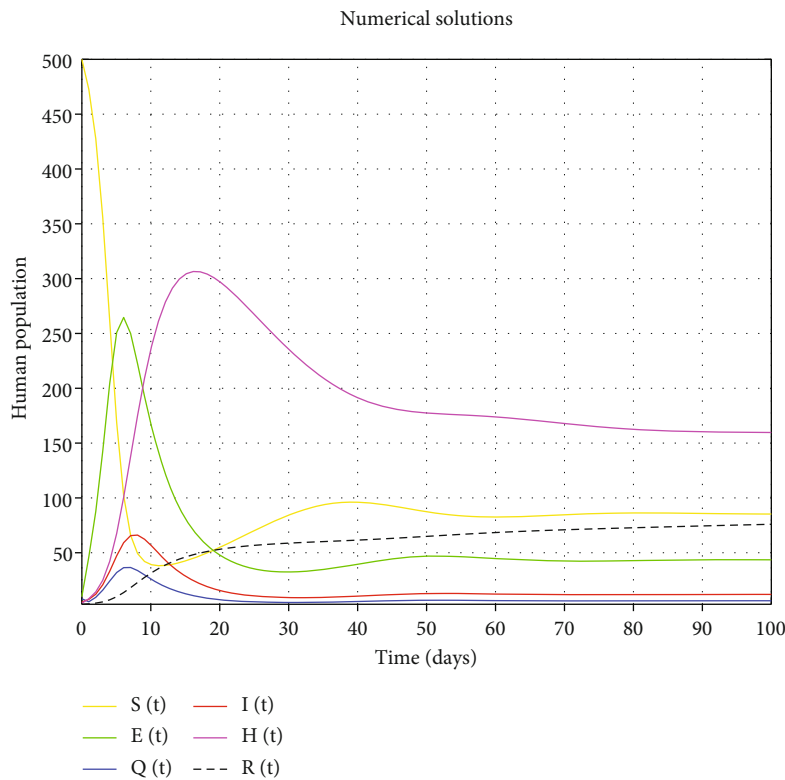
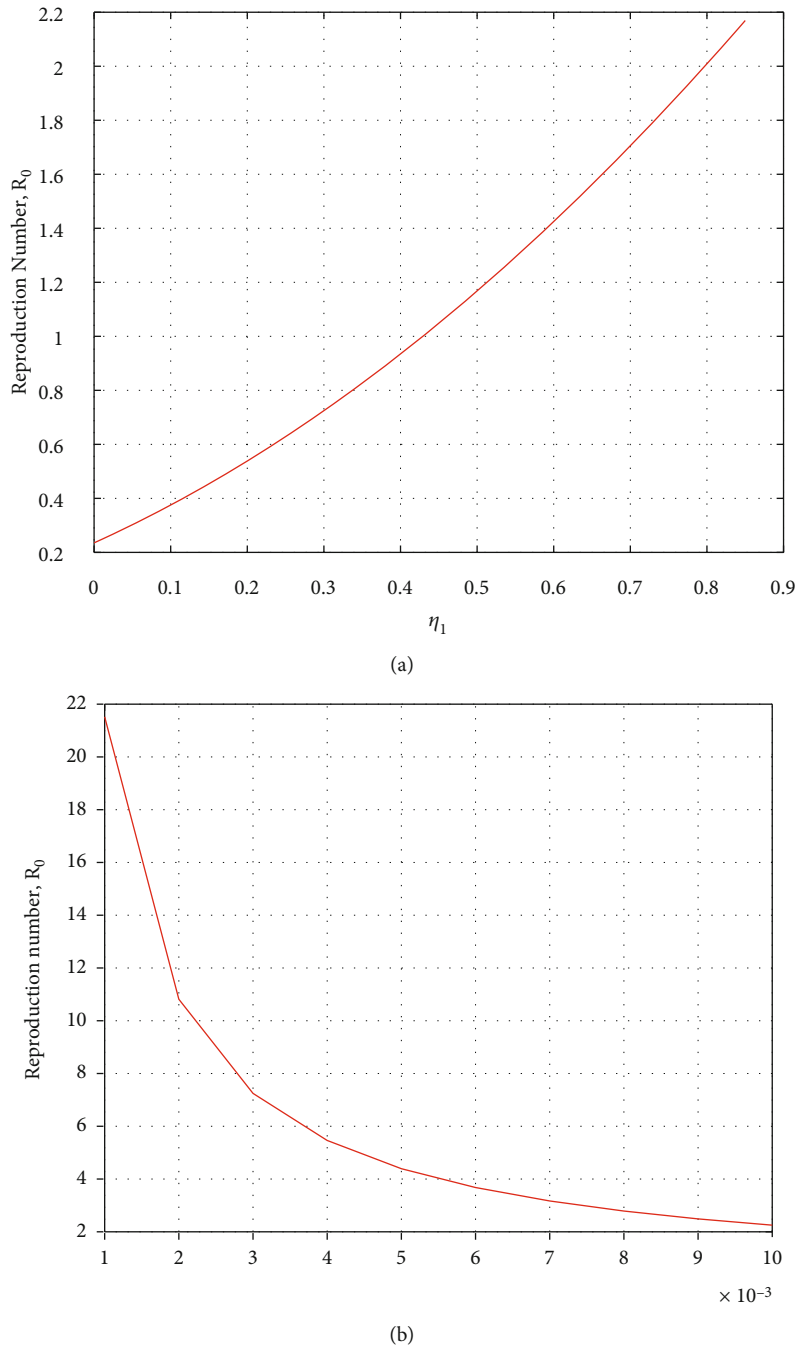


FIGURE 3: Dynamic simulation of a *SEQIHR* model.

FIGURE 4: Effect of stress  $\eta_1$  and natural death  $b$  on  $R_0$ .

where Equation (63) gives

$$\begin{aligned}
 \frac{dW}{dt} = & -bA_1 \frac{(S-S^*)^2}{S} - (\theta + q + b)A_2 \frac{(E-E^*)^2}{E} \\
 & - (\alpha + \eta_1 + b)A_3 \frac{(Q-Q^*)^2}{Q} - (\eta_1 + \nu + \delta + b)A_4 \frac{(I-I^*)^2}{I} \\
 & - (\lambda + \delta + b)A_5 \frac{(H-H^*)^2}{H} - (\rho + b)A_6 \frac{(R-R^*)^2}{R}.
 \end{aligned} \tag{64}$$

□

When  $S \rightarrow S^*$ ,  $E \rightarrow E^*$ ,  $Q \rightarrow Q^*$ ,  $I \rightarrow I^*$ ,  $H \rightarrow H^*$ , and  $R \rightarrow R^*$ . Therefore,  $(dW/dt) \leq 0$  or zero and the function  $W$  is negative when  $W(S, E, Q, I, H, R) \geq 0$ .

By following the approach of [29], the largest invariant set in  $\Delta$  is a singleton set  $W$  which is the endemic equilibrium point, and using LaSalle [30] invariant principle,  $W^*$  is globally asymptotically stable when  $R_0 > 1$  in  $\Delta$ .

#### 4. Numerical Simulation

A series of numerical results for system (2) of the model equations are presented. The explicit Runge-Kutta fourth-

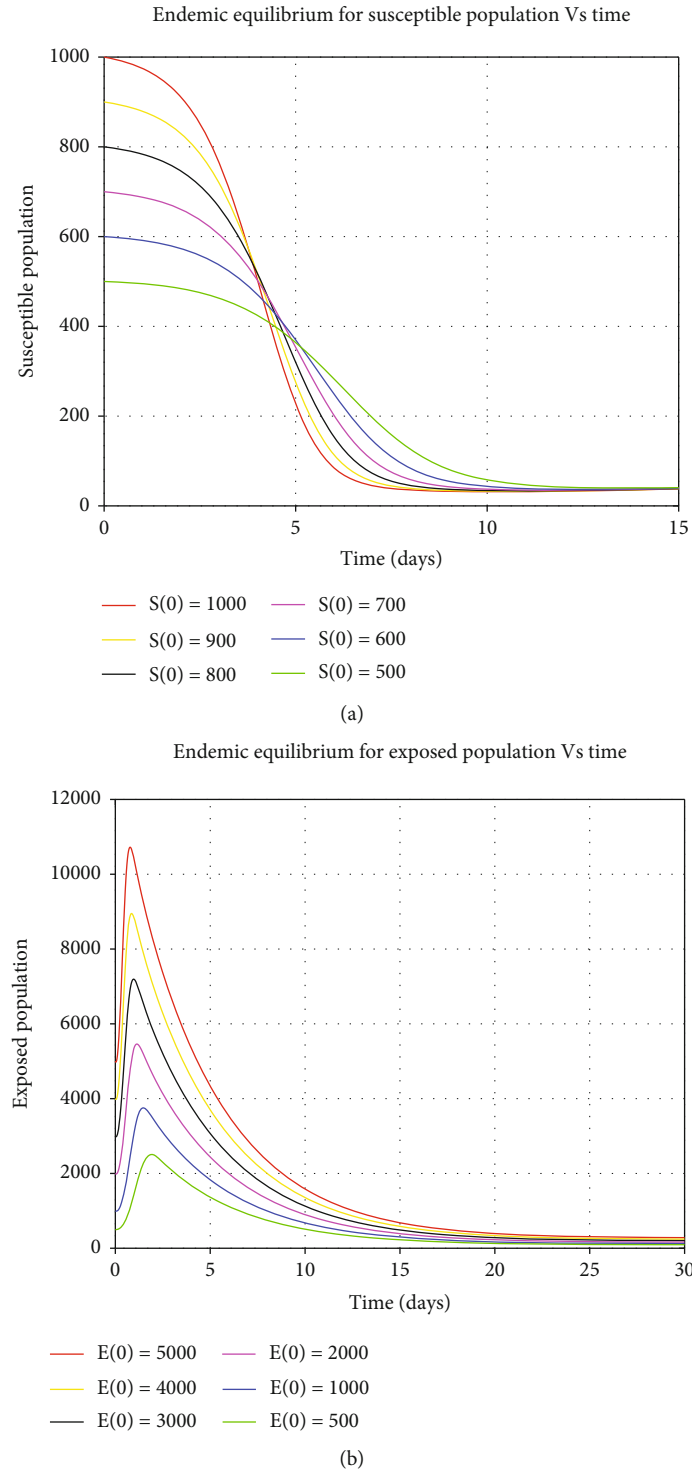


FIGURE 5: Global stability of endemic equilibrium for susceptible and exposed human population.

order method is considered for solving the first-order ordinary differential equations of *SEQIHR* model numerically with a given initial condition. Partial Rank Correlation Coefficient (PRCC) was used to show the sensitivity analysis of the parameters and basic reproduction number. Parameter values from the literature reviews were used, and some were

assumed as shown in Table 3. The data is simulated by substituting them in  $R_0$ . The sensitivity index of each partial basic reproduction number  $R_0$  for its parameters.

**4.1. Sensitivity Analysis and Uncertainty.** The sensitivity analysis for the endemic threshold tells us the importance

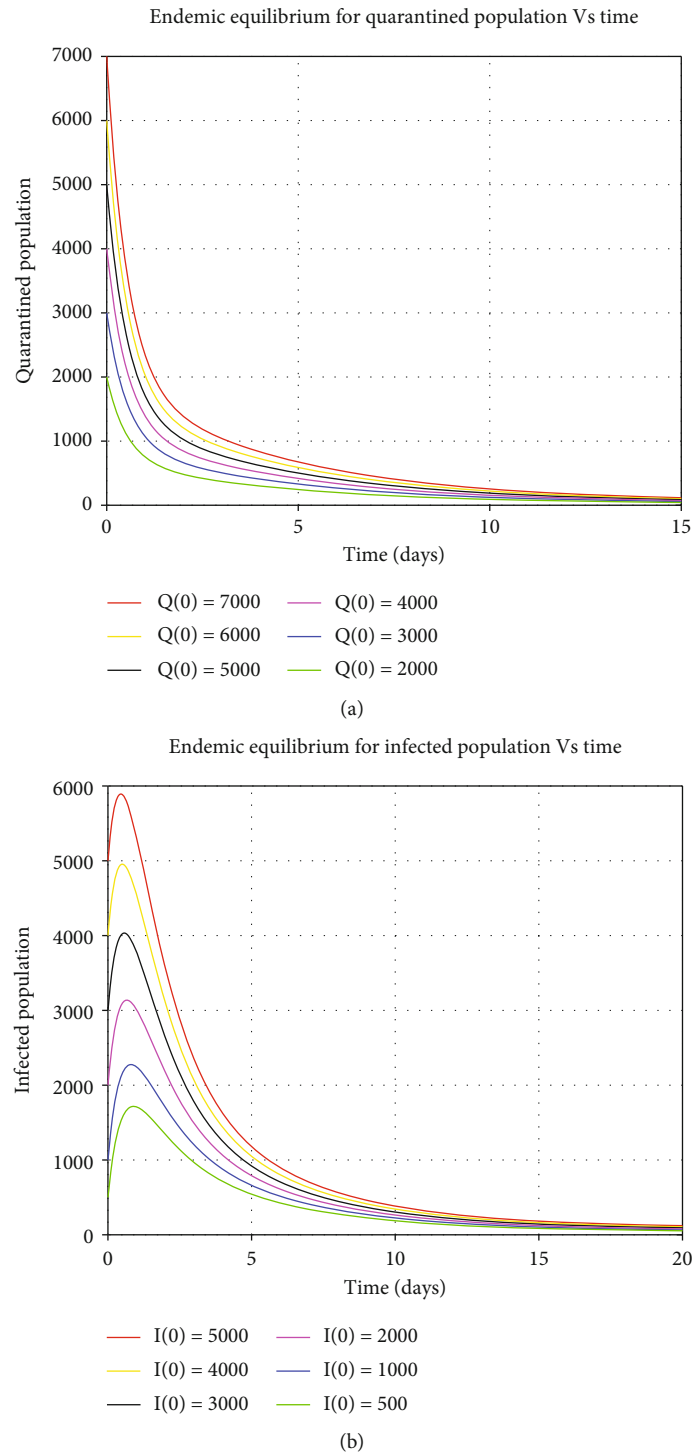


FIGURE 6: Global stability of endemic equilibrium for quarantined and infected human population.

of each parameter for the transmission of COVID-19 disease. The information is crucial for the analysis of complex systems. We used the sensitivity analysis of the parameters to determine the strongness of the *SEQIHR* model predictions for the parameter values. There are usually errors in the data collected and in the initial values assumed for the parameters [35]. The standard equation of a sensitivity index for  $R_0$  is given by

$$\Gamma_L^{R_0} = \frac{\partial R_0}{\partial L} \times \frac{L}{R_0}, \quad (65)$$

From Table 3, it is observed that the  $\eta_1$  parameter is more sensitive since it increases the basic reproductive number by  $\Gamma_L^{R_0} = 1.2813$ . The increase of this parameter means



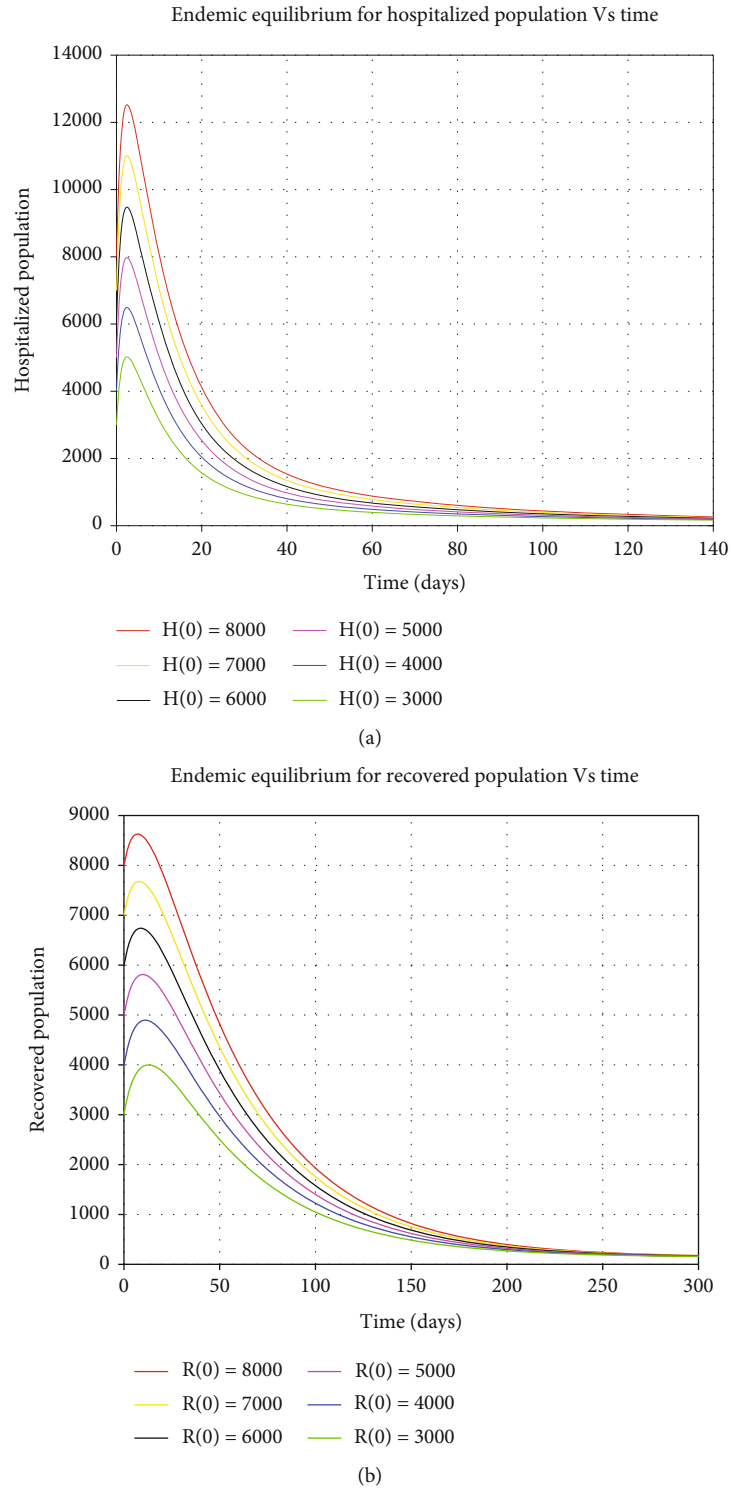
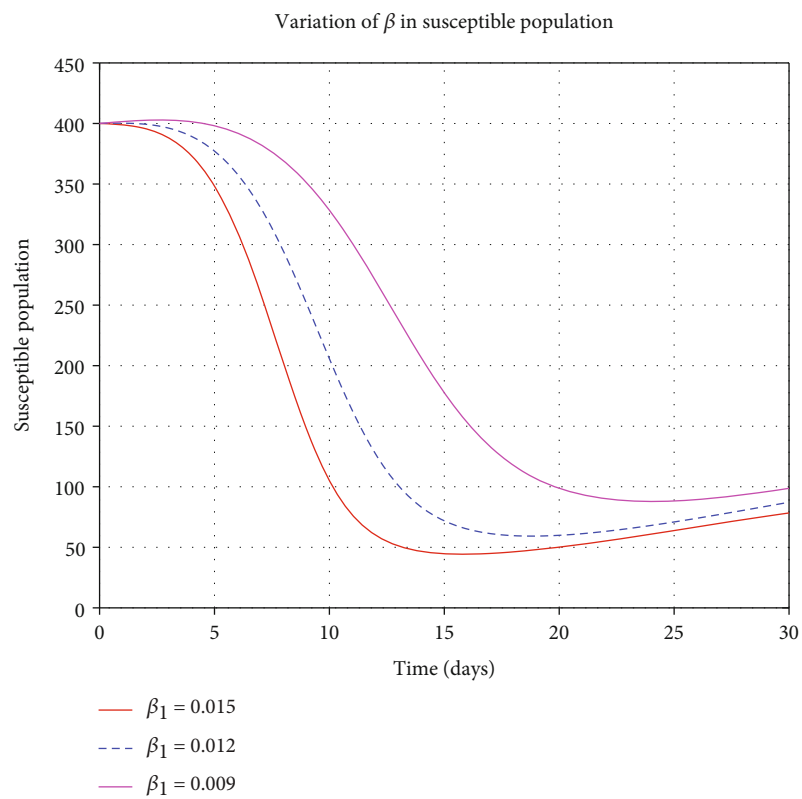


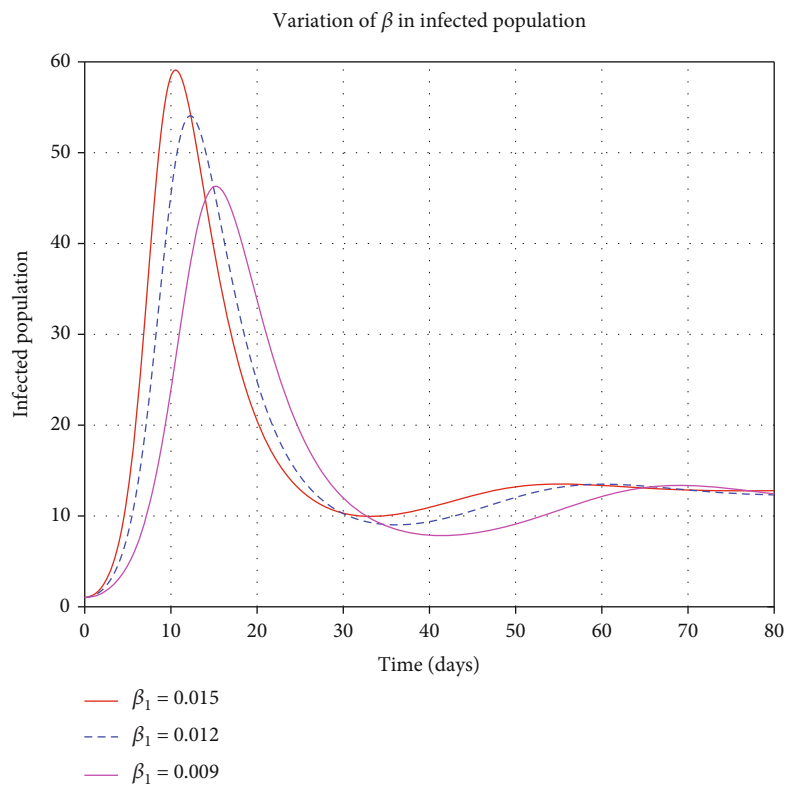
FIGURE 7: Global stability of endemic equilibrium for hospitalized and recovered human population.

that in quarantine, people are more stressed such that the immune system decreases in its efficiency, so the virus spreads within the body. The virus causes blood clotting because the virus fights the respiratory system and enters the bloodstream through lung capillaries that are adjacent to the alveolus [36]. The PRCC supported graphically in Figure 2 shows that  $\eta_1$  has impact on the transmission of

COVID-19 disease. *SEQIHR* model shows that hospitalized patients from the infected class are less stressed than those in quarantine, although it also increases the basic reproduction number by ( $\Gamma_L^{R_0} = 0.8448$ ); then  $\eta_1 > \eta_2$ . Other sensitive parameters are  $\theta$  with  $\Gamma_L^{R_0} = 1.2614$ ,  $\beta$  and  $\mu$  which both have  $\Gamma_L^{R_0} = 1$ . Parameters,  $\omega$  and  $b$ , have the least values which are

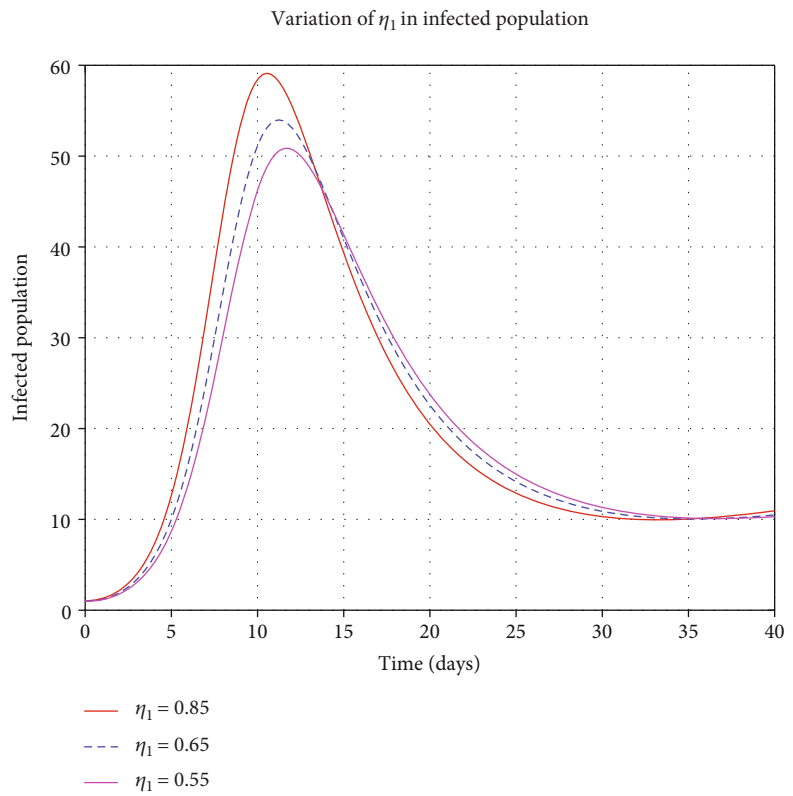


(a)

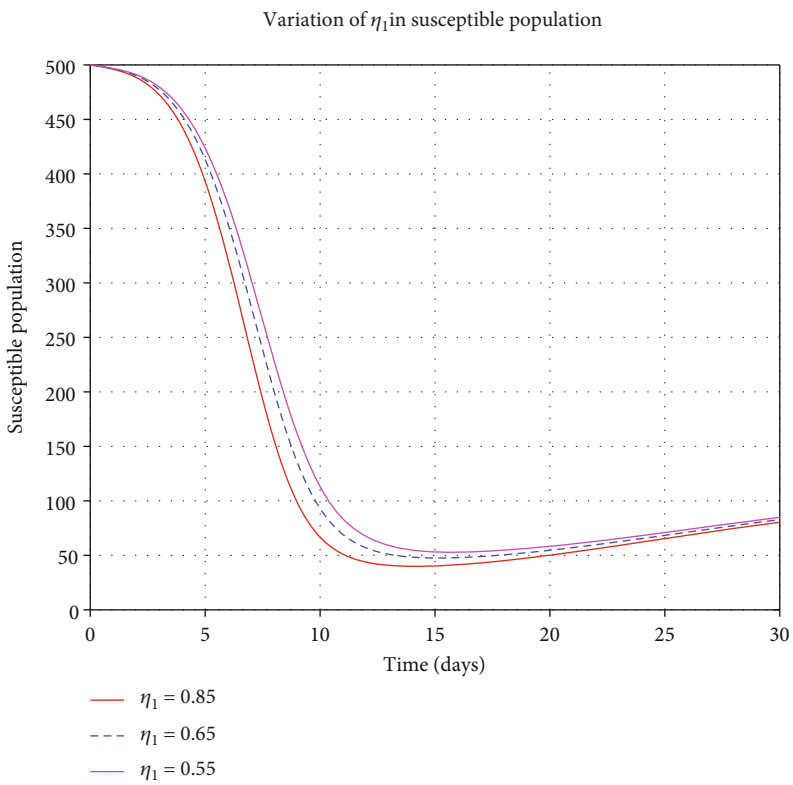


(b)

FIGURE 8: Variation of contact rate  $\beta$  in susceptible and infected population.

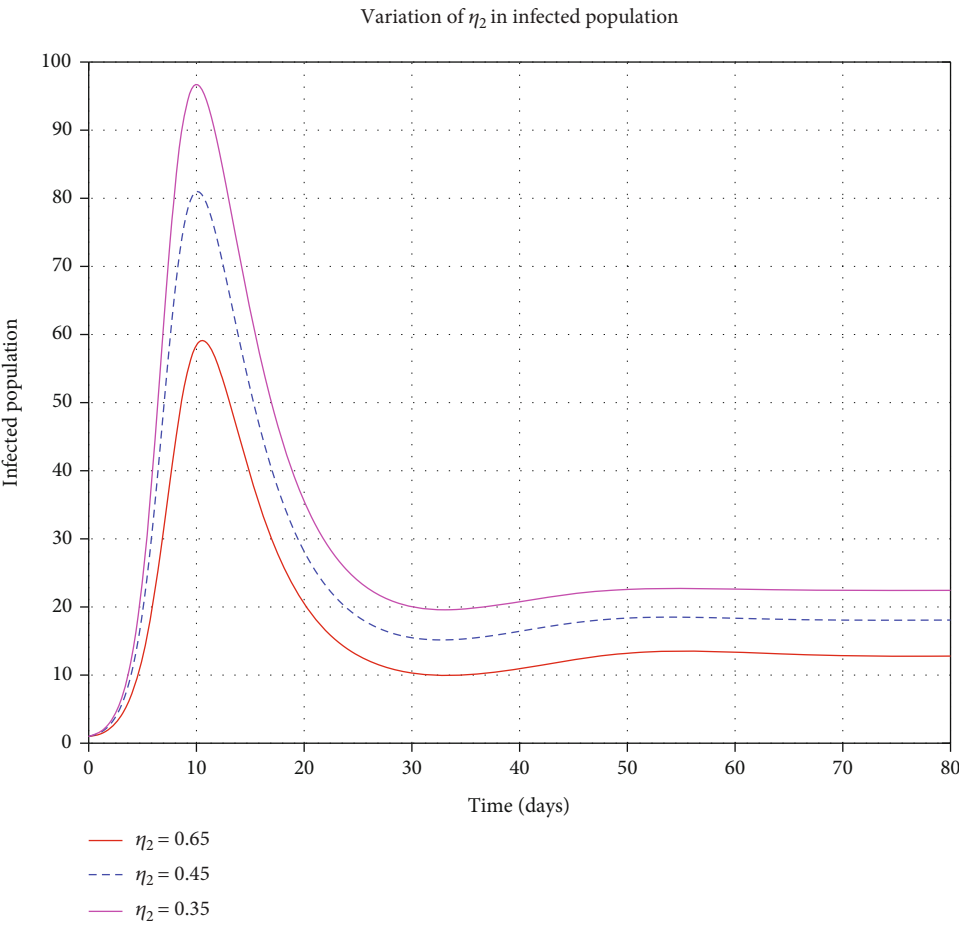


(a)



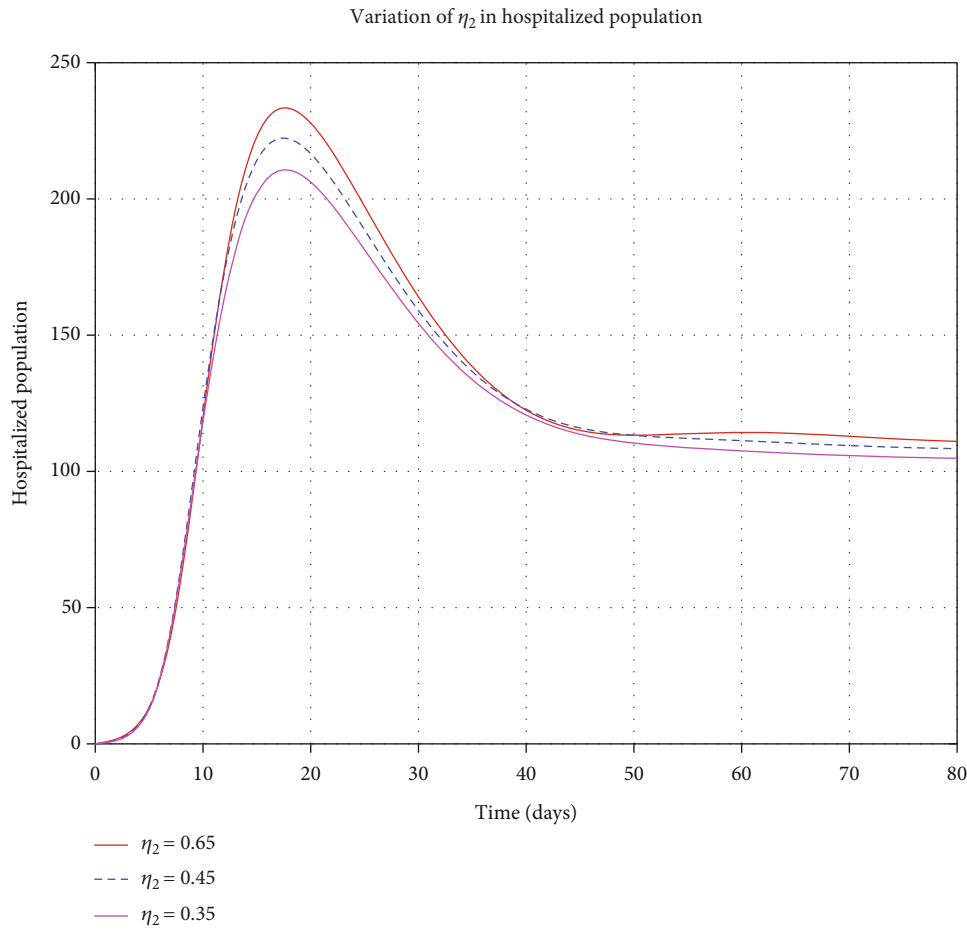
(b)

FIGURE 9: Variation of  $\eta_1$  in susceptible and infected human population.



(a)

FIGURE 10: Continued.



(b)

FIGURE 10: Variation of  $\eta_2$  in infected and hospitalized human population.

-0.0717 and -0.9566, respectively, meaning that decreasing  $\omega$  and  $b$  by a certain percentage always decreases  $R_0$  by the same percentage and the same thing happens if we increase  $R_0$ . It shows that if most of the patients are hospitalized, the disease will decrease, and subsequently, there will be no more transmission within the community. Despite the fact that the other parameters have small values, they still increase  $R_0$  by their respective percentages.

From Figure 2,  $\eta_1$  is positively and highly correlated with  $R_0$  as the absolute value of its PRCC value is higher than the corresponding value of other parameters. Furthermore, natural death  $b$  is highly negatively correlated with  $R_0$ .

**4.1.1. Dynamic Population Simulation with a SEQIHR Model.** The numerical simulation of the SEQIHR model variables is shown in Figure 3. We observe that the susceptible class declines to acquire the endemic equilibrium level exponentially as people die naturally or due to the disease. The exposed, quarantined, and infected populations both assume a parabolic curve which increases exponentially to a certain maximum point before they decelerate to an endemic level. Hospitalized and recovered populations both assumed a parabolic shape as it increases exponentially to a certain maximum point before decelerating to an endemic point.

TABLE 4: Parameter identifiability.

Parameter	Initial values	Estimated values
$\beta$	0.015	0.0147
$\mu$	8.94	9.8
$\omega$	0.083	0.096
$b$	0.0104	0.013
$\alpha$	0.85	1.1
$\nu$	0.07	0.063
$\theta$	0.2435	0.224
$\eta_1$	0.85	0.72
$\eta_2$	0.65	0.51
$\delta$	0.039	0.038
$q$	0.099	0.098
$\rho$	0.003	0.0032
$\lambda$	0.002	0.0018
$\phi$	0.001	0.0009

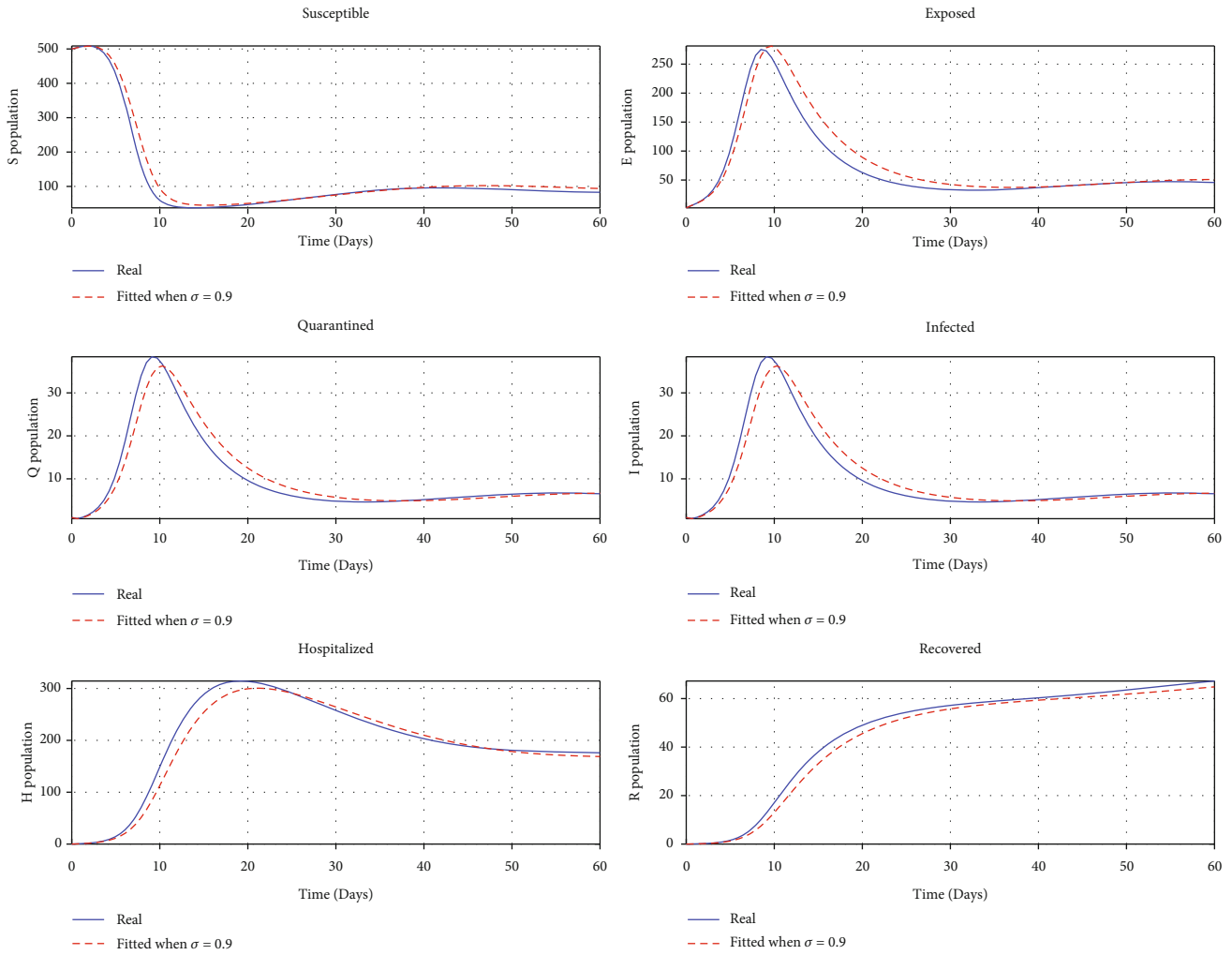


FIGURE 11: Fitted graphs.

**4.1.2. Relationship between Most Positive and Negative Parameters with Basic Reproduction Number  $R_0$ .** From Section 4.1, we observed that the most positive parameter is  $\eta_1$ . The relationship between  $\eta_1$  and  $R_0$  is shown in Figure 4(a), whereby we noticed that the increase of stress results in a quick rise of  $R_0$ . This shows that individuals isolated from their families are more stressed, which increases the disease infection because stress lowers body immunity. Similarly, the natural death  $b$  is the most negative sensitive parameter shown in Figure 4(b), which means that any reduction in it will make the basic reproduction number experience significant exponential retardation.

**4.1.3. Simulation of Stability Analysis of SEQIHR Model.** The numerical simulations for the stability analysis are performed to the analytical results of the model. For the equilibrium point to be globally asymptotically stable, the model trajectories for the state variables should be originated from different initial values and sometimes converge to a common point and maintain an endemic equilibrium point. But if the model trajectories for state variables remain near the equilibrium point and move together in the long run, this implies

that the equilibrium point is globally stable. The six trajectories in each class are represented by different colors as shown by a legend that converge towards equilibrium point as time approaches infinity. The model variables  $S, E, Q, I, H$ , and  $R$  varied by considering Figures 5(a) and 7(b), respectively, are illustrated as follows:

**4.1.4. Control Parameters.** By considering the variation of some control parameters; from Figure 8(a), when the contact rate ( $\beta$ ) increases, the decaying population rate also increases, but when the contact rate decreases, the decaying rate also decreases. From Figure 8(b), when the contact rate increases, the infections also increase and apply the same when the contact rate decreases and the infections decrease. When stress increases in the susceptible class, the rate of decaying increases, and if the stress decreases, the decaying rate decreases, as shown in Figure 9(a). From Figure 9(b), when stress ( $\eta_1$ ) increases, the rate of infection increases, and when  $\eta_1$  decreases, then the rate of infected population decreases. Moreover, when  $\eta_2$  increases, the rate of infected and hospitalized increases and then decreases when  $\eta_2$  decreases as in Figures 10(a) and 10(b).

**4.1.5. Parameter Identifiability and Model Fitting.** The identifiability of parameters is essential to the proposed *SEQIHR* model. Such parameters are  $\beta$ ,  $\mu$ ,  $\omega$ ,  $\alpha$ ,  $\eta_1$ , and  $\eta_2$ . Parameter identifiability is implemented by using the least square method to minimize the sum of squared differences between the observations and the *SEQIHR* model [37] and is defined as

$$SS(\theta) = \sum_{i=1}^n [y_i - f(x_i, \theta)]^2, \quad (66)$$

where  $y_i$  are the observed data of all compartments,  $i$  is the number of compartments (i.e.,  $i = 1, 2, \dots, n$ ), and  $f(x_i, \theta)$  is the solution for all compartments of the *SEQIHR* model. With the initial values of the parameters given as  $\beta$ ,  $\mu$ ,  $\omega$ ,  $\alpha$ ,  $\eta_1$ , and  $\eta_2$ , the least squares identifiabilities are obtained as shown in Table 4 as the initial value and estimated values and used to fit the simulated data as shown in Figure 11. The relationship of initial parameter values and the identifiable values from the least square method is very close.

## 5. Conclusion

COVID-19 pandemic spread rapidly all over the world, which led to the severe human and socioeconomic burden worldwide. In this study, a mathematical model was developed for the transmission of COVID-19 when a human is stressed. The model consists of six compartments: Susceptible ( $S$ ), Exposed ( $E$ ), Quarantined ( $Q$ ), Infectious ( $I$ ), Hospitalized ( $H$ ), and Recovered ( $R$ ) human population. Initially, the model was formulated and some mathematical analyses were presented, including positivity, invariant region, existence, uniqueness of the solution, and stability results for the disease-free equilibrium. The disease-free equilibrium for both local and global is stable when  $R_0 < 1$  was proved. This exploration suggests that the COVID-19 disease can enter and spread to the human population if  $R_0 > 1$  provided that the initial human population is close to the infested region. But also, die out when few initial human populations are infected and  $R_0 < 1$ . The basic reproduction number obtained from this study was 2.1692, which shows that the disease is endemic and unique. The most sensitivity indices are summarized in Table 3, and the least positively and negatively sensitive parameters are crucial for the transmission of COVID-19.

The numerical results in this study showed that stress affects many quarantined people whereby their immune system is disturbed by the COVID-19, and this is most likely because during quarantine, people are isolated from their families and community members, so they develop fear, and later, the body becomes stressed which affects their immune system. When the immune system is disturbed, it fails to fight against the intruders, which leads to the fast spread of COVID-19 throughout the body. Our graphical presentation illustrated that the control parameters showed a great success on minimizing the spread of COVID-19 in the community.

The plan for a future work is to use more detailed and authentic data when having access to COVID-19 data which

will be employed in the *SEQIHR* model. Furthermore, we intend to add a vaccination in our model compartment to implement optimal control strategies and extend to a stochastic model. The limitations of this work are the assumption on an equal death in all compartment while in real situation the infected population has a higher death rate than the susceptible population.

## Data Availability

Some data used in our numerical simulation (as shown in Table 3) are assumed and others from published articles as cited in this work.

## Conflicts of Interest

The authors declare that they have no competing interests.

## Authors' Contributions

James Nicodemus Paul is responsible for the conceptualization, model formulation, model analysis, and drafting of the manuscript. Silas Steven Mirau and Isambi Sailon Mbala-wata are assigned to the model formulation and supervision. All authors read and approved the final manuscript.

## Acknowledgments

The authors acknowledge African Institute for Mathematical Sciences (AIMS) for the support.

## References

- [1] M. Ali, M. Imran, and A. Khan, "Can medication mitigate the need for a strict lock down?: a mathematical study of control strategies for COVID-19 infection," 2020, medRxiv.
- [2] B. Ivorra, M. R. Ferrández, M. Vela-Pérez, and A. M. Ramos, "Mathematical modeling of the spread of the coronavirus disease 2019 (COVID-19) taking into account the undetected infections. The case of China," *Communications in Nonlinear Science and Numerical Simulation*, vol. 88, p. 105303, 2020.
- [3] B. F. Maier and D. Brockmann, "Effective containment explains subexponential growth in recent confirmed COVID-19 cases in China," *Science*, vol. 368, no. 6492, pp. 742–746, 2020.
- [4] J. S. Daks, J. S. Peltz, and R. D. Rogge, "Psychological flexibility and inflexibility as sources of resiliency and risk during a pandemic: modeling the cascade of COVID-19 stress on family systems with a contextual behavioral science lens," *Journal of Contextual Behavioral Science*, vol. 18, pp. 16–27, 2020.
- [5] M. M. Morato, S. B. Bastos, D. O. Cajueiro, and J. E. Normey-Rico, "An optimal predictive control strategy for COVID-19 (SARS-CoV-2) social distancing policies in Brazil," *Annual Reviews in Control*, vol. 50, pp. 417–431, 2020.
- [6] K. Prem, Y. Liu, T. W. Russell et al., "The effect of control strategies to reduce social mixing on outcomes of the COVID-19 epidemic in Wuhan, China: a modelling study," *Public Health*, vol. 5, no. 5, pp. e261–e270, 2020.
- [7] P. V. Savi, M. A. Savi, and B. Borges, "A mathematical description of the dynamics of coronavirus disease 2019 (COVID-19):

- a case study of Brazil,” *Computational and Mathematical Methods in Medicine*, vol. 2020, 2020.
- [8] J. M. V. Grzybowski, R. V. da Silva, and M. Rafikov, “Expanded SEIRCQ model applied to COVID-19 epidemic control strategy design and medical infrastructure planning,” *Mathematical Problems in Engineering*, vol. 2020, 15 pages, 2020.
  - [9] L. Masandawa, S. S. Mirau, and I. S. Mbalawata, “Mathematical modeling of COVID-19 transmission dynamics between healthcare workers and community,” *Results in Physics*, vol. 29, article ???, 2021.
  - [10] M. A. Khan, A. Atangana, and E. Alzahrani, “The dynamics of COVID-19 with quarantined and isolation,” *Adv. Difference Equ.*, vol. 2020, no. 1, pp. 1–22, 2020.
  - [11] S. Ullah and M. A. Khan, “Modeling the impact of non-pharmaceutical interventions on the dynamics of novel coronavirus with optimal control analysis with a case study,” *Chaos, Solitons & Fractals*, vol. 139, article ???, 2020.
  - [12] R. M. Dos Santos, “Isolation, social stress, low socioeconomic status and its relationship to immune response in COVID-19 pandemic context,” *Brain, behavior, & immunity-health*, page, vol. 7, p. 100103, 2020.
  - [13] J. N. Dhanwant and V. Ramanathan, “Forecasting COVID 19 growth in India using susceptible-infected-recovered (sir) model,” 2020, arXiv preprint arXiv: 2004.00696.
  - [14] M. A. Khan and A. Atangana, “Modeling the dynamics of novel coronavirus (2019-nCov) with fractional derivative,” *Alexandria Engineering Journal*, vol. 59, no. 4, pp. 2379–2389, 2020.
  - [15] P. Ashcroft, S. Lehtinen, D. C. Angst, N. Low, and S. Bonhoeffer, “Quantifying the impact of quarantine duration on COVID-19 transmission,” *eLife*, vol. 10, article e63704, 2021.
  - [16] G. Prati, “Mental health and its psychosocial predictors during national quarantine in Italy against the coronavirus disease 2019 (COVID-19),” *Anxiety, Stress, and Coping*, vol. 34, no. 2, pp. 145–156, 2021.
  - [17] A. H. Khan, M. S. Sultana, S. Hossain, M. T. Hasan, H. U. Ahmed, and M. T. Sikder, “The impact of COVID-19 pandemic on mental health & wellbeing among home-quarantined Bangladeshi students: a cross-sectional pilot study,” *Journal of Affective Disorders*, vol. 277, pp. 121–128, 2020.
  - [18] K. Usher, J. Durkin, and N. Bhullar, “The COVID-19 pandemic and mental health impacts,” *International Journal of Mental Health Nursing*, vol. 29, no. 3, pp. 315–318, 2020.
  - [19] M. Mandal, S. Jana, S. K. Nandi, A. Khatua, S. Adak, and T. K. Kar, “A model based study on the dynamics of COVID-19: prediction and control,” *Chaos, Solitons & Fractals*, vol. 136, article 109889, 2020.
  - [20] O. Diekmann and J. Heesterbeek, *Mathematical Epidemiology of Infectious Diseases*, 2000.
  - [21] P. Van den Driessche and J. Watmough, “Reproduction numbers and sub-threshold endemic equilibria for compartmental models of disease transmission,” *Mathematical Biosciences*, vol. 180, no. 1-2, pp. 29–48, 2002.
  - [22] O. Diekmann, J. A. P. Heesterbeek, and J. A. J. Metz, “On the definition and the computation of the basic reproduction ratio  $R_0$  in models for infectious diseases in heterogeneous populations,” *Journal of Mathematical Biology*, vol. 28, no. 4, pp. 365–382, 1990.
  - [23] C. Castillo-Chavez, Z. Feng, and W. Huang, “On the computation of  $R_0$  and its role on global stability,” *IMA Volumes in Mathematics and Its Applications*, vol. 125, pp. 229–250, 2002.
  - [24] N. Chitnis, J. M. Hyman, and J. M. Cushing, “Determining important parameters in the spread of malaria through the sensitivity analysis of a mathematical model,” *Bulletin of Mathematical Biology*, vol. 70, no. 5, pp. 1272–1296, 2008.
  - [25] O. C. Collins and K. J. Duffy, “Optimal control of maize foliar diseases using the plants population dynamics. Acta Agriculturae Scandinavica, Section B—Soil & Plant,” *Science*, vol. 66, no. 1, pp. 20–26, 2016.
  - [26] A. Patil, “Routh-Hurwitz criterion for stability: an overview and its implementation on characteristic equation vectors using MATLAB,” *Emerging Technologies in Data Mining and Information Security*, pp. 319–329, 2021.
  - [27] I. Agmour, N. Achtaich, and Y. E. Foutayeni, “Stability analysis of a competing fish populations model with the presence of a predator,” *Int. J. Nonlinear Sci*, vol. 26, no. 2, p. 108, 2018.
  - [28] B. G. Link and J. C. Phelan, “Conceptualizing stigma,” *Sociology*, vol. 27, no. 1, pp. 363–385, 2001.
  - [29] A. Korobeinikov and G. C. Wake, “Lyapunov functions and global stability for SIR, SIRS, and SIS epidemiological models,” *Applied Mathematics Letters*, vol. 15, no. 8, pp. 955–960, 2002.
  - [30] J. P. LaSalle, “Stability theory and invariance principles,” in *Dynamical Systems*, pp. 211–222, Elsevier, 1976.
  - [31] S. Djaoue, G. G. Kolaye, H. Abboubakar, A. A. A. Ari, and I. Damakoa, “Mathematical modeling, analysis and numerical simulation of the \_COVID-19\_ transmission with mitigation of control strategies used in Cameroon,” *Chaos, Solitons & Fractals*, vol. 139, article ???, 2020.
  - [32] G. O. Agaba, “Modelling the spread of COVID-19 with impact of awareness and medical assistance,” *Mathematical Theory and Modeling*, vol. 10, no. 4, pp. 21–28, 2020.
  - [33] D. Aldila, M. Z. Ndii, and B. M. Samiadji, “Optimal control on COVID-19 eradication program in Indonesia under the effect of community awareness,” *Mathematical Biosciences and Engineering*, vol. 17, no. 6, pp. 6355–6389, 2020.
  - [34] M. Serhani and H. Labbardi, “Mathematical modeling of COVID-19 spreading with asymptomatic infected and interacting peoples,” *Journal of Applied Mathematics and Computing*, pp. 1–20, 2020.
  - [35] D. Carvalho, R. Barbastefano, D. Pastore, and M. C. Lippi, “A novel predictive mathematical model for COVID-19 pandemic with quarantine, contagion dynamics, and environmentally mediated transmission,” 2020, medRxiv.
  - [36] V. Janardhan, V. Janardhan, and V. Kalousek, “COVID-19 as a blood clotting disorder masquerading as a respiratory illness: a cerebrovascular perspective and therapeutic implications for stroke thrombectomy,” *Journal of Neuroimaging*, vol. 30, no. 5, pp. 555–561, 2020.
  - [37] A. Solonen, P. Ollinaho, M. Laine, H. Haario, J. Tamminen, and H. Järvinen, “Efficient MCMC for climate model parameter estimation: parallel adaptive chains and early rejection,” *Bayesian Analysis*, vol. 7, no. 3, pp. 715–736, 2012.



# POSTER: Mathematical Modelling Approach to Investigate Transmission Dynamics of COVID-19 with some Control Parameters

James Nicodemus Paul<sup>1</sup>, Silas Steven Mirau<sup>2</sup>  
& Isambi Sailon Mbalawata<sup>3</sup>

<sup>1,2</sup>The Nelson Mandela African Institution of Science and Technology (NM-AIST)

<sup>3</sup>African Institute for Mathematical Sciences, NEI Global Secretariat, Rue KG590 ST, Kigali - Rwanda



## Introduction

COVID-19 is a world pandemic that has affected and continues to affect the social lives of people. Due to its social and economic impact, different countries imposed preventive measures that aim to reduce the transmission of the disease. Such preventive measures include physical distancing, quarantine, hand-washing, travel and boarder restrictions, lock downs, and the use of hand sanitizers. Some measures used to fight the disease are stressful, for example, quarantine. When people are stressed, their body immunity becomes weak, which leads to multiplying of coronavirus within the body. Hence, there is a need to model the transmission of COVID-19 when a human is stressed.

## Model Formulation

A mathematical model for COVID-19 was formulated based on realistic assumptions. The human population was divided into six classes which are susceptible  $S(t)$ , exposed  $E(t)$ , quarantined  $Q(t)$ , infectious  $I(t)$ , hospitalized  $H(t)$ , and recovered  $R(t)$ . The compartmental diagram is presented in the following figure.

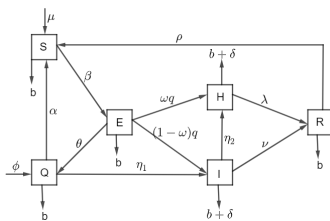


Figure: Model Compartmental Diagram

## Model Properties

The two model properties, **positivity** and **invariant region** make the model to be both mathematically and epidemiologically meaningful because they are positive and bounded respectively. Where for any  $t > 0$ , the model's solutions  $S(t), E(t), Q(t), I(t), H(t), R(t)$  are all positive. And for invariant region

$$\Omega = (S, E, Q, I, H, R) \in \mathbb{R}_+^6 : 0 \leq N(t) \leq \frac{\mu + \phi}{b}$$

## Basic Reproduction Number, $R_0$

The basic reproduction number,  $R_0$  is defined as the spectral radius (dominant eigenvalue) of the matrix.

$$R_0 = \frac{\beta\mu(\eta_1(\theta - \omega q + q) + q(1 - \omega)(\alpha + b))}{b(\alpha + b + \eta_1)(b + \theta + q)(b + \delta + \eta_2 + \nu)}$$

## Local & Global Stability Analysis of $E_0$

$E_0$  is locally asymptotically stable if  $R_0 < 1$  and it is unstable when  $R_0 > 1$ .

## Global Endemic Stability Analysis $E_*$

The endemic equilibrium point  $W^*$  is asymptotically stable when  $R_0 > 1$  and unstable when  $R_0 < 1$ .

## Numerical Simulation Results

Runge-Kutta fourth order method, PRCC method for sensitivity analysis, Least square and MCMC methods for parameter identifiability were used.

## Sensitivity Analysis

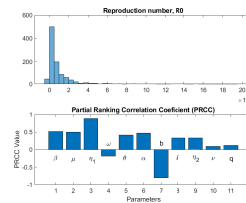


Figure: Sensitivity Analysis by PRCC Method

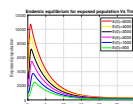


Figure: Endemic Equilibrium

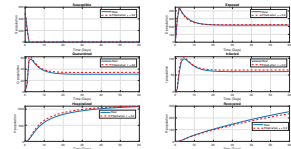


Figure: Model Fitting

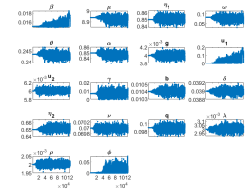


Figure: MCMC Trace Plots

## Conclusion

The numerical results in this study showed that stress affects many quarantined people whereby their immune system is disturbed by the COVID-19 and this is most likely because during quarantine, people are isolated from their families and community members, so they develop fear, and later the body becomes stressed which affects their immune system.

## Recommendation

People should not be quarantined for long and should not be separated from their families.

## References

1. Ashcroft, P., Lehtinen, S., Angst, D. C., Low, N., Bonhoeffer, S. (2021). Quantifying the impact of quarantine duration on COVID-19 transmission. *Elife*, 10, e63704.
2. Barbastefano, R., Carvalho, D., Lippi, M. C., Pastore, D. H. (2020). A novel predictive mathematical model for COVID-19 pandemic with quarantine, contagion dynamics, and environmentally mediated transmission. *medRxiv*.